

Status of Thesis

Title of thesis:

Self-Adaptive Autoreclosing Scheme using Artificial Neural Network and Taguchi's Methodology in Extra High Voltage Transmission Systems

I DESTA ZAHLAY FITIWI hereby allow my thesis to be placed at the information resource centre (IRC) of the Universiti Teknologi PETRONAS (UTP) with the following conditions.

1. The thesis becomes the property of UTP
2. The IRC of UTP may make copies of the thesis for academic purpose only.
3. This thesis is classified as

Confidential

Non-confidential

If this thesis is confidential, please state the reason:

The content of the thesis will remain confidential for _____ years.

Remarks on disclosure:



Signature of Author

Permanent address:

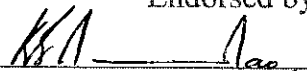
Addis Ababa Kirkos Sub-City

Kebele 08/09, House # 398B

Tel: +251911396499.

Date: 27/07/09

Endorsed by



Signature of Supervisor

Name of Supervisor:

K.S. Rama Rao (A. P. Dr)

Date: 27/07/09

Dr. K.S. Rama Rao
Associate Professor
Electrical & Electronic Engineering
31760 Tronoh Perak
Tel: 06-328 7875 Fax: 365 7443

UNIVERSITI TEKNOLOGI PETRONAS

Approval by Supervisors

The undersigned certify that they have read and recommend to The Postgraduate Studies Programme for acceptance, a thesis entitled "Self-Adaptive Autoreclosing Scheme using Artificial Neural Network and Taguchi's Methodology in Extra High Voltage Transmission Systems" submitted by Desta Zahlay Fitiwi for the fulfillment of the requirements for the degree of Master of Science in Electrical and Electronics Engineering.

27/07/09

Date

Signature



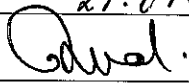
Dr. K.S. Rama Rao
Associate Professor
Electrical & Electronic Engineering
31760 Tronoh Perak
Tel: 05-333 7875 Fax: 365 7443

Main Supervisor: Associate Prof. Dr. K. S. Rama Rao

Date

27.07.2009

Signature



Co-Supervisor : Ir. Perumal A/L Nallagownden

Ir. N. Perumal
Senior Lecturer,
Electrical & Electronic Engineering
Academic Block No 22
Universiti Teknologi PETRONAS
Bandar Seri Iskandar
31750 Tronoh, Perak Darul Ridzuan, MALAYSIA

Date

27/7/09.

UNIVERSITI TEKNOLOGI PETRONAS

Self-Adaptive Autoreclosing Scheme using Artificial Neural Network and
Taguchi's Methodology in Extra High Voltage Transmission Systems

By

© Desta Zahlay Fitiwi

A THESIS

SUBMITTED TO THE POSTGRADUATE STUDIES PROGRAMME

AS A REQUIRMENT FOR THE

DEGREE OF MASTER OF SCIENCE IN ELECTRICAL AND ELECTRONICS

ENGINEERING

DEPARTMENT OF ELECTRICAL AND ELECTRONICS ENGINEERING


BANDAR SERI ISKANDAR, 31750 TRONOH

PERAK DARUL RIDZUAN, MALAYSIA

JULY, 2009

Declaration

I hereby declare that the thesis is based on my original work except for quotations and citations which have been duly acknowledged. I also declare that it has not been previously or concurrently submitted for any other degree at UTP or other institutions.

Signature:  _____

Name : DESTA ZAHLAY FITIWI

Date : JULY 21, 2009

Dedication

“This thesis is dedicated to my wonderful fiancée and my family, who have offered me unconditional love and support throughout the course of this thesis. You have been with me every step of the way, through good and bad times. Thank you for all the unconditional love, guidance, and support that you have always given me, helping me to succeed and instilling in me the confidence that I am capable of doing anything I put my mind to. Thank you for everything. I love you!”

Acknowledgements

From the formative stages of this thesis to the final draft, I owe an immense debt of gratitude to my Supervisor, Associate Professor Dr. K. S. Rama Rao, Senior lecturer at Universiti Teknologi PETRONAS. His sound advice, encouragement, expert guidance and patience towards realizing my research work were invaluable all the time. He has introduced me to new ideas, and allowed me the opportunity to experience a sound research background and perpetual enthusiasm for research. His knowledge and experience contributed significantly to this thesis. I would also like to extend my sincere thanks to my Co-Supervisor Ir. Perumal A/L Nallagownden, Senior lecturer at Universiti Teknologi PETRONAS, for his support and valuable suggestions.

For their efforts and assistance, I extend my deepest appreciation and special thanks as well to Associate Prof. Dr. Mohd Noh Bin Karsiti, Director of the Postgraduate Office, Dr. Nor Hisham Bin Hamid, Head of the Department of Electrical and Electronics Engineering and A.P. Dr. Nordin Bin Saad, senior lecturer at Universiti Teknologi PETRONAS. I would also like to acknowledge the overall support provided by Universiti Teknologi PETRONAS without of which it would be impossible to pursue my studies.

I extend my sincere gratitude to the Postgraduate Office of Universiti Teknologi PETRONAS staff members, Ms. Kamaliah Mohd, Ms. Nurul Aizat Binti Ngah and Mr. Khar for their patience and consistent guidance throughout my study. Many thanks to the staff of the Electrical and Electronics Engineering Department of Universiti Teknologi PETRONAS for providing a stimulating and friendly atmosphere for study and research.

I also thank my external examiner Prof. Dr. Azah Mohamed, my internal examiner Dr. Taib Ibrahim as well as Dr. Vijanth S. A. for their constructive comments. I would like to thank Jigan.

Last but not least, I would like to express my deepest gratitude and personal thanks to those closest to me. In particular, I would like to thank my family for teaching me the value of education, their support and encouragement. I have been overwhelmed by the support from my beloved fiancée Senait Mola. Without her great share, I recognize that my effort wouldn't be fruitful as it is now. I am so delighted to thank my fellow friends Dr. Umesh, Dr. Lemma, Tadesse Weldu, Tedros Mezgebe, Hailay Tsegab and all ESA@UTP members for making my stay at UTP memorable and enjoyable. I would be remiss without mentioning my elder brother Ghirmay Zahlay Fitiwi, whose extreme generosity will be remembered always.

Abstrak

Pada kebiasaannya, sistem penyambungan automatik beroperasi bagi kerosakan kekal, separa kekal ataupun kerosakan sementara terhadap talian penghantaran tanpa membezakan mana-mana kerosakan selepas membenarkan beberapa lengahan masa yang telah dianggarkan. Penyambungan terhadap talian tanpa kerosakan yang diketahui bukan sahaja menyebabkan ketidakstabilan dan ketidaklarasan tetapi juga mendatangkan kerosakan kepada sistem peralatan yang digunakan. Tesis ini memfokuskan mengenai cara-cara untuk membezakan kerosakan sementara terhadap kerosakan kekal, dan seterusnya menentukan dengan tepat 'fault extinction time' di dalam talian EHV voltan terlesih tingsi bagi menghasilkan suatu penyelesaian terhadap 'self-adaptive automatic reclosing scheme'. Pengenalpastian kerosakan yang melibatkan penyambungan ialah melalui pengoptimuman 'artificial neural network' yang terlibat dengan 3 algoritma berkenaan iaitu 'Standard Error Back-Propagation', 'Levenberg Marquardt' dan 'Resilient Back-Propagation'. Di samping itu, metodologi Taguchi digunakan untuk mengoptimumkan parameter-parameter yang digunakan dan juga bagi menentukan bilangan neuron tersembunyi dalam 'neural network'. Bagi tujuan mendapatkan data bagi 'neural network', suatu julat kerosakan disimulasikan berdasarkan kepada 2 kajian kes; 'single machine –infinite bus model' (disambungkan melalui taun penghantaran EHV) dan 'IEEE 9-bus electric system'. Spektrum bagi data voltan rosak kemudiannya dianalisis menggunakan Fast Fourier Transform, dan didapati bahawa AT dan empat komponen harmonic yang pertama mewakili keadaan bagi setiap kerosakan. Bagi setiap kajian kes, 'neural network' dibekalkan dengan tenaga AT ternormal, manakala harmonic teringkas dan empat harmonic terawal dilatih dengan menggunakan satu set data latihan efektif dan disahkan dengan menggunakan data ujian yang diperoleh daripada signal kerosakan voltan terhasil daripada 'IEEE 14-bus electric system model'. Keputusan akhir menunjukkan sejauh mana penggunaan 'self-adaptive automatic reclosing scheme' yang telah dibangunkan ini. Ini menunjukkan bahawa adalah tidak mustahil untuk mengelakkan penyambungan sebelum terjadinya apa-apa kerosakan terhadap talian penghantaran (sama ada kekal ataupun sementara).

Abstract

Conventional automatic reclosures blindly operate for permanent, semi-permanent or transient faults on an overhead line without any discrimination after allowing some estimated time delay. Reclosing onto a line with uncleared fault often results in, not only loss of stability and synchronism but also damage to system equipments, as a consequence. The thesis focuses on methods to discriminate a temporary fault from a permanent one, and accurately determine fault extinction time in an extra high voltage (EHV) transmission line in a bid to develop a self-adaptive automatic reclosing scheme. The fault identification prior to reclosing is based on optimized artificial neural network associated with three training algorithms, namely, Standard Error Back-Propagation, Levenberg Marquardt and Resilient Back-Propagation algorithms. In addition, Taguchi's methodology is employed in optimizing the parameters of each algorithm used for training, and in deciding the number of hidden neurons of the neural network. To get data for training the neural networks, a range of faults are simulated on two case studies –single machine -infinite bus model (connected via EHV transmission line) and a benchmark IEEE 9-bus electric system. The spectra of the fault voltage data are analyzed using Fast Fourier Transform, and it has been found out that the DC, the fundamental and the first four harmonic components can sufficiently and uniquely represent the condition of each fault. In each case study, the neural network is fed with the normalized energies of the DC, the fundamental and the first four harmonics of the faulted voltages, effectively trained with a set of training data, and verified with a dedicated testing data obtained from fault voltage signals generated on IEEE 14-bus electric system model. The results show the efficacy of the developed adaptive automatic reclosing scheme. This effectively means it is possible to avoid reclosing before any fault on a transmission line (be it temporary or permanent) is totally cleared.

Table of Contents

Declaration	iii
Dedication	iv
Acknowledgements	v
Abstrak	vii
Abstract	viii
Table of Contents	ix
List of Tables	xiv
List of Figures	xvi
List of Symbols	xvii
List of Abbreviations	xix
CHAPTER ONE: INTRODUCTION	1
1.1. BACKGROUND	1
1.2. POWER TRANSMISSION LINE FAULTS AND PROTECTION	2
1.3. CONVENTIONAL AUTO-RECLOSURE SCHEME IN EHV LINES.....	5
1.4. MOTIVATION	6
1.5. OBJECTIVE OF THE THESIS.....	8
1.6. SCOPE OF THE THESIS WORK.....	9
1.7. CONTRIBUTION OF THE THESIS	11
1.8. OUTLINE OF THE THESIS.....	12
CHAPTER TWO: LITERATURE REVIEW AND THEORETICAL	
INTRODUCTION TO AUTORECLOSURE SYSTEM.....	14
2.1. INTRODUCTION	14
2.2. HISTORY OF AUTOMATIC RECLOSING	14
2.3. EHV TRANSMISSION LINE FAULTS –AN OVERVIEW	15

2.4.	PRINCIPLES OF AUTOMATIC RECLOSING (AR).....	17
2.4.1.	Definitions of Terms Associated with AR.....	17
2.4.2.	Automatic Reclosing Scheme on EHV Transmission Systems	21
2.4.3.	High Speed Auto-reclosing on EHV Transmission Systems	23
2.4.3.1.	Protection Characteristics	25
2.4.3.2.	Fault Arc De-ionization	25
2.4.3.3.	Characteristics of Circuit Breaker	26
2.4.3.4.	Choice of Dead Time.....	27
2.4.3.5.	Choice of Reclaim Time of a Circuit Breaker	28
2.4.3.6.	Number of Shots.....	28
2.5.	SINGLE-PHASE AUTO-RECLOSING IN EHV TRANSMISSION SYSTEMS.....	28
2.6.	DELAYED AUTORECLOSING ON EHV TRANSMISSION	30
2.6.1.	Operation Scheme of Delayed Auto-reclosing	30
2.6.2.	Synchronism Check Relays	31
2.7.	OPERATING FEATURES OF AR SCHEMES IN EHV SYSTEMS	32
2.7.1.	Initiation of Auto-reclosing	32
2.7.2.	Type of Protection.....	32
2.7.3.	Dead Timer	33
2.7.4.	Reclosing Impulse.....	33
2.7.5.	Anti-Pumping Devices	33
2.7.6.	Reclaim Timer.....	34
2.7.7.	Circuit Breaker Lockout	34
2.7.8.	Manual Closing of a Circuit Breaker	34
2.7.9.	Multi-Shot Schemes in EHV Systems.....	34
2.8.	BENEFITS OF AUTOMATIC RECLOSING	35
2.9.	CHALLENGES IN CONVENTIONAL AUTORECLOSURE	36
2.10.	PREVIOUS WORKS ON INHIBITING RECLOSE ACTION ON TO FAULTS.....	38
2.10.1.	Modification on the Dead Time	38

2.10.2.	Sensing High-Resistance Earth Faults to Block Auto-Reclosing	38
2.10.3.	Development of Adaptive Autoreclosure	39
2.10.4.	Adaptive Autoreclosure Based on Mathematical Algorithms	39
2.10.5.	Artificial Intelligence (AI) Based.....	42
2.11.	PROPOSED TECHNIQUE.....	43
2.12.	SUMMARY.....	44
CHAPTER THREE: ARTIFICIAL NEURAL NETWORKS AND TAGUCHI'S		
OPTIMIZATION METHODS –THEORETICAL REVIEW.....		
3.1.	INTRODUCTION	45
3.2.	ARTIFICIAL NEURAL NETWORKS	46
3.2.1.	Basic Concepts.....	46
3.2.2.	The Mathematical Model of ANN	50
3.2.3.	Classification of ANNs.....	52
3.2.4.	Normalization and ANN Training	53
3.2.5.	Training Algorithms	56
3.2.5.1.	Error Back-Propagation (EBP) Algorithm.....	56
3.2.5.2.	The Resilient Back-propagation algorithm (RPROP)	58
3.2.5.3.	The Levenberg Marquardt (LM) Algorithm	63
3.2.6.	Advantages and Applications of ANN in Power Systems	67
3.3.	OPTIMIZATION METHOD -TAGUCHI'S METHODOLOGY.....	69
3.4.	SUMMARY.....	72
CHAPTER FOUR: MODEL POWER SYSTEM SIMULATIONS AND DATA		
GATHERING		
4.1.	INTRODUCTION	73
4.2.	CASE STUDY I: A SINGLE MACHINE - INFINITE BUS SYSTEM	75
4.2.1.	Introduction.....	75
4.2.2.	Fault Simulations on SMIB Electric Power System Model	76
4.2.3.	Feature Extraction and Selection	79

4.3.	CASE STUDY II: IEEE 9-BUS ELECTRIC POWER SYSTEM	85
4.3.1.	Introduction.....	85
4.3.2.	Fault Simulations on IEEE 9-Bus Electric Power System Model	86
4.3.3.	Feature Extraction	87
4.4.	CASE STUDY III: IEEE 14-BUS ELECTRIC POWER SYSTEM	92
4.4.1.	Introduction.....	92
4.4.2.	Fault Simulations on IEEE 14-Bus Electric Power System	93
4.4.3.	Feature Extraction and Selection	94
4.5.	SUMMARY	96
CHAPTER FIVE: DESIGN AND OPTIMIZATION OF ANN USING TAGUCHI'S METHODOLOGY AND TEST RESULTS		97
5.1.	INTRODUCTION	97
5.2.	ANN SIMULATION AND TAGUCHI'S EXPERIMENTS WITH DATA FROM SMIB MODEL –CASE STUDY I	97
5.2.1.	Method of Training Neural Network.....	97
5.2.2.	Normalization of Input Data.....	100
5.2.3.	Choice of Transfer Function	101
5.2.4.	Application of Taguchi's Methodology for Optimization.....	101
5.3.	ANN SIMULATION AND TAGUCHI'S EXPERIMENTS WITH DATA FROM IEEE 9-BUS POWER SYSTEM MODEL	108
5.3.1.	Method of Training Neural Network and Normalization.....	108
5.3.2.	Taguchi's Experimentation for Optimization	110
5.3.3.	Validation	115
5.4.	TESTING RESULTS WITH DATA FROM IEEE 14-BUS MODEL.....	116
5.5.	ACCURATE DETERMINATION OF FAULT EXTINCTION TIME ...	117
5.6.	SUMMARY.....	118
CHAPTER SIX: CONCLUSIONS AND RECOMMENDATIONS		120
6.1.	CONCLUSIONS.....	120

6.2. RECOMMENDATIONS	122
PUBLICATIONS	124
APPENDIX A: DISTRIBUTED TRANSMISSION LINE PARAMETERS	133
APPENDIX B: TRAINING DATA PATTERNS AND TESTING RESULTS OF NEURAL NETWORK	135
APPENDIX C: SOME OF THE DATA PATTERNS FOR TRAINING ANN WITH TARGET VALUES.....	138
APPENDIX D: A SET UP OF IEEE 9-BUS POWER SYSTEM MODEL IN SIMULINK	139
APPENDIX E: FFT OUTPUTS OF TEMPORARY FAULT AFTER AND BEFORE EXTINCTION.....	140
APPENDIX F: A SET UP OF IEEE 14-BUS POWER SYSTEM MODEL IN SIMULINK	141
APPENDIX G: MATLAB CODES	142

List of Tables

Table 2.1: Typical circuit breaker trip-close operation times (in seconds)	20
Table 2.2: Fault arc de-ionization times	26
Table 3.1: Some activation functions of artificial neural networks	49
Table 4.1: Some simulated data patterns for training ANN and the target values	82
Table 4.2: Maximum and minimum values of features extracted.....	92
Table 4.3: Generated faults and their variable parameter settings	93
Table 4.4: Extracted data patterns (immediately after fault inception and 10 th cycles)	95
Table 5.1: Control parameters and their corresponding levels for LMA	103
Table 5.2: L ₁₆ Orthogonal arrays for 4 parameters each with 4 Levels and their corresponding error index and epochs for LM algorithm	104
Table 5.3: Average % EI for each factor and level in LM.....	106
Table 5.4: Average epochs (n) for each factor and level in LM	106
Table 5.5: Average ε for each factor and each level in LM.....	106
Table 5.6: Control parameters and their corresponding levels for RPROP.....	106
Table 5.7: Average ε for each factor and each level - RPROP	107
Table 5.8: Control parameters and their corresponding levels for EBP	107
Table 5.9: Average ε for each factor and each level for EBP	107
Table 5.10: Accuracy and convergence rate of the three algorithms	108
Table 5.11: Control Parameters and Corresponding Levels	111
Table 5.12: Results of Taguchi's experiment for LM algorithm	111
Table 5.13: Average ε for each CP and each level –LM	113
Table 5.14: Average ε for each CP and each level –RPROP.....	113
Table 5.15: Average ε for each CP and each level –EBP.....	113
Table 5.16: Optimized values of CPs and corresponding accuracies.....	114
Table 5.17: Test results of optimized ANN for the data generated from IEEE 14 ...	117

List of Figures

Figure 1.1: An onset of transmission line fault (a) and its consequence (b)	3
Figure 1.2: Sample voltage and current waveforms before, during and after a fault	4
Figure 1.3: Transmission line protective relaying schematic diagram	5
Figure 1.4: Schematic diagram of the proposed auto-reclosure activation.....	10
Figure 1.5: Functional steps for the fault identification process	10
Figure 2.1: Operation of single-shot auto-reclose scheme for a permanent fault	18
Figure 2.2: Operation of single-shot auto-reclose scheme for a temporary fault.....	18
Figure 2.3: Typical circuit breaker trip-close operation time instants.....	20
Figure 2.4: Effect of high-speed three-phase auto-reclosing on system stability	23
Figure 2.5: Network diagram	31
Figure 3.1: A 5x7x1 feed-forward neural network.....	48
Figure 3.2: A single processing unit.....	51
Figure 3.3: Supervised neural network learning scheme	52
Figure 3.4: A training process flowchart of error back propagation algorithm	58
Figure 3.5: Training flowchart of LM algorithm	65
Figure 3.6: A schematic diagram demonstrating the use of Taguchi's experiment	70
Figure 4.1: Schematic outline of the simulation work.....	73
Figure 4.2: Single machine infinite bus (SMIB) power system.....	76
Figure 4.3: Single line diagram of line model used in the study.....	77
Figure 4.4: A setup of SMIB model in Simulink	77
Figure 4.5: Temporary a-phase-to-ground fault voltage waveform	78
Figure 4.6: Permanent three-phase-to-ground fault voltage waveform.....	78
Figure 4.7: FFT of voltage signal for single-phase-to-ground temporary fault	81
Figure 4.8: FFT of voltage signal for three-phases-to-ground permanent fault.....	82
Figure 4.9: A stacked column representation of temporary and cleared fault	83
Figure 4.10: A stacked column representation of temporary fault patterns.....	84
Figure 4.11: A stacked column representation of cleared fault patterns	84

Figure 4.12: Stacked column representation of permanent fault patterns	85
Figure 4.13: Single line diagram of an IEEE 9-bus system used in the study.....	86
Figure 4.14: Temporary single-phase-to-ground fault voltage	87
Figure 4.15: Permanent three-phase-to-ground fault voltage	87
Figure 4.16: FFT analysis of a sample taken from temporary 2-phase-to ground.....	88
Figure 4.17: Stacked column representation of temporary and cleared fault data.....	89
Figure 4.18: Energies of temporary and cleared fault samples vs. location of fault ...	90
Figure 4.19: Energies of harmonic components of temporary fault vs. location.....	90
Figure 4.20: Cleared fault cases with increasing location of fault	91
Figure 4.21: Energies of harmonic components of permanent fault vs. location	91
Figure 4.22: IEEE 14-bus system.....	92
Figure 4.23: Recorded temporary ABG –HIF fault (at 100 km) – IEEE 14.....	94
Figure 4.24: Recorded temporary ABG fault (at 50 km) – IEEE 14-bus system	95
Figure 5.1: A plot of harmonic components of data patterns and their corresponding neural network outputs.....	98
Figure 5.2: A GUI for training neural network.....	99
Figure 5.3: A generalized GUI for training neural network	99
Figure 5.4: Schematic of Taguchi’s experimentation on selected parameters of	104
Figure 5.5: Training Performance before and after optimization.....	108
Figure 5.6: A stacked column representation of harmonic components of fault sample patterns (a), and their corresponding neural network output (b).	109
Figure 5.7: Performance (a) before and (b) after optimization for LM algorithm ...	115
Figure 5.8: Performance (a) before and (b) after optimization for RPROP.....	115
Figure 5.9: ANN output patterns for temporary and permanent faults	118

List of Symbols

$\% EI$	Percent Error Index
Δ	Change in
Δ_0	Initial update value
Δ_{ij}	Update value for weight connecting i^{th} and j^{th} neurons
\circ	Degree
a	Actual value
A	Actual Value vector
a_j	Output of j^{th} neuron
d	Desired value
e	Error
E	Total Error
E_P	Error for pattern P
f	Activation function
$F(.)$	Error function
h	Number of hidden neurons
H_i	Highest desired input value
J	Jacobian Matrix
L_o	Lowest desired input value
M	Number of hidden layers
n	Number of iterations
net_j	Net input to j^{th} neuron
N_i	Number of hidden units
N_I	Number of input units
N_o	Number of output units
P	Training pattern
T	Target Value Vector
t	Time
τ	Transpose
w	Weight vector

X	Raw data value
x	Scaled input data vector
x_i	Outputs of previous layer
α	momentum term/ weight decay parameter
β	Decay rate
β_i	Bias of j^{th} neuron
ε	Modified Error Index
η^-	Decrement factor
η	Learning rate
η^+	Increment factor
λ	Learning parameter

List of Abbreviations

AB	Phases A and B short circuit fault
ABCG	Phases A, B and C to Ground fault
ABG HIF	Phases A and B to Ground High Impedance Fault
ABG	Phases A and B to Ground fault
AG HIF	Phase A to Ground High Impedance Fault
AG	Phase A to Ground fault
AI	Artificial Intelligence
ANN	Artificial Neural Network
AR	Auto-Reclosure
CB	Circuit Breaker
COOCG	Close-Opening – Open-Closing
CSG	Conjugate Scaled Gradient
CT	Current Transformer
CVT	Capacitor Voltage Transformer
DC	Direct Current
DFT	Discrete Fourier Transform
DW	Data Window
DWT	Discrete Wavelet Transform
EBP	Error Back-Propagation
EHV	Extra High Voltage
EI	Error Index
ER	Energy Ratio
ES	Expert System
FFT	Fast Fourier Transform
FL	Fuzzy Logic
FST	Fuzzy Set Theory
GA	Genetic Algorithm
GUI	Graphical User Interface

HDI	Harmonic Distortion Index
HIF	High Impedance Fault
HSR	High Speed Reclosing
HV	High Voltage
Hz	Hertz
IEEE	Institute of Electrical and Electronics Engineers
km	Kilo meters
kV	Kilo Volt
LM	Levenberg Marquardt
MLP	Multi-Layer Perceptron
MSE	Mean Square Error
MV	Medium Voltage
OA	Orthogonal Array
RBNN	Radial Basis Feed-forward Neural Network
RMS	Root Mean Square
RMSE	Root Mean Square Error
RPROP	Resilient Back-Propagation
s	Second
SB	Smaller-the-Better
SMIB	Single Machine Infinite Bus
TM	Taguchi's Method
UHV	Ultra High Voltage
WA	Wavelet Analysis

CHAPTER ONE

INTRODUCTION

1.1. BACKGROUND

An electric power system comprises of generation, transmission and distribution of electric energy. Studies show electrical power distribution systems were first introduced towards the end of the last century. In comparison to today's systems, they were relatively simple, usually consisting of small generating stations that provided the needs of their immediate vicinities. As demand increased and growth in power systems blossomed, larger systems are introduced, where widely scattered and numerous substations and generating plants are connected by transmission lines into a huge network [P.M. Anderson and A.A. Fouad, 2003]. The direct benefit of these connections is to enable the transfer of electric power from the producer to the consumer across regions.

In particular, Extra High Voltage (EHV) transmission lines (whose line-to-line voltage level lies between 345 kV and 765 kV) are designed to transfer large amount of power from one location to another over a long distance. The length exposed to the environment is a major reason for occurrence of faults on the lines. A fault on an EHV transmission line affects the stability of the overall power system, which sometimes leads to permanent damage of equipments. For this reason, the proper functioning of a modern power system is heavily dependent upon the healthy operation of the transmission lines within it. In other words, transmission line should be adequately protected to avoid damage to equipments while maintaining the continuity of supply.

A power system, most of the time, operates in a steady state but disturbances, temporary and permanent, occur occasionally by the presence of large number of components which are susceptible to failures caused due to natural calamities, human

errors and aging [Leonard L. Grigsby, 2007]. Faults cause large amounts of currents to flow in the components that would burn out if current flows are not promptly interrupted. Basically, the voltages of the faulted phases decrease on the occurrence of a fault, but the currents shoot up. Therefore, faults, if not detected and eliminated quickly, may cause severe reduction in system voltage, loss of synchronism, loss of revenue and may damage the equipment permanently. They can be minimized by proper power system planning and using sophisticated equipment but the occurrence of faults cannot be eliminated fully. It is, therefore, necessary to protect power systems from faults.

1.2. POWER TRANSMISSION LINE FAULTS AND PROTECTION

Many items of equipments in power system grid are very expensive, and so the complete power system represents a very large capital investment [P.M. Anderson, 1999]. To maximize the return on this outlay, the system must be utilized as much as possible within the applicable constraints of security and reliability of supply. Safety and reliability are two of the most important aspects of electric power supply systems. More fundamental, however, is that the power system should operate in a safe manner at all times.

Recently, increasing transmission requirements and environmental pressures are forcing utilities to increase loading on existing transmission networks as an alternative to system reinforcements. Consequently, increased loading inevitably results in a reduction in the transient stability margins of the system. This requires fast fault clearing times because of the reduced stability margins. Particularly, EHV transmission lines are vulnerable to such types of instabilities and irregularities. This is due to the fact that EHV transmission lines span over long distances and are usually connected to huge power stations and/or substations.

When today's EHV transmission lines are exposed to treacherous weather, they are very likely to be subjected to faults. Insulator failure may result in short circuits

among phases and ground conductors. A lightning strike may break down the dielectric between phases and cause a short circuit between the phases and the ground conductors via arcing. A fault occurring on the transmission line may subsequently lead to a collapse at the system level if it is improperly handled. No matter how well designed, faults will always occur on a power system, and these faults may represent a risk to life and/or property. Figure 1.1(a) shows an onset of a fault on an overhead line [Laszlo Prikler, et al. 2002].

The destructive power of a fault arc carrying a high current is very great; it can burn through copper conductors or weld together core laminations in a transformer or machine in a very short time – some tens or hundreds of milliseconds. Figure 1.1(b) provides an illustration of the consequences of failure to provide appropriate protection [Laszlo Prikler, et al. 2002]. Even away from the fault arc itself, heavy fault currents can cause damage to plant if they continue for more than a few seconds. Figure 1.2 shows sample voltages and current waveforms recorded before, during and after a fault on a model transmission line. The provision of adequate protection to detect and disconnect elements of the power system in the event of a fault is therefore an integral part of power system design. Only by so doing can the objectives of the



(a)

(b)

Figure 1.1: An onset of transmission line fault (a) and its consequence (b)

[Laszlo Prikler, et al. 2002]

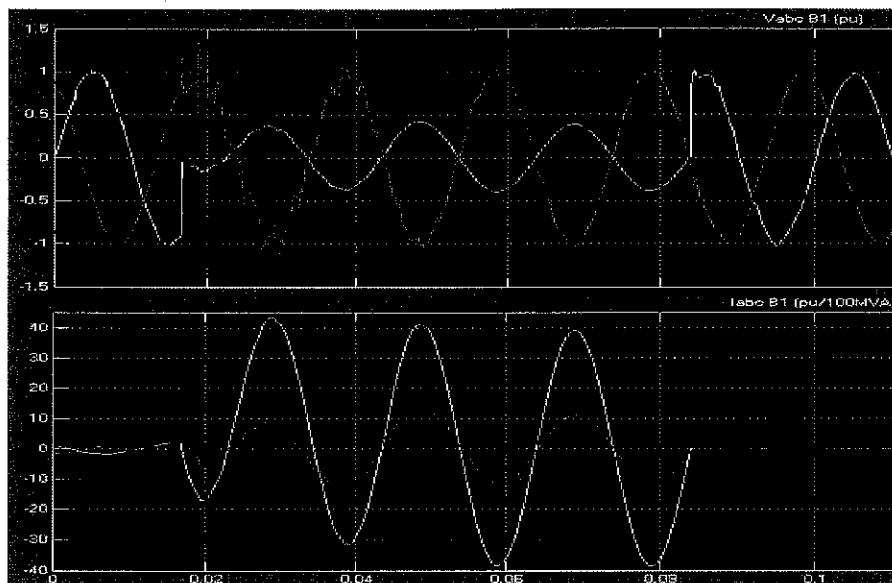


Figure 1.2: Sample voltage and current waveforms before, during and after a fault

power system be met and the investment be protected. So, proper operation and protection of EHV transmission lines to minimize the consequences of faults is unquestionable.

Protective relays are installed at various places in the power system to detect faults and isolate the faulted part from the remaining system. Depending on the application, relays receive voltages and/or currents as inputs from a power system via voltage and current transformers. Figure 1.3 is a typical power system protective relaying for EHV transmission line. In modern transmission lines, distance relaying is a well established technique for protecting the transmission lines against electrical fault conditions. By monitoring the line voltage and current as measured at the relaying point, the distance relay compares the system impedance with a pre-set reference representing the impedance of the protected line, and decides whether or not a fault condition exists on that line. If a fault is detected, the relay output provides instruction to the relevant circuit isolation equipment to disconnect the faulted section.

On the other hand, the continuity of supply is another key issue that has to be taken into consideration in power systems. To meet this condition, it is required that a transmission line, isolated following a fault occurrence, be reclosed within possible

short duration of time. This in turn improves not only the continuity of supply but also the maintenance of the power system stability and synchronism, particularly to EHV systems.

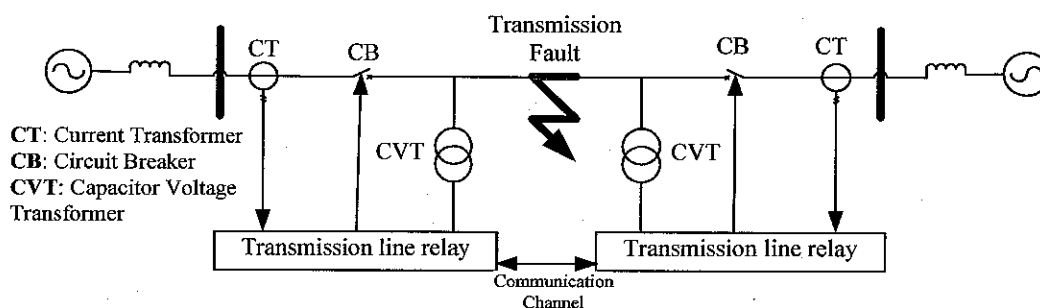


Figure 1.3: Transmission line protective relaying schematic diagram

1.3. CONVENTIONAL AUTO-RECLOSURE SCHEME IN EHV LINES

An auto-reclosure is a mechanism that can automatically close a circuit breaker after it has been opened due to a fault on a transmission line; this re-energizes the power transmission line. As explained in Section 1.2, a transmission line is protected by tripping its circuit breakers following a fault. Allowing an isolated transmission line for a prolonged time usually results in adverse affects on the continuity of supply and stability of the system. Thus, automatic reclosing of the faulted transmission line is an imperative concern in modern transmission lines. The most important consideration in the application of auto-reclosing to EHV transmission lines is the maintenance of system stability and synchronism. Hence, to improve the continuity of supply and the maintenance of power system stability and synchronism, particularly to EHV systems, automatic reclosure (or simply auto-reclosure) schemes have been introduced for many years. These schemes have significantly enhanced the stability and reliability of power industries.

However, auto-reclosures have certain drawbacks that necessitate considerable attention. An automatic reclosure acts for permanent, semi-permanent or temporary

faults on an overhead line without any discrimination after allowing some estimated time delay prior to reclosing. A closing decision is usually issued after the fault occurred considering a certain fixed time delay, which is deliberately set to allow a transient fault to fully extinguish so that reclosing will be safe. For a temporary fault, subsequent re-energizing of the line will usually be successful. However, if it is a permanent or a semi-permanent fault, excessive breaking duty is undesirably applied to the breaker unit resulting in potential damage to the system, in general. Besides, the faults on transmission lines, particularly temporary faults, are extremely random in nature whose arcing duration lasting from a few milliseconds to several seconds or minutes. Thus, the estimated time delay is not sometimes long enough to allow a transient fault or semi-permanent fault to vanish before reclosing which leads to a fault arc re-strike followed by other severe consequences. Or, the fixed time delay is excessively long where unnecessary delay is introduced after arc ionization. This results in a further short duration fault (like lightning storms) that occurs during the time delay be judged to be a repeat of the original temporary fault, and a further reclose is locked out. In this situation, it is very inefficient to have a fixed time delay before reclosing is taken place. In any case, reclosing before a fault is totally cleared potentially brings about possible damage of system equipments. Therefore, discrimination of temporary fault from the permanent fault, and accurate determination of fault extinction time is highly demanded before any reclosing action is taken. This thesis outlines a method to resolve this problem based on artificial intelligence for the fault identification. The details of the proposed method will be discussed in Chapter 2.

1.4. MOTIVATION

Nowadays, the demand for a power quality increase forces utilities to meet an acceptable level of the fundamental parameters of electrical energy. A continuous power supply is most important to consumers of electricity. Thus, an auto-reclosure (AR) technique has become an acceptable means for restoring transmission lines after fault clearance and improving stability of particularly EHV transmission systems. In

other words, automatic reclosing of the tripped line offers a substantial improvement on the reliability, stability and security of the overall power system. These improvements are based on the assumption that majority of faults on a transmission line are transient in nature (i.e. once the fault arc has been extinguished by isolating the line under fault, it does not restrike). However, acute system stability conditions result in a necessity of improving AR schemes used so far. The risk of unsuccessful reclosing emanates if the line under fault is exposed to an elongated arc or permanent fault; hence, the reliability, stability and security of the power system grid are put in danger. Hitherto, utilized AR methods often lead to a multiple restrike of the fault path in the case of a permanent fault occurred. Moreover, the isolated transmission line is reclosed after a fixed time referred to as a dead time, which is of the order of about 0.5 s. A strategy of increasing the dead time guarantees (non-optimal) safety margin preventing a restrike of the fault, yet then the power system stability can be endangered.

One of the challenges in auto-reclosure applications is to prevent the breaker on a transmission line from reclosing before the fault extinguishes or during a permanent fault case. Basically, conventional reclosures operate for permanent and transient faults without any discrimination i.e. whenever there is a fault on a certain part of a power system transmission line, the common practice is to automatically reclose circuit breakers after some estimated delay into the faulted system regardless of the fault nature (permanent or transient). This is due to the fact that existing AR schemes practice employing fixed dead time (the time delay required prior to reclosing). Thus, closing decision is issued following circuit breaker opening [Kothari and Nagrath (2004)]. For a temporary fault whose extinction time is less than the fixed time delay used by the AR system, subsequent re-energizing of the line will usually be successful. However, if it is a permanent fault or an extended arcing fault, excessive breaking duty is undesirably applied to the breaker unit resulting in not only an unsuccessful reclosure but also possible shock and damage to the system in general.

Reclosing applications under permanent fault and/or without arc extinction provides added power system damage and compromises system stability and can jeopardize power system operation if the fault condition has not disappeared before the reclosing attempt; that is, the breaker closes under fault condition, making the power system

prone to instability and damage. In the case of permanent fault, reclosing could lead to even worse damage of power system equipments. It is obvious this adversely affects the power system stability and eventually results in loss of synchronism, particularly in EHV systems.

Ideally, it is required the breaker to close if and only if there is no fault on the line. Accurate determination of the arc extinction time also prevents reclosing under fault conditions and optimizes the dead time (this is discussed in detail in Chapter 2). In any case, reclosing before a fault is totally cleared would potentially bring about irreparable damage to system equipments. Discrimination of temporary fault from the permanent one and accurate determination of fault extinction time is highly demanded before any action is executed. To mitigate these inconveniences, some features have to be introduced to auto-reclosure schemes.

Thus, it is of no question to develop a method to identify whether or not the fault is cleared prior to reclosing order to circuit breaker. The fault extinction time (also known as dead time) should as well be accurately determined in order to avoid reclosing into an uncleared temporary fault.

1.5. OBJECTIVE OF THE THESIS

The following are the major objectives of this study.

- To develop a knowledge-based and self-adaptive auto-reclosure scheme that is able to identify type of fault (temporary from permanent) in a transmission line, and inhibit reclosing of power system grid onto a line under fault. This is supported by an optimized neural network.
- To precisely determine the fault extinction time for a temporary fault so as to alleviate early reclosing while the fault is not completely extinguished.
- To employ Taguchi's methodology, a smart-way optimization technique, in optimizing values of key parameters associated with neural network training.

- To improve and enhance the stability and the protection of a power system so as to add significant value to the quality and reliability of the power system upon modifying the conventional auto-reclosure with the proposed auto-reclosure scheme.

1.6. SCOPE OF THE THESIS WORK

The schematic diagram of the proposed automatic reclosure is shown in Figure 1.4. The figure illustrates the series of tasks carried out to realize the proposed method of automatic reclosing. Data acquisition process from Capacitor Voltage Transformer (CVT) is followed by signal pre-processing (which includes FFT analysis and normalization). ANN processing and optimization tasks are executed in succession. The start and activation logics are included for the purpose of initiating and activating the outputs of the whole process, respectively.

The functional steps for identification of a permanent from a temporary fault or vice-versa, or detection of exact temporary fault extinction time are shown in Figure 1.5. This Figure summarizes the processes that are handled by the proposed AR scheme while it sorts out what type of fault occurred on the transmission line.

The scheme process, shown in Figure 1.5, is initiated whenever the start logic is activated i.e. when there is a fault on a transmission network. In this process, one sample i.e. one full cycle at the power frequency is passed to the feature extraction process, which measures the energy contained in the DC, fundamental and the first four harmonic components. These features are passed to the ANN input layer which scales the values to fall within a suitable range for the activation function used. The ANN calculates a scaled output value in a range of 0 to +1 or -1 to +1 that indicates the class in which the network considers the input to be. The window of data from which the features are calculated is then moved on by the next cycle. Included in the scheme is a timer (activation logic) which causes the relay to lock out if reclosure is not initiated within a prescribed time and send a reclose signal to circuit breaker if ever identified as safe.

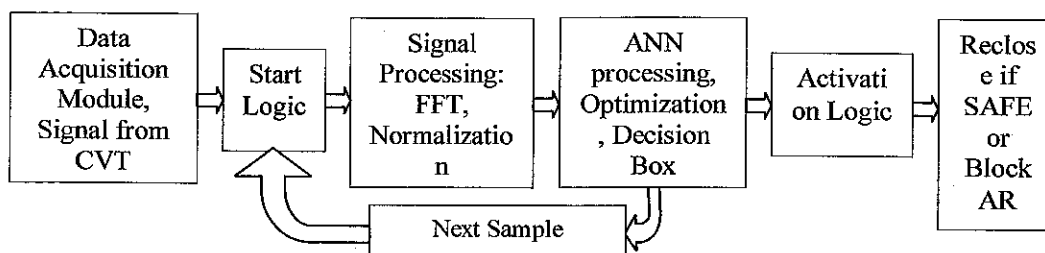


Figure 1.4: Schematic diagram of the proposed auto-reclosure activation

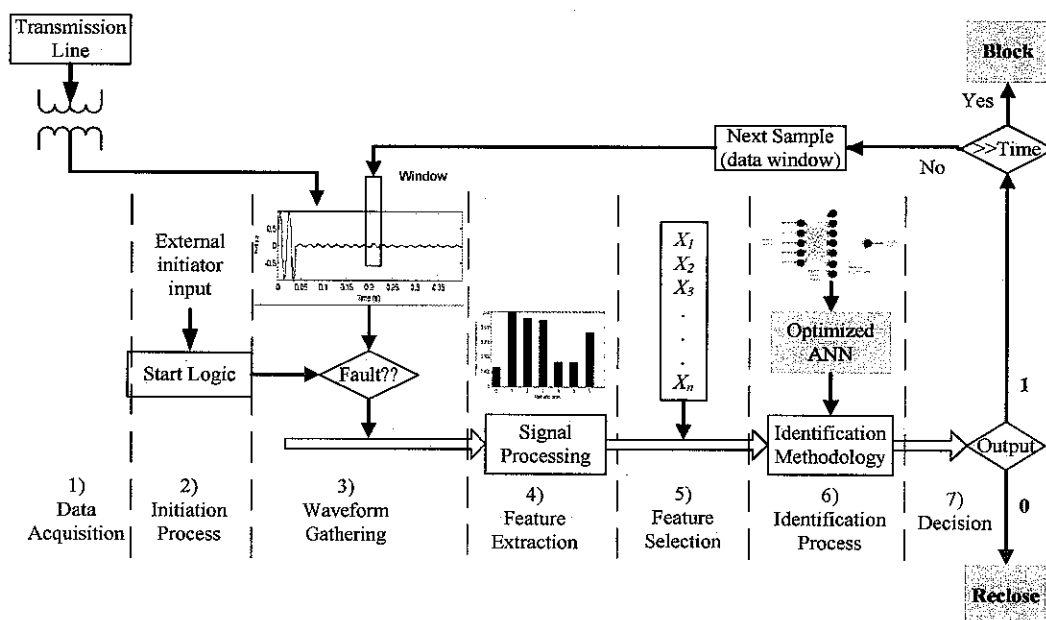


Figure 1.5: Functional steps for the fault identification process

Basically, the following work is carried out to meet the objectives of the thesis.

- Performing extensive literature review.
- Modeling a power system network using MATLAB software package in which a specified EHV transmission line with series and parallel compensators are connected in a bid to represent most modern transmission systems and distributed line model is employed to calculate transmission parameters.

- Simulating several faults (both permanent and transient) by varying different factors that have significant influence on the faults; typically, fault inception, fault resistance, fault duration and location
- Analyzing and processing the fault voltage signals using Fast Fourier Transform (FFT) to make them ready as inputs to the neural network
- Finding optimal neural network using Taguchi's methodology that is able to furnish the desired output with negligible error during identification of fault and decision-making
- Applying three different algorithms, namely, Error Back-Propagation (EBP), Levenberg Marquardt (LM) and Resilient Back-Propagation (RPROP), to spot out the best training algorithm for the proposed neural network.
- Finally, putting forward a real implementation of the proposed auto-reclosure for practical applications.

In a practical system, the output of the network would be compared with a threshold value over some period of time, i.e. some number of consecutive outputs of the network, and then a decision would be made whether to reclose, or lock out.

1.7. CONTRIBUTION OF THE THESIS

This thesis mainly focuses on developing an adaptive auto-reclosure which provides a prompt solution for improper reclosing action of a conventional auto-reclosure onto a faulted line in EHV systems. This is achieved by using an optimized ANN algorithm which effectively distinguishes a temporary fault from permanent, and takes appropriate decision, either to allow or block reclosing action.

Three different training algorithms, namely, Error Back-Propagation (EBP), Levenberg Marquardt (LM) and Resilient Back-Propagation (RPROP), have been

utilized as training means for the neural network. The parameters decisive in the application of ANN throughout the process are optimized using Taguchi's Methodology, a powerful and robust process optimization technique. The theoretical details of the neural network, algorithms and Taguchi's Methodology are discussed in the next Chapters.

In the case of temporary faults, a method using ANN is developed to accurately determine fault extinction time (dead time). This offers tremendous advantages such as increased rate of successful reclosure, improved system stability and a reduction in system-equipment damage under a permanent fault. The technique proposed in this report transforms the conventional auto-reclosure system which is based on 'restore service' into 'reclose only if safe'.

1.8. OUTLINE OF THE THESIS

This thesis is organized in five Chapters. The first Chapter provides a brief review of areas relevant to the thesis work and outlines the material presented in the thesis. The problems associated with conventional auto-reclosures are also introduced in this Chapter. The motivation, objectives of the thesis, and methodology used in the thesis are clearly presented in the first Chapter.

The second Chapter brings in previous research works that used different approaches to solve the problems associated with conventional auto-reclosure. The subjects of auto-reclosure and artificial intelligence are discussed in detail in this Chapter. Also, a brief description of the properties and behaviors of transmission line faults is reported.

The third Chapter introduces artificial intelligence specifically artificial neural networks (ANNs) and the algorithms used in this thesis to train the ANN, typically, the standard Error Back-Propagation (EBP) algorithm, the Levenberg Marquardt (LM) algorithm, and Resilient back-PROPagation (RPROP). This Chapter also elucidates the concepts associated with Taguchi's Methodology (TM) and its application as an optimization tool in the thesis.

The fourth Chapter presents a technique which is used to discern a temporary fault from a permanent fault based on optimized artificial neural network. Simulations, carried out in MATLAB –SimPowerSystems by varying different parameters like transmission line length, fault type, fault resistance and fault inception angle, so as to generate a set of fault data for training, testing, and validating the neural network are also presented in this Chapter.

Discussion, summary of the thesis and conclusions drawn from the whole work are presented in Chapter 5. Recommendations are also reported in this Chapter.

CHAPTER TWO

LITERATURE REVIEW AND THEORETICAL INTRODUCTION TO AUTORECLOSURE SYSTEM

2.1. INTRODUCTION

This Chapter presents theoretical reviews of automatic reclosing technique including its history, principles of operation, associated transmission line faults, modes of operation, operating features, its benefits and existing challenges. Previous works to improve the performance of conventional reclosing technique are discussed in detail. The Chapter concludes with explanations about the proposed reclosing scheme to mitigate the existing problems of automatic reclosing, and the methods developed in this thesis to improve the successful rate of automatic reclosing are introduced.

2.2. HISTORY OF AUTOMATIC RECLOSING

Automatic reclosing was first applied in the early 1900's [IEEE PSRC, 1984] on radial feeders protected by instantaneous relays and fuses. These schemes reclosed the power system circuit two or three times prior to lockout, with a 73 % to 88 % success rate on the first reclose actions, and covered both radial and looped circuits, predominantly at distribution voltages, but also including 154 kV.

It was reported in [Jackson, et al. 1979] that high-speed reclosing (HSR) was first used by American Electric Power System in 1935 as a means to defer construction of redundant transmission lines. System continuity was maintained on these radial lines by rapidly reclosing a single line rather than providing a second, redundant path for power to flow.

Modern systems, with single radial lines to transmit power from one point to another, are usual. It is also more common to have a network with parallel transmission lines.

HSR is used more for maintaining system stability and synchronism than for point-to-point continuity. The development of high-speed breakers for transmission lines by the late 1930's led to the application of high-speed reclosing (HSR) on these lines, resulting in improved system stability. Probability studies of the insulator flashover were initiated to determine minimum reclosing times that still permitted enough time for arc de-ionization. Early applications of HSR on multi-terminal lines tripped all terminals and then reclosed the circuit breaker at high-speed at one terminal. If this high-speed recloser was successful, the remaining terminals were reclosed with time delay to complete the circuit [IEEE PSRC, 1984].

The preceding historical information touches on a number of reasons for using auto-reclosing in transmission systems, particularly on EHV lines. The various advantages are discussed in Section 2.7. This does not, however, mean that auto-reclosing techniques implemented in modern transmission and sub transmission systems flawlessly work throughout the system. There have been some misdeeds of the conventional auto-reclosure technique observed in its application so far. Details of some of the disadvantages of conventional auto-reclosure are reported in Section 2.8.

2.3. EHV TRANSMISSION LINE FAULTS –AN OVERVIEW

In an electric power system comprising of different complex interacting elements, there always exists a possibility of disturbance and fault. Faults, typically on EHV transmission system, fall into one of the following two categories: temporary (also known as transient) and permanent.

A transient fault is a fault which is cleared by the immediate tripping of one or more circuit breakers to isolate the fault, and does not recur when the line is re-energized after certain delay time. Transient faults are commonly caused by lightning and temporary contact with foreign objects. The immediate tripping of one or more circuit breakers clears the fault. Subsequent re-energizing (reclosing) of the line is usually successful. Various studies have shown that anywhere from 70 % to 90 % of faults on most overhead lines are transients (temporary faults) [IEEE Power System Relaying

Committee, 2003]. Since electrical power systems contain passive elements in the form of inductances and capacitances of electrical components and inertia of rotating machines, any abrupt change in such systems will give rise to such type of faults. Depending upon the duration of the transients, they are generally classified into three groups.

Ultra-fast transients- These types of transients are caused either by lightning or by the abrupt but normal network changes resulting from regular switching operations. These transients are entirely electrical in nature and they generally last only for a few milliseconds. Such transients give rise to high voltages much higher than the nominal system voltages.

Medium-fast transients- These transients occur due to abrupt short-circuit in the system causing abnormal changes in the system. They are also entirely electrical in nature, and are responsible for excessive currents in the system. Short-circuit transients last in the system for a longer period, and are of greatest practical importance for nearly 10 cycles of the power frequency source voltage (i.e. for about 200 milliseconds in a 50 Hz system).

Slow transients- These are electromechanical in nature causing mechanical oscillations of rotors of synchronous machine. Such oscillations may cause instability of the interconnected power systems by putting some or all of the synchronous machines out of synchronism. These transients exist in the system for a much longer period ranging from a fraction of a second to a second or more.

On the other hand, permanent faults, which account for the remaining 10 % to 30 %, are those that do not vanish upon tripping and reclosing [IEEE Power System Relaying Committee, 2003]. These faults are classified as semi-permanent and permanent. A small tree branch falling on the line could cause a semi-permanent fault. The cause of the fault would not be removed by the immediate tripping of the circuit, but could be burnt away during a time-delayed trip. EHV overhead lines in forest areas are prone to this type of fault. Permanent faults, such as broken conductors, and faults on underground cable sections, must be located and repaired before the supply

can be restored. Equivalently saying, auto-reclose application to a line under fault would mean aggravating the fault condition; and hence, permanent faults should be cleared before any action of automatic recloser.

2.4. PRINCIPLES OF AUTOMATIC RECLOSING (AR)

2.4.1. Definitions of Terms Associated with AR

Before discussing the issues involved in the application of auto-reclosing schemes, it is useful to define some of the terms in common usage. The majority of these definitions are taken from reference [IEEE Std., 1992], IEEE Standard Definitions for Power Switchgear, IEEE Std.C37.100-1992. Several of the terms defined below are illustrated in Figures 2.1 and 2.2, which show the sequence of events in a typical auto-reclosing operation, where the circuit breaker makes one attempt at reclosure after tripping to clear a fault. Two conditions are shown in Figures 2.1 and 2.2: an unsuccessful reclosure followed by lockout of the circuit breaker if the fault is permanent, and a successful reclosure in the event of transient or temporary fault. The detailed description of the operation principles of auto-recloser for both types of faults is discussed in the next Sections.

Dead Time (of a circuit breaker) –The dead time of a circuit breaker on a reclosing operation is defined in IEEE Std. C37.100-1992 as the interval between interruption in all poles on the opening stroke and reestablishment of the circuit on the reclosing stroke. The dead time of an arcing fault on a reclosing operation is not necessarily the same as the dead time of the circuit breakers involved, since the dead time of the fault is the interval during which the line under fault is de-energized from all terminals. The choice of high-speed versus delayed auto-reclosing has a direct effect on the amount of dead time, as will be explained later in this Chapter.

Dead Time (of a reclosing relay) –The dead time of a reclosing relay is similar to the dead time of a circuit breaker. It is the amount of time between the auto-reclose

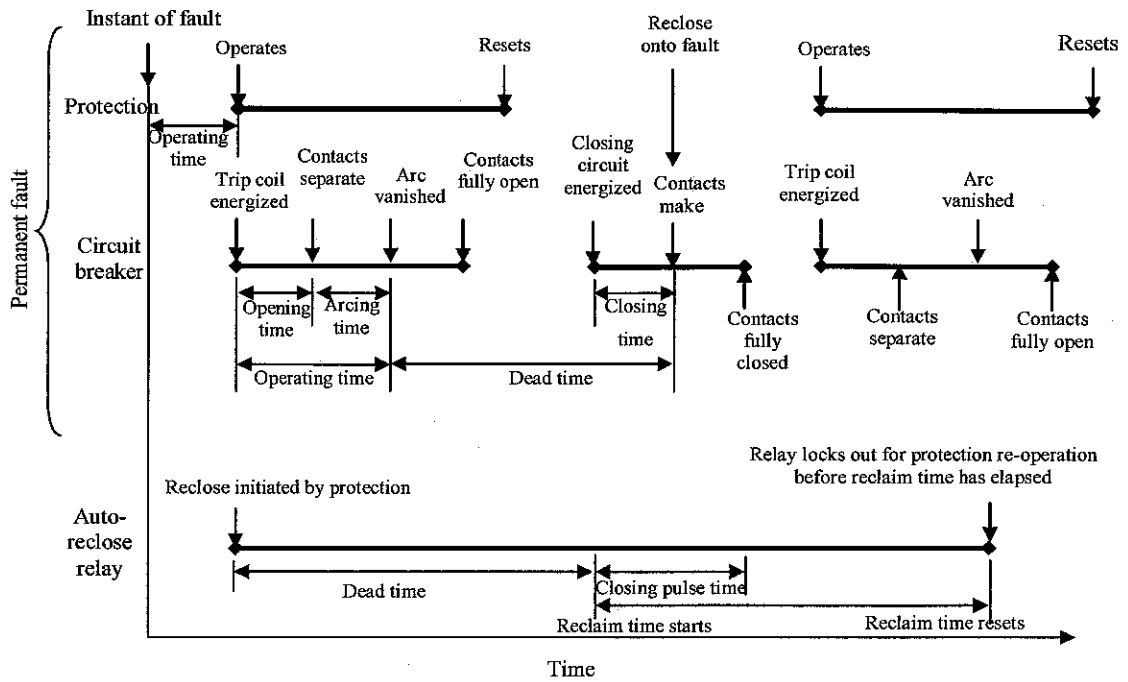


Figure 2.1: Operation of a single-shot auto-reclose scheme for a permanent fault
[GEC Alstom T&D, 1987]

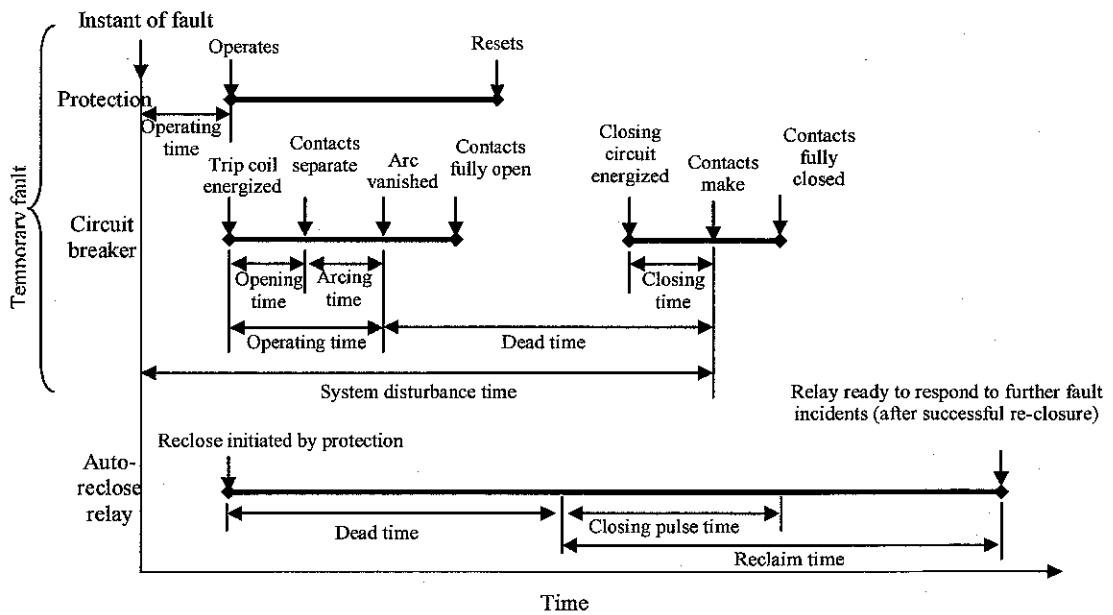


Figure 2.2: Operation of a single-shot auto-reclose scheme for a temporary fault
[GEC Alstom T&D, 1987]

scheme being initiated (e.g., by the operation of a protective element) and the operation of the 'reclose' contacts, which energize the circuit breaker closing coil.

Arcing time (of a mechanical switching device) – This is the interval of time between the instant of the first initiation of the arc and the instant of final arc extinction in all poles

Reset Time – Reset or reclaim time of an automatic circuit recloser is defined in IEEE Std. C37.100-1992 as the time required, after one or more counting operations, for the counting mechanism to return to the starting position. In an auto-reclosing relay, the reset time is the time following a successful closing operation, measured from the instant the auto-reclose relay closing contacts make, which must elapse before the auto-reclose relay initiates a new reclosing sequence in the event of a further fault incident.

Breaker reclosing time – This is the elapsed time between the energizing of the breaker trip coil and the closing of the breaker contacts to reestablish the circuit by the breaker primary contacts on the reclose stroke (i.e. breaker operating time plus breaker dead time).

Closing time (of a mechanical switching device) – This is the interval of time between the initiation of the closing operation and the instant when metallic continuity is established in all poles. Equivalently saying, this is the time interval between the energization of the closing mechanism and the making of the contacts. This time highly depends on the type of the circuit breaker. Figure 2.3 illustrates the performance of modern HV and EHV circuit breakers in this respect. Older circuit breakers may require longer times than those shown.

De-ionizing time – This represents the time following the extinction of an overhead line fault arc necessary to ensure dispersion of ionized air so that the arc does not re-strike when the line is re-energized.

Operating time (circuit breaker) – This refers to the time from the energizing of the trip coil until the fault arc is extinguished.

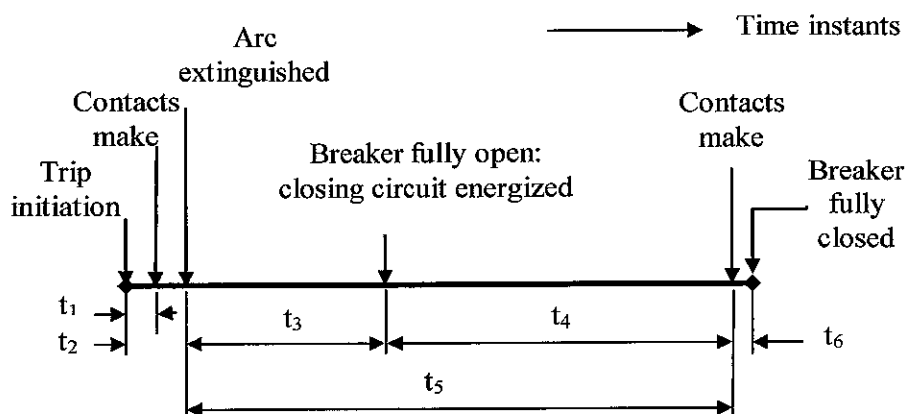


Figure 2.3: Typical circuit breaker trip-close operation time instants

Table 2.1: Typical circuit breaker trip-close operation times (in seconds)

	Oil 11 kV	Vacuum 15 kV	Oil 132 kV	Air 400 kV	SF6 132 kV	SF6 400 kV
t_1	0.06	0.038	0.03	0.035	0.04	0.02
t_2	0.1	0.053	0.06	0.045	0.07	0.05
t_3	0.08	0.023	0.2	0.0235	0.03	0.01
t_4	0.16	0.048	0.35	0.065	0.08	0.06
t_5	0.24	0.28	0.55	0.3	0.11	0.07
t_6	0.02	0.07	0.01	0.02	0.12	0.04

Operating time (protection) –This is the time from the inception of the fault to the closing of the tripping contacts. Where a separate auxiliary tripping relay is employed, its operating time is included.

Reset time (of an automatic circuit recloser) –This is the time required, after one or more counting operations, for the counting mechanism to return to the starting position.

System disturbance time –This corresponds to the time between the inception of the fault and the circuit breaker contacts making on successful reclosing.

Delayed auto-reclosing –This is auto-reclosing of a circuit breaker after a time delay that is intentionally longer than for high-speed auto-reclosing. The application of

delayed auto-reclosing particularly to EHV systems is discussed in detail in Section 2.5.

High-speed auto-reclosing – This is auto-reclosing of a circuit breaker after a necessary time delay (typically less than one second) to permit fault arc de-ionization with due regard to coordination with all relay protective systems. This type of auto-reclosing is generally not supervised by voltage magnitude or phase angle. The concept of high-speed auto-reclosing and application to EHV systems is explained in Section 2.3.

Single-shot reclosing – It is an operation sequence that provides only one reclosing operation followed by lockout of the circuit breaker occurring on subsequent tripping.

2.4.2. Automatic Reclosing Scheme on EHV Transmission Systems

It is well realized that transient faults which are most frequent in occurrence do not usually result in permanent damage to the system as they are transitory in nature. These faults disappear if the line is disconnected from the system momentarily in order to allow the arc to extinguish. After the arc path has become sufficiently de-ionized, the line is reclosed to restore normal service. Not always, reclosing could also be achieved with semi-permanent faults but with delayed action, e.g. a small tree branch falling on the line, in which case the cause of the fault would not be removed by the immediate tripping of the circuit breaker but could be burnt away during a time delayed trip, and thus the line is reclosed to restore service. Now, should the fault be permanent, reclosing is of no use, as the fault still remains on reclosing and the fault has to be cleared manually. However, if the fault does not disappear after the first trip and closure, double or triple-shot reclosing is used in many cases before pulling the line out of service.

Unlike the medium/high voltage transmission lines (where the main aim of auto-reclosure is to restore service), the most important consideration in the application of auto-reclosing to EHV transmission lines is the maintenance of system stability and synchronism. When a line is fed from both ends as in Figure 2.4, the generators at the two ends of the line drift apart in phase. In EHV circuits where the fault levels

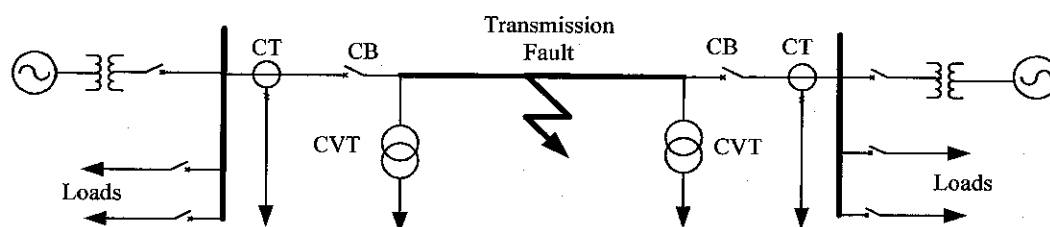
associated are extremely high, it is essential that the dead time be kept to a few cycles so that the generators do not drift apart. On occurrence of the fault, the breakers at the two ends must be reclosed simultaneously before the generators drift too far apart for synchronism to be maintained. Such a reclosure increases the stability limit considerably.

The stability and synchronism issues involved are, however, dependent on whether the transmission system is weak, for example, with two power systems connected by a single tie line, or, conversely, highly interconnected (strong), in which case maintaining synchronism during auto-reclosing is much easier. With a weak system, loss of a transmission link may lead quickly to an excessive phase angle across the circuit breaker (CB) used for re-closure, thus preventing a successful re-closure. In a relatively strong system, the rate of change of phase angle will be slow, so that delayed auto-reclose can be successfully applied.

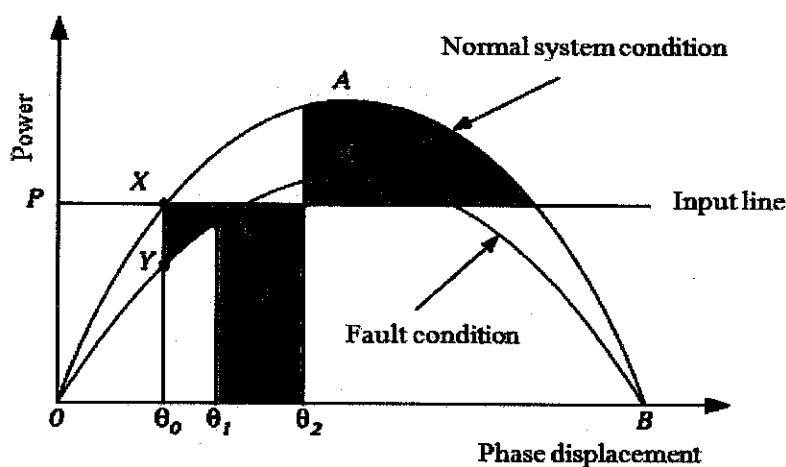
An illustration is the interconnector between two power systems, as shown in Figure 2.4a. The power-angle curves during normal and fault system condition are shown in Figure 2.4b [Kimbark and Wilson, 1998]. Under healthy conditions, the amount of synchronizing power transmitted P crosses the power vs. angle curve OAB at point X, showing that the phase displacement between the two systems is θ_0 . Under fault conditions, the curve OCB is applicable, and the operating point moves to Y. Assuming constant power input to both ends of the line, there is now an accelerating power XY. As a result, the operating point moves to Z, with an increased phase displacement, θ_1 , between the two systems. At this point, the circuit breakers trip and break the connection. The phase displacement continues to increase at a rate dependent on the inertia of the two power sources. To maintain synchronism, the circuit breaker must be reclosed before the phase angle exceeds θ_2 . This angle is such that the area (2) stays greater than the area (1), which is the condition for maintenance of synchronism [Anderson and Fouad, 1977].

The example, given in Figure 2.4 for a weak system, shows that the successful application of auto-reclosing in such a case needs high-speed protection with short dead time and high speed circuit breakers. On strong systems, synchronism is unlikely

to be lost by the tripping out of a single line. For such systems, an alternative policy of delayed auto-reclosing is adopted. This enables the power swings on the system resulting from the fault to decay before reclosure is attempted. The various factors to be considered when using EHV auto-reclose schemes are now dealt with. High-speed and delayed auto-reclose schemes are discussed separately in the following sub sections.



(a) Power system



(b) Power curve before and after fault demonstrating equal area criteria

Figure 2.4: Effect of high-speed three-phase auto-reclosing on system stability for a weak system (a) power system network (b) power curve

2.4.3. High Speed Auto-reclosing on EHV Transmission Systems

The first requirement of high-speed auto-reclosing application is knowledge of the system disturbance time that can be tolerated without loss of system stability. This

normally requires transient stability studies to be conducted for a defined set of power system configurations and fault conditions. High speed reclosure in extra high voltage circuits improves the stability to a considerable extent on single-circuit ties. However, the successful application of high speed auto-reclose to high voltage systems interlinking a number of sources depends on the following factors:

- The maximum time available for opening and closing the circuit breakers at each end of the faulty line, without loss of synchronism.
- The time required to de-ionize the arc at the fault, so that it does not restrike when the breakers are reclosed.
- The speed of operation on opening and closing of the circuit breakers.
- The probability of transient faults, that allows high speed reclosure of the faulty lines.

Some of these conditions are conflicting, e.g. the faster the breakers are reclosed the greater the power that can be transmitted without loss of synchronism, provided that the arc does not restrike. But here, the probability of arc restriking is greater. An unsuccessful reclosure is more detrimental to stability than no reclosure at all specially in EHV systems. For this reason, the time allowed to de-ionize the line must not be less than the critical time for which the arc hardly ever restrikes. The reduction of reclosing time obtained by high speed relaying is, however, preferred as it reduces the duration of arc. Indeed, the increase in power limit due to reclosing is much greater with very rapid fault clearing than with slower fault clearing. For best results, the circuit breakers at both ends of the faulty line must be opened simultaneously. Any time during which one circuit breaker is open in advance of the other represents an effective reduction of the breaker electrical dead time and may well jeopardize the chances of a successful reclosure.

To determine the electrical dead time for circuit breaker used in a high speed auto-reclose scheme, it is essential to know the time interval during which the line must be kept de-energized in order to allow for the complete de-ionization of the arc and ensure that it will not restrike when the line is reconnected to the system. The deionization time of an arc is discussed in the following Sections.

With knowledge of protection and circuit breaker operating characteristics and fault arc de-ionization times, the feasibility of high-speed auto-reclosing can then be assessed. These factors are discussed in the following subsections.

2.4.3.1. Protection Characteristics

The use of high-speed protection equipment, such as distance or unit protection schemes, giving operating times of less than 50 ms, is essential. In conjunction with fast operating circuit breakers, high-speed protection reduces the duration of the fault arc and; thus, the total system disturbance time. It is important that the circuit breakers at both ends of a fault line be tripped as rapidly as possible. The time that the line is still being fed from one end represents an effective reduction in the dead time, and may well jeopardize the chances of a successful reclosure. When distance protection is used, and the fault occurs near one end of the line, special measures have to be adopted to ensure simultaneous tripping at each end.

2.4.3.2. Fault Arc De-ionization

It is important to know the time that should be allowed for complete de-ionization of the arc, to prevent arc re-striking when the voltage is re-applied. The de-ionization time of an uncontrolled arc, in free air depends on the circuit voltage, conductor spacing, fault currents, fault duration, wind speed and capacitive coupling from adjacent conductors. Of these, the circuit voltage is the most important, and as a general rule, the higher the voltage, the longer the time required for deionization. Typical values of de-ionization time for an arc in free air are shown in Table 2.2 [ABB, 1994 and Basler Electric, 1998].

If single-phase tripping and auto-reclosing is used, capacitive coupling between the healthy phases and the faulty phase tends to maintain the arc and hence extend the dead time required. This is a particular problem on long distance EHV transmission lines. Accurate determination of the fault de-ionization time is required to alleviate the problems that arise due to reclosing onto a line under fault.

Table 2.2: Fault arc de-ionization times

Line Voltage (kV)	Minimum de-ionization time (seconds)
66	0.2
110	0.28
132	0.3
220	0.35
275	0.38
400	0.45
525	0.55

2.4.3.3. Characteristics of Circuit Breaker

The high fault levels involved in EHV systems imposes a very severe duty on the circuit breakers used in high-speed auto-reclose schemes. The accepted breaker cycle of break-make-break requires the circuit breaker (CB) to interrupt the fault current, reclose the circuit after a time delay of greater than 0.2 s and then break the fault current again if the fault persists. But this practice usually endangers the expensive equipments in the power system grid.

The types of circuit breaker commonly used on EHV systems are oil, air blast and SF6 types. Oil circuit breakers are used for transmission voltages up to 300 kV, and can be subdivided into two types: 'bulk oil' and 'small oil volume'. The latter is a design aimed at reducing the fire hazard associated with the large volume of oil contained in the bulk oil breaker. The operating mechanisms of oil circuit breakers are of two types, 'fixed trip' and 'trip free', of which the latter is the most common. With trip-free types, the reclosing cycle must allow time for the mechanism to reset after tripping before applying the closing impulse. Special means have to be adopted to obtain the short dead times required for high-speed auto-reclosing. Various types of tripping mechanism have been developed to meet this requirement. The three types of closing mechanism fitted to oil circuit breakers are solenoid, spring and pneumatic.

Circuit breakers with solenoid closing are not suitable for high-speed auto-reclose due to the long time constant involved. Spring, hydraulic or pneumatic closing mechanisms are universal at the upper end of the EHV range and give the fastest

closing time. Figure 2.3 and Table 2.1 show the operation times for various types of EHV circuit breakers, including the dead time that can be attained.

Air blast breakers have been developed for voltages up to the highest at present in use on transmission lines. They fall into two categories: pressurized head circuit breakers and non-pressurized head circuit breakers

In pressurized head circuit breakers, compressed air is maintained in the chamber surrounding the main contacts. When a tripping signal is received, an auxiliary air system separates the main contacts and allows compressed air to blast through the gap to the atmosphere, extinguishing the arc. With the contacts fully open, compressed air is maintained in the chamber. Loss of air pressure could result in the contacts reclosing, or, if a mechanical latch is employed, restriking of the arc in the de-pressurized chamber. For this reason, sequential series isolators, which isolate the main contacts after tripping, are commonly used with air blast breakers. Since these are comparatively slow in opening, their operation must be inhibited when auto-reclosing is required. A contact on the auto-reclose relay is made available for this purpose. Non-pressurized head circuit breakers are slower in operation than the pressurized head type and are not usually applied in high-speed reclosing schemes.

Most EHV circuit breaker designs now manufactured use SF₆ gas as an insulating and arc-quenching medium. The basic design of such circuit breakers is in many ways similar to that of pressurized head air blast circuit breakers, and normally retains all, or almost all, of their voltage withstand capability, even if the SF₆ pressure level falls to atmospheric pressure. Sequential series isolators are therefore not normally used, but they are sometimes specified to prevent damage to the circuit breaker in the event of a lightning strike on an open ended conductor. Provision should therefore be made to inhibit sequential series isolation during an auto-reclose cycle.

2.4.3.4. Choice of Dead Time

At voltages of 220 kV and above, the de-ionization time will probably dictate the minimum dead time, rather than any circuit breaker limitations. This can be deduced from Table 2.2. The dead time setting on a high-speed auto-reclose relay should be

long enough to ensure complete de-ionization of the arc or there should be a means to accurately determine the dead time so that improper reclosing is avoided. On EHV systems, an unsuccessful reclosure is more detrimental to the system than no reclosure at all. So, the choice of dead time is pivotal to avoid the detrimental effect on the system due to automatic reclosing before a fault extinguishes. A method developed to accurately determine the de-ionization time is discussed Section 2.11.

2.4.3.5. Choice of Reclaim Time of a Circuit Breaker

Where EHV oil circuit breakers are concerned, the reclaim time should take account of the time needed for the closing mechanism to reset ready for the next reclosing operation. Reclosing before the closing mechanism resets categorically results in not only unsuccessful reclosure but also damage to the system, in general.

2.4.3.6. Number of Shots

High-speed auto-reclosing on EHV systems is customarily single shot followed by the locked out of circuit breakers after one unsuccessful attempt. However, multiple shots are still implemented in many EHV systems. There is no doubt about it; repeated reclosure attempts with high fault levels would have serious consequences on system stability.

2.5. SINGLE-PHASE AUTO-RECLOSING IN EHV TRANSMISSION SYSTEMS

Single phase to earth faults account for the majority of overhead line faults. When three-phase auto-reclosing is applied to single circuit interconnectors between two power systems, the tripping of all three phases may cause the two systems to drift apart in phase, as described in Section 2.3.2. No interchange of synchronizing power can take place during the dead time. If only the faulty phase is tripped, synchronizing power can still be interchanged through the healthy phases. Any difference in phase between the two systems will be correspondingly less, leading to a reduction in the disturbance on the system when the circuit breaker recloses.

For single-phase auto-reclosing, each circuit breaker pole must be provided with its own closing and tripping mechanism; this is normal with EHV air blast and SF6 breakers [IEEE Power System Relaying Committee, 2003]. The associated tripping and reclosing circuitry is therefore more complicated, and, except in distance schemes, the protection needs the addition of phase selection logic. On the occurrence of a phase-earth fault, single-phase auto-reclose schemes trip and reclose only the corresponding pole of the circuit breaker. The auto-reclose function in a relay therefore has three separate elements, one for each phase. Operation of any element energizes the corresponding dead timer, which in turn initiates a closing pulse for the appropriate pole of the circuit breaker. A successful reclosure results in the auto-reclose logic resetting at the end of the reclaim time, ready to respond to a further fault incident. If the fault is persistent and reclosure is unsuccessful, it is usual to trip and lock out all three poles of the circuit breaker. The above describes only one of many variants. Other possibilities are:

- three-phase trip and lockout for phase-phase or 3-phase faults, or if either of the remaining phases should develop a fault during the dead time
- use of a selector switch to give a choice of single or three-phase reclosing
- combined single and three-phase auto-reclosing; single phase to earth faults initiate single-phase tripping and reclosure, and phase-phase faults initiate three-phase tripping and reclosure

Modern numerical relays often incorporate the logic for all of the above schemes, for the user to select as required. The advantages of single-phase auto-reclosing are:

- The maintenance of system reliability.
- On multiple earth systems, negligible interference with the transmission of load. This is because the current in the faulted phase can flow through earth via the various earthing points until the fault is cleared and the faulty phase restored

The main disadvantage is the longer de-ionization time resulting from capacitive coupling between the faulty and healthy lines. This leads to a longer dead time being

required. Mal-functioning of earth fault relays on double circuit lines owing to the flow of zero sequence currents also occurs. These are induced by mutual induction between faulty and healthy lines.

2.6. DELAYED AUTORECLOSING ON EHV TRANSMISSION SYSTEMS

On highly interconnected transmission systems, where the loss of a single line is unlikely to cause two sections of the system to drift apart significantly and lose synchronism, delayed auto-reclosing can be employed. Dead times of the order of 5 s - 60 s are commonly used [IEEE Power System Relaying Committee, 2003]. No problems are presented by fault arc de-ionization times and circuit breaker operating characteristics, and power swings on the system decay before reclosing. In addition, all tripping and reclosing schemes can be three-phase only, simplifying control circuits in comparison with single phase schemes. In systems on which delayed auto-reclosing is permissible, the chances of a reclosure being successful are somewhat greater with delayed reclosing than would be the case with high-speed reclosing. Delayed reclosing cannot, however, be applied to weak systems as this will put system stability in immense danger.

2.6.1. Operation Scheme of Delayed Auto-reclosing

Figure 2.5 shows a transmission line connecting two substations A and B, with the circuit breakers at A and B tripping out in the event of a line fault. Synchronism is unlikely to be lost in a system that employs delayed auto-reclose. However, the transfer of power through the remaining tie-lines on the system could result in the development of an excessive phase difference between the voltages at points A and B. The result, if reclosure takes place, is an unacceptable shock to the system. It is therefore usual practice to incorporate a synchronism check relay into the reclosing system to determine whether auto-reclosing should take place.



Figure 2.5: Network diagram

After tripping on a fault, it is normal procedure to reclose the breaker at one end first, a process known as ‘live bus/dead line charging’. Reclosing at the other end is then under the control of a synchronism check relay element for what is known as ‘live bus/live line reclosing’. For example, if it is decided to charge the line initially from station A, the dead time in the auto-reclose relay at A will be set at, say, 5 seconds, while the corresponding timer in the auto-reclose relay at B will be set at, say, 15 seconds. The circuit breaker at A will then reclose after 5 seconds provided that voltage monitoring relays at A indicates that the bus-bars are alive and the line is dead. With the line recharged, the circuit breaker at B will then reclose with a synchronism check, after a 2 second delay imposed by the synchronism check relay element. If for any reason the line fails to ‘dead line charge’ from end A, reclosure from end B will take place after 15 seconds. The circuit breaker at A will then be given the opportunity to reclose with a synchronism check.

2.6.2. Synchronism Check Relays

In some cases, synchronism-check logic is incorporated with an auto-reclose relay as means to prevent auto-reclosing when the phase angle difference has moved outside specified limits. The synchronism check relay element commonly provides a three-fold check: phase angle difference, voltage and frequency difference. The phase angle setting is usually set to between $20^\circ - 45^\circ$, and reclosure is inhibited if the phase difference exceeds this value. The scheme waits for a reclosing opportunity with the phase angle within the set value, but locks out if reclosure does not occur within a defined period, typically 5 s.

A voltage check is incorporated to prevent reclosure under various circumstances. A number of different modes may be available. These are typically under voltage on either of the two measured voltages, differential voltage, or both of these conditions.

The logic also incorporates a frequency difference check, either by direct measurement or by using a timer in conjunction with the phase angle check. In the latter case, if a 2 second timer is employed, the logic gives an output only if the phase difference does not exceed the phase angle setting over a period of 2 seconds. This limits the frequency difference (in the case of a phase angle setting of 20°) to a maximum of 0.11 % of 50 Hz, corresponding to a phase swing from $+20^\circ$ to -20° over the measured 2 seconds. While a significant frequency difference is unlikely to arise during a delayed auto-reclosing sequence, the time available allows this check to be carried out as an additional safeguard.

2.7. OPERATING FEATURES OF AR SCHEMES IN EHV SYSTEMS

The extensive use of auto-reclosing has resulted in the existence of a wide variety of different control schemes. Some of the most important variations in the operating features of AR schemes in EHV systems are explained in the following subtopics.

2.7.1. Initiation of Auto-reclosing

Modern auto-reclosing schemes are invariably initiated by the tripping command of a protection relay function. Some older schemes may employ a contact on the circuit breaker. Modern digital or numerical relays often incorporate a comprehensive auto-reclose facility within the relay, thus eliminating the need for a separate auto-reclose relay and any starter relays.

2.7.2. Type of Protection

In most cases, the auto-reclose relay provides a means of isolating the instantaneous relay after the first trip. In older schemes, this may be done with a normally closed contact on the auto-reclose starting element wired into the connection between the instantaneous relay contact and the circuit breaker trip coil. With digital or numerical relays with in-built auto-reclose facilities, internal logic facilities are normally used.

With certain supply authorities, it is the rule to fit tripping relays to every circuit breaker. If auto-reclosing is required, electrically reset tripping relays must be used, and a contact must be provided either in the auto-reclose logic or by separate trip relay resetting scheme to energize the reset coil before reclosing can take place.

2.7.3. Dead Timer

This will have a range of settings to cover the specified high-speed or delayed reclosing duty. Any interlocks that are needed to hold up reclosing until conditions are suitable are mostly connected into the dead timer circuit.

2.7.4. Reclosing Impulse

The duration of the reclosing impulse must be related to the requirements of the circuit breaker closing mechanism. On auto-reclose schemes using spring-closed breakers, it is sufficient to operate a contact at the end of the dead time to energize the latch release coil on the spring-closing mechanism. A circuit breaker auxiliary switch can be used to cancel the closing pulse and reset the auto-reclose relay. With solenoid operated breakers, it is usual to provide a closing pulse of the order of 1-2 seconds, so as to hold the solenoid energized for a short time after the main contacts have closed. This ensures that the mechanism settles in the fully latched-in position. The pneumatic or hydraulic closing mechanisms fitted to oil, air blast and SF₆ circuit breakers use a circuit breaker auxiliary switch for terminating the closing pulse applied by the auto-reclose relay.

2.7.5. Anti-Pumping Devices

The function of an anti-pumping device is to prevent the circuit breaker closing and opening several times in quick succession. This might be caused by the application of a closing pulse while the circuit breaker is being tripped via the protection relays. Alternatively, it may occur if the circuit breaker is closed on to a fault, and the closing pulse is longer than the sum of protection relay and circuit breaker operating times. Circuit breakers with trip free mechanisms do not require this feature.

2.7.6. Reclaim Timer

Electromechanical, static or software-based timers are used to provide the reclaim time, depending on the relay technology used. If electromechanical timers are used, it is convenient to employ two independently adjustable timed contacts to obtain both the dead time and the reclaim time on one timer. With static and software-based timers, separate timer elements are generally provided.

2.7.7. Circuit Breaker Lockout

If reclosure is unsuccessful the auto-reclose relay locks out the circuit breaker. Some schemes provide a lockout relay with a flag, with provision of a contact for remote alarm. The circuit breaker can then only be closed by hand; this action can be arranged to reset the auto-reclose relay element automatically. Alternatively, most modern relays can be configured such that a lockout condition can be reset only by operator action. Circuit breaker manufacturers state the maximum number of operations allowed before maintenance is required. A number of schemes provide a fault trip counting function and give a warning when the total approaches the manufacturer's recommendation. These schemes will lock out when the total number of fault trips has reached the maximum value allowed.

2.7.8. Manual Closing of a Circuit Breaker

It is undesirable to permit auto-reclosing if circuit breaker closing is manually initiated. Auto-reclose schemes include the facility to inhibit auto-reclose initiation for a set time following manual CB closure. The time is typically in the range of 2-5 seconds.

2.7.9. Multi-Shot Schemes in EHV Systems

Schemes providing up to three or four shots, timing circuits are often included in an auto-reclose relay to provide different, independently adjustable, dead times for each shot. Instantaneous protection can be used for the first trip, since each scheme provides a signal to inhibit instantaneous tripping after a set number of trips. The

scheme resets if reclosure is successful within the chosen number of shots, ready to respond to further fault incidents.

2.8. BENEFITS OF AUTOMATIC RECLOSING

As stated in the previous Chapter, the intent of auto-reclosing on transmission systems, other than the maintenance of stability, is to return the system to its normal configuration with minimum outage of the line and with the least expenditure of manpower. System restoration becomes increasingly important when applied to lines that interconnect systems, and are critical for reliable power exchange between the systems. Individual utility policy and system requirements dictate the complexity and variety of automatic reclosing schemes in service today.

Instantaneous tripping on EHV systems reduces the duration of the power arc resulting from an overhead line fault to a minimum. The chance of permanent damage occurring to the line and terminal equipments is reduced. However, the application of instantaneous protection may result in non-selective tripping of a number of circuit breakers and an ensuing loss of supply to a number of healthy sections. Auto-reclosing allows these circuit breakers to be reclosed within a few seconds. With transient faults, the overall effect would be loss of supply for a very short time but affecting a larger number of consumers. If only time-graded protection without auto-reclose was used, a smaller number of consumers might be affected, but for a longer time period.

The main use of an auto-reclose scheme is to re-energize a line after a fault trip which permits successful re-energization of the line. Sufficient time must, however, be allowed after tripping for the fault arc to de-energize prior to reclosing; otherwise, the arc will re-strike. Such schemes have been the cause of a substantial improvement in continuity of supply. A further benefit, particularly to EHV systems, is the maintenance of system stability and synchronism. A typical single-shot auto-reclose scheme is shown in Figures 2.1 and 2.2. Figure 2.1 shows a successful reclosure in the

event of a transient fault, and Figure 2.2 an unsuccessful reclosure followed by lockout of the circuit breaker if the fault is permanent.

The preceding historical information touches on a number of reasons for using auto-reclosing on transmission systems [IEEE Power System Relaying Committee, 2003].

Following is a summary of reasons for using auto-reclosing:

- Minimizing the interruption of the supply to customer; hence, improvement of supply continuity
- Maintenance of system stability and synchronism (due to high-speed tripping and auto-reclosing on overhead transmission lines)
- Restoration of system capacity and reliability with minimum outage and least expenditure of manpower (reduction of substation visits)
- Restoration of critical system interconnections
- Restoration of service to critical loads
- Higher probability of some recovery from multiple unforeseen outages
- Reduction of fault duration, resulting in less fault damage and fewer permanent faults
- Ability to run substations unattended, minimizing substation visits resulting in saved wages
- Relief for system operators in restoration during system outages

2.9. CHALLENGES IN CONVENTIONAL AUTORECLOSURE

Basically, the application of auto-reclosing requires the evaluation of many factors. These factors vary considerably depending upon the system configuration, the system components, and the reclosing philosophy utilized by the protection engineer or company. The following factors are of fundamental concerns:

- The benefits and possible problems associated with reclosing
- The choice of dead time

- The choice of reset time
- The decision to use single- or multiple-shot reclosing

Some of the benefits associated with auto-reclosing are noted in Section 2.7. These benefits must be incorporated with any potential problems that may arise when applying auto-reclosing.

With a conventional circuit breaker, a transient fault would open the breaker, disabling the line until a technician could manually close the circuit breaker. But an auto-reclosure makes several pre-programmed attempts to re-energize the line. If the transient fault has cleared, the auto-reclosed circuit breaker remains closed and normal operation of the power line resumes. If the fault is some sort of a permanent fault (downed wires, tree branches lying on the wires, etc.), the auto-reclosure will exhaust its pre-programmed attempts to re-energize the line and remain tripped off until manually commanded to try again. One of the challenges in auto-reclosure applications is to prevent the breaker on a transmission line from reclosing before the fault extinguishes or during a permanent fault case. Reclosing under fault provides added power system damage and compromises system stability. Hence, there has to be a means to identify the type of a fault on the transmission and accurately determine the fault extinction time to avoid improper reclosing. The previously reported means to tackle this problem are discussed in the following section (Section 2.9).

In power industry, although auto-reclosing success rates vary from one system to another, the majority of faults on a transmission line can be successfully cleared by the proper use of tripping. This de-energizes the line long enough for the fault source to pass and the fault arc to de-energize, then automatically recloses the line to restore service. Thus, auto-reclosing can significantly reduce the outage time due to faults and provide a higher level of service continuity to the customer.

Various studies have shown that 70 % to 90 % of faults on most overhead lines are transients in which automatic reclosing following the protection process is usually successful. Whereas, the remaining 10 % to 30 % of faults are of semi-permanent or

permanent in nature. In this case, an immediate de-energizing of the line and subsequent auto-reclosing does not clear the fault.

2.10. PREVIOUS WORKS ON INHIBITING RECLOSE ACTION ON TO FAULTS

2.10.1. Modification on the Dead Time

There are several approaches set forth to prevent the damaging conditions which arise from reclosing while a fault on a transmission line is not cleared fully. One of the most common approaches is to add shunt and neutral reactors [Ban G., 1999] and [Kimbark, 1964] to suppress the secondary arc present during the pole-open condition and have a dead time (open phase interval) long enough to allow for arc suppression and air de-ionization. Another approach is to increase the dead time and expect the secondary arc to be self-extinguished. Unfortunately, extending the fault clearing time can lead to instability in the system. None of these approaches verify cessation of the arc before the breaker pole recloses. Moreover, these two approaches cannot guarantee an unprecedented complete protection during high impedance fault or permanent faults, in general.

2.10.2. Sensing High-Resistance Earth Faults to Block Auto-Reclosing

Most of the time, normal protection relays face difficulty to pick up when high-impedance faults occur on a transmission line. This situation has become increasingly problematic in the era of power transmission line protection. Recently, it is a common practice to fit sensitive earth-fault protection to supplement the normal protection in order to detect high resistance earth faults. This protection cannot possibly be stable on through faults, and is therefore, set to have an operating time longer than that of the main protection. This longer time may have to be taken into consideration when deciding on a reclaim time. A broken overhead conductor in contact with dry ground or a wood fence may cause this type of fault. It is therefore common practice to use a contact on the sensitive earth fault relay to block auto-reclosing, and lock out the

circuit breaker [Aucoin and Jones, 1996]. This approach appreciably solved the handicap nature of protection relays for high-impedance earth faults. However, the extended delay of the operating time may be unsafe and may aggravate the situation in some circumstances, particularly when dealing with EHV systems. Moreover, due to the random nature of faults on transmissions, it is hard to say to what extent the method would be effective and robust.

2.10.3. Development of Adaptive Autoreclosure

Recent studies reported development of adaptive auto-reclosure system, an approach to curb the previously stated setbacks of conventional auto-reclosure, using diverse methodologies. The methodologies used in this regard, in general, fall in to either of the two approaches: pure mathematical based and artificial intelligence based. Both approaches are separately discussed in the following subsections.

2.10.4. Adaptive Autoreclosure Based on Mathematical Algorithms

Different mathematical manipulations, models and/or algorithms have been suggested to develop an adaptive auto-reclosure system. A single-phase auto-reclosure was proposed based on investigating the differential approach of zero sequence power during the secondary period of arcing faults [N.I. Elkalashy, et al. 2007]. However, this scheme requires communication channels at both the line terminals. Moreover, the work did not prove that the method developed works for the vast types of faults on a transmission line.

It has been reported in [M.E. Golshan, et al. 2005] that an adaptive auto-reclosure based on tracking harmonic distortion index (HDI) from the behavior of the low frequency components of the faulted phase voltage or sound current signals as a means to avoid the improper reclosing of conventional auto-reclosure and boost successful reclosing. And, a decision-making index is defined based on properties of the tracked HDI.

Another approach [K.J. Zoric, et al. 1997] developed an adaptive auto-reclosure based on estimating arc voltage minimal-maximal amplitude, and compared it with a pre-

defined threshold value for distinguishing a temporary from a permanent fault. However, determining the threshold value is a problem because it depends on fault conditions and transmission line characteristics.

Other algorithms are based on magnitude of the induced voltage on the faulted phase owing to capacitive and electromagnetic coupling of the faulted phase and sound phases. In [Yaozhong, et al. 1989], the induced voltage magnitude has been used to identify transient and permanent faults.

Detecting amplitude of a resonant component has been reported a useful ingredient in the identification of transient and permanent faults [Zengping, et al. 2006]. According to this report, in the case of a permanent fault, after the secondary arc extinguishes, the voltage at the end of the opened phase is a power frequency voltage. However, in case of a temporary fault, the voltage consists of not only a power frequency component but also a resonant component. This method may, however, be flawed for high impedance permanent faults that closely resemble to the temporary faults.

In [Sang-Pil Ahn, et al. 2001], a tracked RMS value of a faulted phase voltage waveform has been used to determine the final arc extinction time. Accordingly, when the difference value between the present and previous RMS values at each time step is greater than a prescribed threshold, successful reclosing can be made. If difference values do not exceed the threshold after a sufficient time delay, the fault is permanent and reclosing will not be permitted.

[P.K. Aggarwal et al. 1993] also demonstrated an adaptive auto-reclosure technique based on defining and identifying the waveform patterns of the voltage transients following initial breaker opening. The decision making of this method is based on comparing a streaming voltage sample values to a pre-determined threshold voltage. If the voltage compared with the threshold is less than the threshold, the fault is considered to be transient, and reclosing can be triggered. This may give sense to some extent. Due to the tremendous causes of faults on a transmission line, there is no guarantee that the method would apply to all types of faults.

A study on an adaptive single phase reclosing scheme on EHV/UHV transmission lines based on calculation of Bergeron model by utilizing harmonics energy ratio to identify arc extinguishment [Li Bin, et al. 2008], by considering a secondary arc model rooted in gray-box model [Alessandr,et al. 2008], and by distinguishing transient faults from permanent faults based on the carrier channel of carrier protections of EHV transmission lines [Huang Qiang, et al. 2002] are reported in recent times.

A different approach for adaptive AR with reference to power system stability based on multi agent system using java agent development framework has been also proposed [You-Jin Lee, et al. 2008]. A self-adaptive auto-reclosure criterion using dual-window transient energy ratio (ER) for transmission line is proposed, and a novel concept of close-opening - open-closing morphological gradient (COOCG) is put forward [Xiangning Lin, et al. 2008].

More to come, a numerical algorithm for determining adaptive dead time, and blocking automatic reclosing during permanent faults on overhead lines which is based on terminal voltage input data processing has been proposed [Radojevic, et al. 2008]. In this case, the decision if ever to reclose is determined by the total harmonic distortion factor of the fault voltage signal that is calculated by discrete Fourier transform (DFT).

However, the mathematical optimizations so far failed to encompass all possible types of faults that occur on a transmission line. In other words, a model developed based on certain assumptions may fail at some point due to the uncertainties and randomness of faults on a transmission system. Most of the approaches discussed exhibit wide range limitations due to many causes of faults e.g. high-impedance permanent faults that closely resemble to arcs may not be categorically identified. Mostly, it is difficult to say how robust those approaches would be because they are developed under certain assumptions. Moreover, most of the methods do not consider the suppression effect of shunt reactors. And, since transmission lines are currently series-compensated to boost their loading capacity; the effect of series compensators is not taken into consideration

2.10.5. Artificial Intelligence (AI) Based

Application of artificial intelligence, which includes expert systems (ES), artificial neural network (ANN), genetic algorithm (GA), fuzzy logic (FL), etc, has recently become evident in solving power system problems. AI's have been crucial in solving long standing problems in the area of power system protection, control and planning. The detail description of artificial intelligence and different algorithms implemented in this thesis is presented in the next Chapter.

Recently, faults on EHV lines have been classified as phase to ground fault, two phases to ground fault, three phases to ground fault, etc using radial basis function neural networks (RBFNN) up on utilizing faulted voltage and current signals at the receiving end of the line only [M. Joorabian, et al. 2004]. The application of ANNs in classifying faults paved the way to the developments of methods to identify permanent faults from temporary ones. For instance, recent studies proposed a new adaptive auto-reclosure of transmission system for different levels of voltages - High Voltage (HV) as in [A.I. Megahed, et al. 2006], Medium Voltage (MV) as in [V.V. Terzija, et al. 2004] and EHV as in [Lukowicz, 2004]. The data presented to the neural networks for identification purpose (training, testing and validation) were taken from extracted features of a real time one terminal voltage and/ or current signals.

An auto-reclosure which utilizes ANN as a pattern classifier and different harmonic components of positive sequence of voltage as inputs to ANN is developed by [Khorashadi-Zadeh, 2005]. Similarly, a research group [El-Hadidy, et al. 2004] suggested a single-phase AR technique which uses information extracted from residual voltage of a tripped phase using Discrete Wavelet Transform (DWT) as input to an ANN for classification.

[Yu and Song, 1998] carried out a research on wavelet analysis and neural network based adaptive single-pole auto-reclosure scheme for EHV transmission systems. Wavelet analysis is used to analyze and extract the features of the transient and permanent faults. The decision is made by the help of a supervised training neural network fed with the extracted features.

None of the above reports, adopted to alleviate the previously mentioned problems of AR, showed any means to optimize the parameters which are very decisive in training process of the neural network. Almost all parameters have been selected randomly which is ineffective, and may not guarantee the desired outcome. Moreover, the validity of the algorithms, developed in each report, seems to have major concerns of generalizations. It is not clearly put in place how far each approach would go in depth of the problems stated earlier.

2.11. PROPOSED TECHNIQUE

This thesis mainly focuses on developing an adaptive auto-reclosure which provides a prompt solution for the improper reclosing action of a conventional auto-reclosure on to a line under fault, particularly in EHV systems. This is achieved with the help of an optimized and well-trained artificial neural network algorithm which effectively discerns a temporary from a permanent fault, and takes appropriate decision, either to allow if safe or block in severe and uncleared fault conditions.

Fault data are gathered by generating a number of faults on three power system models, namely, SMIB, IEEE 9-bus and IEEE 14-bus electric systems. Three different training algorithms (Error Back-Propagation, Resilient Back-Propagation and Levenberg Marquardt) are employed as a training means for the neural network. The parameters of each of these algorithms and the number of hidden neurons are optimized using Taguchi's methodology, a powerful and robust optimization technique.

In the case of temporary faults, a method using ANN is developed to accurately determine fault extinction time. This is due to the fact that the trained ANN has the ability to detect a fault when it extinguishes out (i.e. when secondary arc vanishes).

The techniques adopted in this thesis offer tremendous advantages such as increased rate of successful reclosure, improved system stability and a reduction in system equipment damage under a permanent or elongated arcing fault, etc.

2.12. SUMMARY

In this Chapter, theoretical review of automatic reclosing technique including its history, principles of operation, associated transmission line faults, modes of operation, operating features, its benefits and existing challenges have been dealt in Sections 2.1 through 2.9. Previous works to improve the performance of conventional reclosing technique have been also discussed in detail. In connection to these, the drawbacks and disadvantages of the previously proposed works with regard to the automatic reclosing flaws have been pointed out in Section 2.10. The Chapter concluded with the proposed method to mitigate the existing problems of automatic reclosing.

CHAPTER THREE

ARTIFICIAL NEURAL NETWORKS AND TAGUCHI'S OPTIMIZATION METHODS –THEORETICAL REVIEW

3.1. INTRODUCTION

Various optimization techniques have been applied to solve power system problems so far. Among these, mathematical optimization methods have been used over the years for many power systems planning, operation, and control problems. Mathematical formulations of real-world problems are derived under certain assumptions, and even with these assumptions, the solution to problems in large-scale power systems is not simple. On the other hand, there are many uncertainties in power system problems because power systems are large, complex, and geographically widely distributed. It is desirable that solutions of power system problems should be optimum globally, but solutions searched by mathematical optimizations are usually optima locally. These facts make it difficult to deal effectively with many power system problems through strict mathematical formulation alone.

Artificial intelligences have been widely applied to solve many real world problems. The wide applications of artificial intelligence have led many researchers to investigate its applications in power system engineering [S. Kak, 1998]. Therefore, artificial intelligence (AI) techniques such as expert systems (ES), artificial neural network (ANN), genetic algorithm (GA) and fuzzy logic, which promise a global optimum or nearly so, have emerged in recent years in power systems as a complement tool to mathematical approaches. Artificial Intelligences are among the techniques widely used in power systems in recent years which have clearly demonstrated their ability in solving some long standing problems where conventional techniques have had difficulty or have been unable to meet functional requirements. They have been proposed and implemented for different applications in power systems including fault detection and classification, fault direction discrimination, fault location, machine diagnosis, power system control and protection, etc. [R.C. Bansal, 2005]. In general, recent works on wide areas of power system prove the

versatility of AI's in solving power system problems. The detailed explanation of each of the above-mentioned artificial intelligence tools (other than ANNs), and their applications to electric power systems is beyond the scope of this thesis.

As mentioned in Chapter 2, ANNs have been employed in this research work for tackling the problem which this thesis is based on. But before the detailed use of ANNs in this study are presented, it is imperative to present a brief review of ANNs. This Chapter presents a theoretical review of ANNs, discusses the details of three algorithms selected for training the neural network, namely, standard Error Back-Propagation (EBP), Levenberg-Marquardt (LM) and Resilient Back-Propagation (RPROP). In addition, it gives details about the useful optimization technique - Taguchi's Methodology (TM), which is helpful in optimizing certain parameters of the neural network and its training algorithm.

3.2. ARTIFICIAL NEURAL NETWORKS

3.2.1. Basic Concepts

An ANN is a powerful data modeling tool that is able to capture and represent complex input/output relationships. The motivation for the development of neural network technology is stemmed from the desire to develop an artificial system that could perform intelligent tasks similar to those performed by the human brain. This is based on a parallel distributed information processing structure consisting of processing units or neurons each of which perform two functions: aggregation of its inputs from other neurons or the external environment, and generation of an output from the aggregated inputs. These units, working in unison to solve specific problems, are interconnected via unidirectional signal channels called connections. In other words, an ANN is an interconnected group of artificial neurons that uses a mathematical or computational model for information processing based on a connectionist approach to computation. Each processing unit has a single output connection that branches into as many collateral connections as desired; each carries the same signal - the processing element output signal, which can be of any

mathematical type desired. A connection between a pair of neurons has an associated numerical strength called synaptic weight [R.D. Reeds and R.J. Marks, 1999].

Neural networks are different from conventional computing or statistical systems. As stated earlier, the networks were inspired by the structure and operation of biological neurons. They are composed of many simple elements called neurons (processing units) that are interconnected by links and act like axons to determine an empirical relationship between the inputs and outputs of a given system. Knowledge is stored in the topology of the network itself rather than in explicitly coded data structures. The simple processing units or artificial neurons, joined through numerous interconnections, are usually organized into groups called layers. The input layer is connected to the output layer through junctions with a hidden layer or a number of hidden layers.

Basically, one of the most popular neural network paradigms is the feed-forward neural network. In a feed-forward neural network, the neurons are usually arranged in layers [Battiti R., 1992]. A feed-forward neural network is denoted as $N_I \times N_1 \times \dots \times N_i \times \dots \times N_M \times N_O$, where:

- N_I represents the number of input units;
- M represents the number of hidden layers;
- N_i represents the number of units from the hidden layer, $i = 1, 2, \dots, M$;
- N_o represents the number of output units.

The feed-forward neural networks are the first and simplest type of neural networks. In this network, the information moves in only one direction which is forward from the input nodes, through the hidden nodes and to the output nodes. The connections are formed by connecting each of the nodes in a given layer to all of the neurons in the next layer. In this way, every node in a given layer is connected to every other node in the next layer. Usually there are at least three layers [Yam and Chow, 1999] to a feed-forward network which are an input layer, a hidden layer, and an output layer. By convention, the input layer does not count, since the input units are not processing units, they simply pass on the input vector x . It is where the data is fed into the network via the hidden layer. The hidden layer, in turn, feeds into the output layer.

The actual processing in the network occurs in the nodes of the hidden layer and the output layer. Units from the hidden layers and output layer are, however, processing units. Multiple layers arrangement of a typical and fully connected 2-layer feed-forward interconnected neural network with $5 \times 7 \times 1$ structure is shown in Figure 3.1. It consists of an input layer, an output layer, and one hidden layer with different roles. Each connecting line has an associated weight, and each processing unit has an activation function, $f(x)$, linked with it.

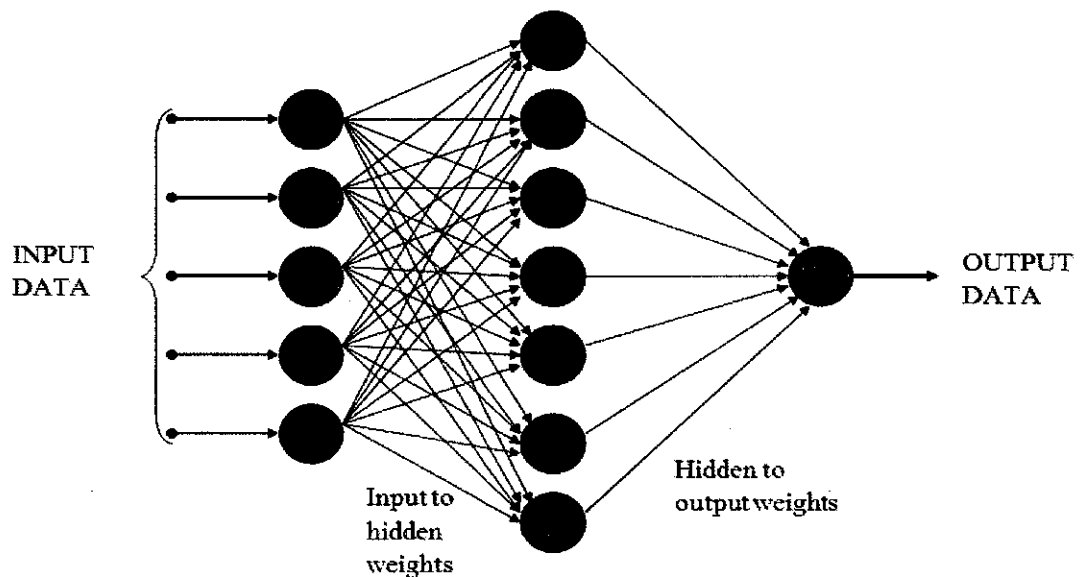


Figure 3.1: A $5 \times 7 \times 1$ feed-forward neural network

Activation Functions –Activation functions are functions needed specially to introduce nonlinearity for the hidden units into the network. Without nonlinearity, hidden units would not make networks more powerful than just plain networks (which do not have any hidden units, just input and output units). The reason is that a linear function of linear functions is again a linear function. However, it is the nonlinearity (i.e. the capability to represent nonlinear functions) that makes multilayer networks so powerful. Some of the nonlinear functions frequently used in neural networks are shown in Table 3.1. For some learning algorithms, the activation function must be differentiable, and it helps if the function is bounded; the sigmoid functions such as *logistic*, *hyperbolic tangent* and *Gaussian* function are the most common choices.

Functions such as *hyperbolic tangent* or *arctangent* that produce both positive and negative values tend to yield faster training than functions that produce only positive values such as *logistic*, because of better numerical conditioning. Another benefit from these functions is typically the squashing effect to the output of each unit which an activation function is associated with. In other words, they limit the output of each processing unit to a range between either 0 and 1 or -1 and 1 depending on the kind of activation function used.

Table 3.1: Some activation functions of artificial neural networks

Function	Definition	Range
Linear	X	$(-\infty, +\infty)$
Logistic	$\frac{1}{1 + e^{-x}}$	$(0, +1)$
Hyperbolic tangent	$\frac{e^x - e^{-x}}{e^x + e^{-x}}$	$(-1, +1)$
Negative exponential	e^{-x}	$(0, +\infty)$
Inverse tangent	$\arctan(x)$	$(-\pi/2, +\pi/2)$
Softmax	$\frac{e^x}{\sum_i e^{x_i}}$	$(0, +1)$
Unit sum	$\frac{x}{\sum_i x_i}$	$(0, +1)$
Square root	\sqrt{x}	$(0, +\infty)$
Sine	$\sin(x)$	$[0, +1]$
	$-1; x \leq -1$	$[-1, +1]$
Ramp	$x; -1 < x < +1$	
	$+1; x \geq +1$	
Step (threshold)	$0; x < 0$	$[0, +1]$
	$+1; x \geq 0$	

For hidden units, sigmoid activation functions are usually preferable to threshold activation functions. It has been verified that networks with threshold units are difficult to train because the error function is stepwise constant, hence the gradient either does not exist or is zero, making it impossible to use back-propagation or more

efficient gradient-based training methods Even for training methods that do not use gradients –such as simulated annealing and genetic algorithms –sigmoid units are easier to train than threshold units. This is due to the fact that with sigmoid units, a small change in the weights will usually produce a change in the outputs, which makes it possible to tell whether that change in the weights is good or bad. With threshold units, a small change in the weights will often produce no change in the outputs. Details of these terminologies will be discussed in the next Subsections.

For the output units, an activation function suited to the distribution of the target values is usually chosen. For instance,

- For binary (0/1) targets, the logistic function is an excellent choice.
- For categorical targets using 1-of-C coding, the softmax activation function is the logical extension of the logistic function.
- For continuous-valued targets with a bounded range, the *logistic* and *hyperbolic tangent* functions can be used, provided that either the outputs are scaled to the range of the targets or the targets to the range of the output activation function. Technically speaking, scaling means multiplying by and adding appropriate constants.
- If the target values are positive but have no known upper bound, an exponential output activation function is usually used.
- For continuous-valued targets with no known bounds, the linear activation function is used [Jordan, 1995].

3.2.2. The Mathematical Model of ANN

When creating a functional model of the biological neuron, there are three basic components of importance. First, the synapses of the neuron are modeled as weights. The strength of the connection between an input and a neuron is noted by the value of the weight. Negative weight values reflect inhibitory connections, while positive values designate excitatory connections [S. Haykin, 1998]. The next two components model the actual activity within the neuron. This is demonstrated by the single neuron connection phenomenon as in Figure 3.2. The output from a given neuron is calculated by applying a transfer function to a weighted summation of its input to give

an output, which can serve as input to other neurons, as shown in Equation (3.1). Thus, an adder sums up all the inputs modified by their respective weights, which is referred to as linear combination. Finally, an activation function, usually associated to each processing unit in the neural network, controls the amplitude of the output of the neuron. As mentioned previously, the activation function acts as a squashing function, such that the output of a neuron in a neural network is between certain values. An acceptable range of the output, which depends up on the activation, lies between 0 and 1 (refer to Equation (3.1)) or between -1 and +1[Gharbi, 1997].

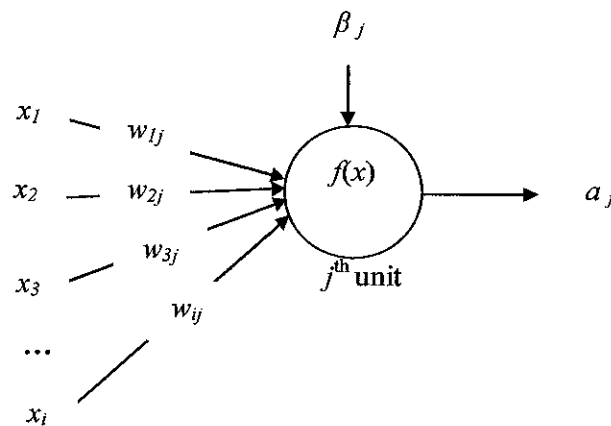


Figure 3.2: A single processing unit

A simple yet useful mathematical model which shows the net input to j^{th} processing unit is given by Equation (3.1).

$$net_j = \sum_{i,j} w_{ij} x_i + \beta_j \quad (3.1)$$

where x_i 's are the outputs from the previous layer, w_{ij} is the weight (connection strength) of the link connecting unit i to unit j , and β_j is the bias of unit j , which determines the location of the activation function on the x -axis. When logistic activation function is employed, the activation output value of unit j is represented by Equation (3.2). As a matter of fact, net_j is now mapped in to a value a_j which is squashed as a result of the activation function into $0 \leq a_j \leq 1$.

$$a_j = f(\text{net}_j) = \frac{1}{1 + e^{-\text{net}_j}} \quad (3.2)$$

3.2.3. Classification of ANNs

ANNs can be classified as either feed-forward, recurrent, modular, and stochastic or many others, depending on how data is processed through the network. Another way of classifying ANNs is by their method of learning, as some ANN employs supervised learning while others are referred to as unsupervised or self-organizing. Yet, there are other categories of ANNs which impart reinforcement learning method. Each of these categories is explained below.

Supervised Learning or Associative Learning –The supervised ANN requires a set of inputs and matching output patterns provided for its training. During the training, the output from the ANN is compared with the desired output (target) and the difference (error) is reduced by employing some training algorithms. This training is repeated till the actual output acquires an acceptable level. These input-output pairs can be provided by an external teacher, or by the system which contains the neural network (self-supervised) as shown in Figure 3.3. The most common neural network model, feed-forward network multilayer perceptron (MLP), is known as a supervised network because it requires a desired output in order to learn. The goal of this type of network is to create a model that correctly maps the input to the output using historical data so that the model can then be used to produce the output when the desired output is unknown.

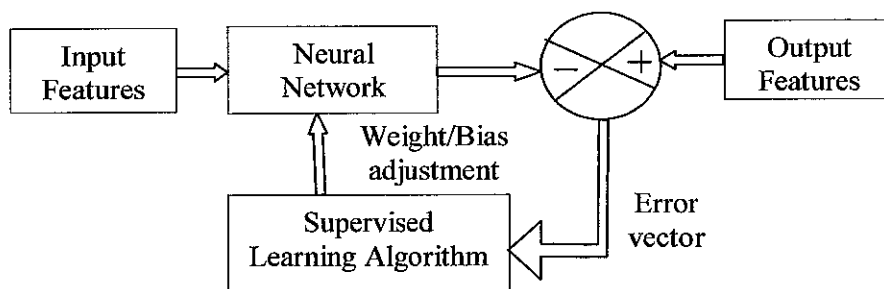


Figure 3.3: Supervised neural network learning scheme

Unsupervised Learning or Self-organization –The artificial neural network which does not require a supervisor or teacher for training is in this category. In competitive or unsupervised learning units of the output layer compete for the chance to respond to a given input pattern. In this paradigm, the system is supposed to discover statistically salient features of the input population. Unlike the supervised learning paradigm, there is no a priori set of categories into which the patterns are to be classified; rather the system must develop its own representation of the input stimuli.

Reinforcement Learning –This type of learning may be considered as an intermediate form of the above two types of learning. Here, the learning machine does some action on the environment and gets a feedback response from the environment. The learning system grades its action good (rewarding) or bad (punishable) based on the environmental response and accordingly adjusts its parameters. Generally, parameter adjustment is continued until an equilibrium state occurs, following which there will be no more changes in its parameters. The self-organizing neural learning may be categorized under this type of learning.

3.2.4. Normalization and ANN Training

Normalization – is a process of scaling the numbers in a data set into a specified range, to improve the accuracy of the subsequent numeric computation, computations. Normalization of input and output data is very critical. The values in the external data files are not always well suited for directly copying to network activities. This is because the activities in the network are normally in the range $[-1,1]$, and if some activities differ significantly from this behavior, training performance is often degraded. Hence, without normalization, there is a tendency that the signal or value of large magnitude will be too dominating. If the input and output variables are not of the same order of magnitude, some variables may appear to have more significance than they actually do. The training algorithm has to compensate for order-of-magnitude differences by adjusting the network weights, which is not very effective in many of the training algorithms such as back propagation algorithm. For example, if one input variable has a value of thousands and other input variable has a

value in tens, the assigned weight for the second variable entering a node of hidden layer 1 must be much greater than that for the first. In addition, typical transfer functions such as a sigmoid function, or hyperbolic tangent function, cannot distinguish between two values of inputs when both are very large, because both yield identical threshold output values of 1.

In general, proper normalization of particularly input data makes training algorithms numerically robust and leads to a faster convergence. The common normalization method is to normalize each pattern in such a way that the minimum value is mapped to -1 and the maximum value is mapped to +1. In this report, the input data patterns are normalized between between -1 and +1.

Training (Learning) –is the process of modifying the weights of a neural network in order to produce a network that performs some function. The goal of learning is to create a model that correctly maps the input to the output using historical data so that the model can then be used to produce the output when the desired output is unknown. This is met by adjusting all the connection weights and biases of the network, so that the calculated outputs may be approximated by the desired values.

Basically, the development of ANN involves two phases: training or learning phase and testing phase. Neural networks develop information processing capabilities by learning from examples called training set (a collection of input-output patterns that are used to train the network). Hence, the network learns by a process involving the modification of the connection weights between neurons and layers. As soon as the network has learnt the problem, it is tested with new unknown patterns, and its efficiency is checked.

As mentioned previously, learning techniques can be either supervised or unsupervised. Supervised learning requires a set of examples for which the desired network response is known. The learning process consists then in adapting the network in a way that it will produce the correct response for the set of examples. The resulting network should then be able to generalize (give a good response) when presented with cases not found in the set of examples. Whereas, in unsupervised learning, the neural network is autonomous; it processes the data it is presented with,

finds out about some of the properties of the data set, and learns to reflect these properties in its output. What exactly these properties are, that network can learn to recognize, depends on the particular network model and learning method.

The supervised learning type has been utilized in this study. Hence, all explanations following this will be based on this category.

The objective of different supervised learning algorithms is the iterative optimization of a so called error function representing a measure of the performance of the network. For obvious reason, the training process requires a proper set of data, i.e. input and target output, and a proper mapping of the input to the output. The error function that is usually used for training process is defined as the mean square sum of differences between the values of the output units of the network and the desired target values, calculated for the whole input pattern set. More specifically, the error for a pattern p is given by Equation (3.3):

$$E_p = \sum_{j=1}^{N_o} (d_{pj} - a_{pj})^2 \quad (3.3)$$

where d_{pj} and a_{pj} are the target and the actual response values of j^{th} output neuron corresponding to the pattern p .

Thus, the total mean square error and the root mean square error (a typical performance function that is used for training feed forward neural networks) are given as in Equations (3.4) and (3.5), respectively.

$$E = \frac{1}{P} \sum_{p=1}^P E_p = \frac{1}{P} \sum_{p=1}^P \sum_{j=1}^{N_o} (d_{pj} - a_{pj})^2 \quad (3.4)$$

$$RMSE = \sqrt{\frac{E}{P * N_o}} \quad (3.5)$$

where P is the number of the training patterns and N_o is the number of outputs.

During training process, a set of pattern examples is used, each example consisting of a pair with the input and corresponding target output. The patterns are presented to the network sequentially, in an iterative manner, the appropriate weight corrections being

performed during the process to adapt the network to the desired behavior [Demuth and Beale, 2002]. This iteration process continues until the connection weight values allow the network to perform the required mapping. Each presentation of the whole pattern set is named an epoch. The iteration process is governed by different types of training algorithms which will be discussed in the following subsection.

3.2.5. Training Algorithms

3.2.5.1. Error Back-Propagation (EBP) Algorithm

One of the most popular supervised learning algorithms for feed-forward neural networks is error back-propagation [Minai A., 1990] and [Battiti R., 1992]. It is a supervised learning method, a multilayer feed-forward network with hidden layers between the input and output, and is an implementation of the delta rule [Osman and Al-MArhoun, 2002]. It requires a teacher that knows, or can calculate, the desired output for any given input. It is the most useful algorithm for feed forward networks (networks that have no feedback or simply, that have no connections that loop).

With back-propagation, the input data is repeatedly presented to the neural network. With each presentation, the output of the neural network is compared to the desired output, and an error is computed. This error is then fed back (back-propagated) to the neural network and used to adjust the weights such that the error decreases with each iteration and the neural model gets closer and closer to producing the desired output.

The simplest implementation of back propagation learning algorithm is the network weights and biases updates in the direction of the negative gradient that the performance function decreases most rapidly. Thus, the minimization of the error function is carried out using a gradient-descent technique. The necessary corrections to the weights of the network for each moment t are obtained by calculating the partial derivatives of the error function in relation to each weight w_{ij} . A gradient vector representing the steepest increasing direction in the weight space is thus obtained. The next step is to compute the resulting weight update. In its simplest form, the weight update is a scaled step in the opposite direction of the gradient. Hence, the weight update rule is given by Equation (3.6).

$$\Delta_p w_{ij}(t) = -\eta * \frac{\partial E_p}{\partial w_{ij}}(t) \quad (3.6)$$

where η is a parameter determining the step size, and is called the learning rate whose value is usually selected with in the range of 0 and 1 i.e. $\eta \in (0,1)$. A momentum is usually used with the idea of incorporating in the present weight update, some influence of the past iteration. Thus, the weight update rule becomes as in Equations (3.7) and (3.8).

$$\Delta_p w_{ij}(t) = -\eta * \frac{\partial E_p}{\partial w_{ij}}(t) + \alpha * \Delta_p w_{ij}(t-1) \quad (3.7)$$

$$w_{ij}(t+1) = w_{ij}(t) + \Delta w_{ij}(t) \quad (3.8)$$

where α is the momentum term and determines the amount of influence from the previous iteration to the present one, and η is the learning rate. Both these parameters are useful ingredients in the overall performance of the neural network training; hence, their values should be carefully chosen. The overall flow chart of error back-propagation is depicted in Figure 3.4.

Figure 3.4 implies that the errors (and therefore the learning) propagate backwards from the output nodes to the inner nodes as the long as the stopping criterion (minimum error or maximum number of epochs) is not satisfied. So, technically speaking, back-propagation is used to calculate the gradient of the error of the network with respect to the network's modifiable weights. And, the weight updates are based on the equations explained previously (Equations 3.7 through 3.9).

It is important to note that back propagation networks are necessarily multilayer perceptron (usually with one input, one hidden, and one output layer). In order for the hidden layer to serve any useful function, multilayer networks must have non-linear activation functions for the multiple layers: a multilayer network using only linear activation functions is equivalent to some single layer, linear network. Non-linear activation functions that are commonly used are included in Table 3.1 of Subsection 3.2.1.

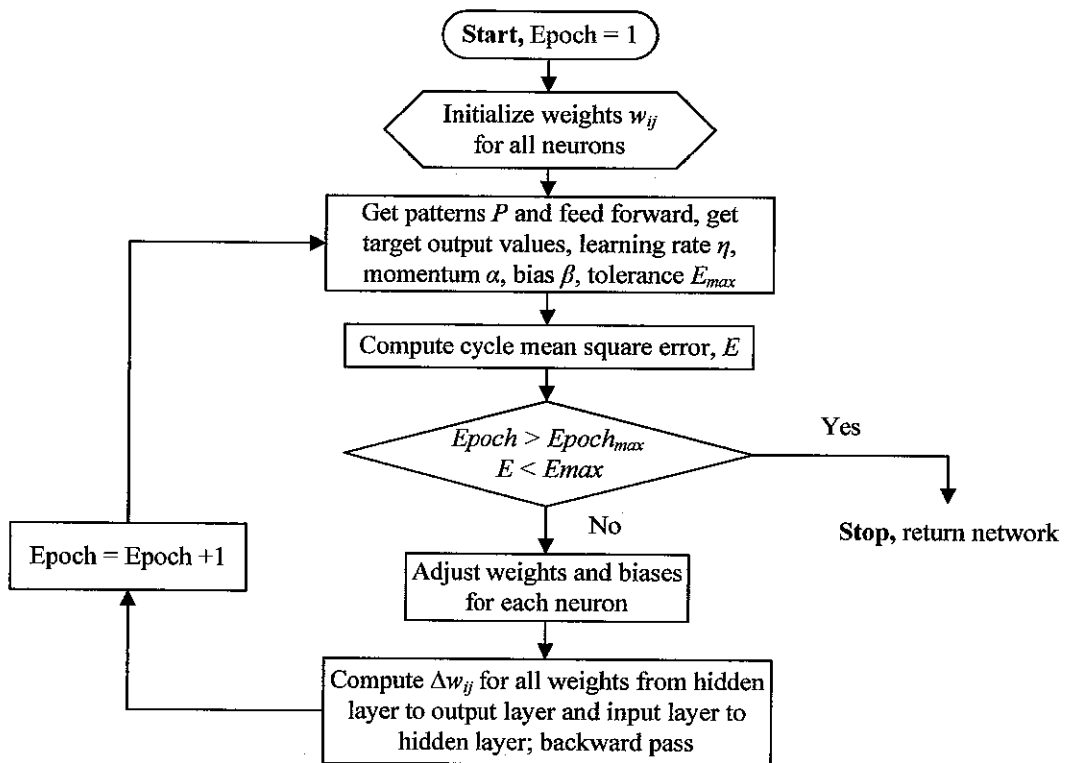


Figure 3.4: A training process flowchart of error back propagation algorithm

Other than the standard error back propagation algorithm, there are various back propagation algorithms such as Scaled Conjugate Gradient (SCG), Levenberg-Marquardt (LM) and Resilient Back-propagation (RPROP). These algorithms proved a much improved training performance over the standard EBP, and are more practiced nowadays. Among these, LM is the fastest training algorithm for networks of moderate size, and it has the memory reduction feature to be used when the training set is large. LM and RPROP will be discussed in detail in the following subsections.

3.2.5.2. The Resilient Back-propagation algorithm (RPROP)

RPROP algorithm is a local adaptive learning scheme, performing supervised batch learning in feed-forward neural networks. It is a very promising algorithm for feed-forward neural networks, introduced by [M. Riedmiller, 1993]. The basic principle of RPROP is to eliminate the harmful influence of the size of the partial derivative on the weight step. As a consequence, only the sign of the derivative is considered to

indicate the direction of the weight update. To achieve this, for each weight w_{ij} , its individual update-value $\Delta_{ij}(t)$ is introduced which solely determines the size of the weight-update.

A second learning rule is introduced. This determines the evolution of the update-value $\Delta_{ij}(t)$. This estimation is based on the observed behavior of the partial derivative during two successive weight-steps as in Equation (3.9).

$$\Delta_{ij}(t) = \begin{cases} \eta^+ \cdot \Delta_{ij}(t-1), & \text{if } \frac{\partial E}{\partial w_{ij}}(t) \cdot \frac{\partial E}{\partial w_{ij}}(t-1) > 0 \\ \eta^- \cdot \Delta_{ij}(t-1), & \text{if } \frac{\partial E}{\partial w_{ij}}(t) \cdot \frac{\partial E}{\partial w_{ij}}(t-1) < 0 \\ \Delta_{ij}(t-1), & \text{else} \end{cases} \quad (3.9)$$

where $0 < \eta^- < 1 < \eta^+$. In words, the adaptation rule works as follows. Every time the partial derivative of the corresponding weight w_{ij} changes its sign, which indicates that the last update was too big and the algorithm has jumped over a local minimum, the update-value $\Delta_{ij}(t)$ is decreased by the factor η^- . If the derivative retains its sign, the update-value is slightly increased in order to accelerate convergence in shallow regions.

Once the update-value for each weight is adapted, the weight-update itself follows a very simple rule: if the derivative is positive (increasing error), the weight is decreased by its update-value, if the derivative is negative, the update-value is added as shown in Equations (3.10) and (3.11).

$$\Delta w_{ij}(t) = \begin{cases} -\Delta_{ij}(t), & \text{if } \frac{\partial E}{\partial w_{ij}}(t) > 0 \\ \Delta_{ij}(t), & \text{if } \frac{\partial E}{\partial w_{ij}}(t) < 0 \\ 0, & \text{else} \end{cases} \quad (3.10)$$

$$w_{ij}(t+1) = w_{ij}(t) + \Delta w_{ij}(t) \quad (3.11)$$

However, there is one exception. If the partial derivative changes sign, that is the previous step was too large and the minimum was missed, the previous weight-update is reverted as in Equation (3.12).

$$\Delta w_{ij}(t) = -\Delta w_{ij}(t-1) \quad \text{if} \quad \frac{\partial E}{\partial w_{ij}}(t) \cdot \frac{\partial E}{\partial w_{ij}}(t-1) < 0 \quad (3.12)$$

Due to that ‘backtracking’ weight-step, the derivative is supposed to change its sign once again in the following step. In order to avoid a double punishment of the update-value, there should be no adaptation of the update-value in the succeeding step. In practice, this can be done by setting $\frac{\partial E}{\partial w_{ij}}(t-1) = 0$ in the Δ_{ij} update-rule above. The partial derivative of the total error is given by Equation (3.13).

$$\frac{\partial E}{\partial w_{ij}}(t) = \frac{1}{2} \sum_{p=1}^P \frac{\partial E_p}{\partial w_{ij}}(t) \quad (3.13)$$

Hence, the partial derivatives of the errors must be accumulated for all P training patterns. This means that the weights are updated only after the presentation of all training patterns.

[M. Riedmiller, 1994] introduced a *weight-decay* parameter α . This parameter determines the relationship of two goals, namely, to reduce the output error (the standard goal) and to reduce the size of the weights (to improve generalization). The composite error function is given by Equation (3.14).

$$E = \frac{1}{2} \sum_{p=1}^P \sum_{j=1}^{N_o} (d_{pj} - a_{pj})^2 + \frac{1}{10^\alpha} \cdot \sum_{i,j} w_{ij}^2 \quad (3.14)$$

The *weight-decay* parameter α denotes the exponent, to allow comfortable input of very small values. Hence, a choice of $\alpha = 4$ corresponds to a ratio of weight decay term to output error of 1:10000.

Parameter Settings –In order to reduce the number of freely adjustable parameters, often leading to a tedious search in parameter space, the increase and decrease factors η^+ and η^- are set to values: $\eta^- \leq 1.0$ and $\eta^+ \geq 1.0$. At the beginning of the

algorithm, all update-values Δ_{ij} are set to an initial value Δ_0 whose value is adapted as learning proceeds. It is evident that careful choice of these parameters improves the training performance of learning ability of the neural network. In addition, to prevent the weights from becoming too large, the maximum weight-step determined by the size of the update-value is limited. The upper bound is set to Δ_{\max} , which is set somewhat arbitrarily to $\Delta_{\max} = 50.0$. Usually, the convergence is rather insensitive to this parameter as well. The minimum step size is constantly fixed to $\Delta_{\min} = 1e^{-6}$.

The following pseudo-code fragment shows the kernel of the RPROP adaptation and learning process. The minimum (maximum) operator is supposed to deliver the minimum (maximum) of two numbers; the sign operator returns +1 if the argument is positive, -1 if the argument is negative and 0, otherwise.

$$\forall i, j : \Delta_{ij}(t) = \Delta_0 ; \forall i, j : \frac{\partial E}{\partial w_{ij}}(t-1) = 0$$

REPEAT

 Compute Gradient $\frac{\partial E}{\partial w_{ij}}(t)$

 For all weights and biases {

$$\text{IF} \left[\frac{\partial E}{\partial w_{ij}}(t-1) * \frac{\partial E}{\partial w_{ij}}(t) > 0 \right],$$

 THEN { $\Delta_{ij}(t) = \min(\Delta_{ij}(t-1) * \eta^+, \Delta_{\max})$

$$\Delta w_{ij}(t) = -\text{sign}\left(\frac{\partial E}{\partial w_{ij}}(t)\right) * \Delta_{ij}(t)$$

$$\Delta w_{ij}(t+1) = \Delta w_{ij}(t) + \Delta w_{ij}(t)$$

$$\frac{\partial E}{\partial w_{ij}}(t-1) = \frac{\partial E}{\partial w_{ij}}(t)$$

 }

$$\text{ELSE IF } \left[\frac{\partial E}{\partial w_{ij}}(t-1) * \frac{\partial E}{\partial w_{ij}}(t) < 0 \right],$$

$$\text{THEN } \{ \Delta_{ij}(t) = \max(\Delta_{ij}(t-1) * \eta^-, \Delta_{\min})$$

$$\frac{\partial E}{\partial w_{ij}}(t-1) = 0$$

$$\}$$

$$\text{ELSE IF } \left[\frac{\partial E}{\partial w_{ij}}(t-1) * \frac{\partial E}{\partial w_{ij}}(t) = 0 \right],$$

$$\text{THEN } \{ \Delta w_{ij}(t) = -\text{sign}\left(\frac{\partial E}{\partial w_{ij}}(t)\right) * \Delta_{ij}(t)$$

$$\Delta w_{ij}(t+1) = \Delta w_{ij}(t) + \Delta w_{ij}(t)$$

$$\frac{\partial E}{\partial w_{ij}}(t-1) = \frac{\partial E}{\partial w_{ij}}(t)$$

$$\}$$

$$\}$$

UNTIL (convergence criterion is met)

To sum up, the basic principle of RPROP is the direct adaptation of the weight update value Δ_{ij} . In contrast to learning rate based algorithms (as for example gradient descent), RPROP modifies the size of the weight step directly by introducing the concept of resilient update-values. As a result, the adaptation effort is not blurred by unforeseeable gradient behavior. Due to the clarity and simplicity of the learning laws, there is only a slight expense in computation compared with ordinary back-propagation. Besides fast convergence, one of the main advantages of RPROP lies in the fact that for many problems no choice of parameters is needed at all to obtain optimal or at least nearly optimal convergence times.

Another often discussed aspect of common gradient descent is that the size of the derivative decreases exponentially with the distance between the weight and the output-layer, due to the limiting influence of the slope of the activation function.

Consequently, weights far away from the output layer are less modified and do learn much slower. Using RPROP, the size of the weight step is only dependent on the sequence of signs, not on the magnitude of the derivative. For that reason, learning is spread equally all over the entire network; weights near the input layer have the equal chance to grow and learn as weights near the output layer.

3.2.5.3. The Levenberg Marquardt (LM) Algorithm

The Levenberg-Marquardt algorithm is an iterative technique that locates the minimum of a multivariate function that is expressed as the sum of squares of non-linear real-valued functions. It has become a standard technique for non-linear least-squares problems [H.D. Mittelmann, 2004], widely adopted in a broad spectrum of disciplines. LM can be thought of as a combination of steepest descent and the Gauss-Newton method [K. Madsen, 2004]. When the current solution is far from the correct one, the algorithm behaves like a steepest descent method: slow, but guaranteed to converge. When the current solution is close to the correct solution, it becomes a Gauss-Newton method. Next, a short description of the LM algorithm based on the material in [K. Madsen, 2004] is supplied.

Gradient-based training algorithms, like back-propagation, are most commonly used by researchers. They are not efficient due to the fact that the gradient vanishes at the solution. Hessian-based algorithms used [Bartolac et al., 1993] allow the network to learn more subtle features of a complicated mapping. The training process converges quickly as the solution is approached, because the Hessian does not vanish at the solution. The LM algorithm is basically a Hessian-based algorithm for nonlinear least squares optimization, and is widely accepted as the most efficient one in the sense of realization accuracy.

In LM algorithm, the performance index $F(w)$ to be minimized is defined as the sum of squared errors between the target outputs and the actual outputs as in Equation (3.15).

$$F(w) = \sum_{p=1}^P \sum_{k=1}^K (d_{kp} - o_{kp})^2 \quad (3.15)$$

where $w = [w_1, w_2, \dots, w_N]^T$ consists of all weights of the network, d_{kp} is the desired value of the k^{th} output and the p^{th} pattern, o_{kp} is the actual (target) value of the k^{th} output and the p^{th} pattern, N is the number of weights, P is the number of patterns, and K is the number of network outputs. Equivalently, Equation (3.15) can be rewritten as in Equation (3.16).

$$F(w) = E^T E \quad (3.16)$$

where E is the cumulative error vector given by $E = [e_{11} \dots e_{k1}, e_{12} \dots e_{k2}, \dots, e_{1P} \dots e_{KP}]^T$ for all patterns, and $e_{kp} = d_{kp} - o_{kp}$, $k = 1, 2 \dots K$, $p = 1, 2 \dots P$. And, the increment of weights Δw , as dictated by Levenberg Marquardt, can be obtained as in Equation (3.17).

$$\Delta w = [J^T J + \lambda I]^{-1} J^T E \quad (3.17)$$

where J is Jacobian matrix defined as in Equation (3.18), λ is learning parameter which is to be updated using either a decay rate β ($0 \leq \beta \leq 1$) or an increment λ^+ and decrement λ^- factors depending on the outcome; I is identity matrix. The updated weights are expressed by Equations (3.19) and (3.20).

$$J(w) = \begin{bmatrix} \frac{\partial e_{11}}{\partial w_1} & \frac{\partial e_{11}}{\partial w_2} & \dots & \frac{\partial e_{11}}{\partial w_N} \\ \frac{\partial e_{21}}{\partial w_1} & \frac{\partial e_{21}}{\partial w_2} & \dots & \frac{\partial e_{21}}{\partial w_N} \\ \vdots & \vdots & \ddots & \vdots \\ \frac{\partial e_{1P}}{\partial w_1} & \frac{\partial e_{1P}}{\partial w_2} & \dots & \frac{\partial e_{1P}}{\partial w_N} \\ \frac{\partial e_{2P}}{\partial w_1} & \frac{\partial e_{2P}}{\partial w_2} & \dots & \frac{\partial e_{2P}}{\partial w_N} \\ \vdots & \vdots & \ddots & \vdots \\ \frac{\partial e_{KP}}{\partial w_1} & \frac{\partial e_{KP}}{\partial w_2} & \dots & \frac{\partial e_{KP}}{\partial w_N} \end{bmatrix} \quad (3.18)$$

$$w_{t+1} = w_t + \Delta w_t \quad (3.19)$$

$$w_{t+1} = w_t + [J_t^T J_t + \lambda_t I]^{-1} J_t^T E_t \quad (3.20)$$

Figure 3.5 shows the flowchart for training a neural network using Levenberg-Marquardt algorithm.

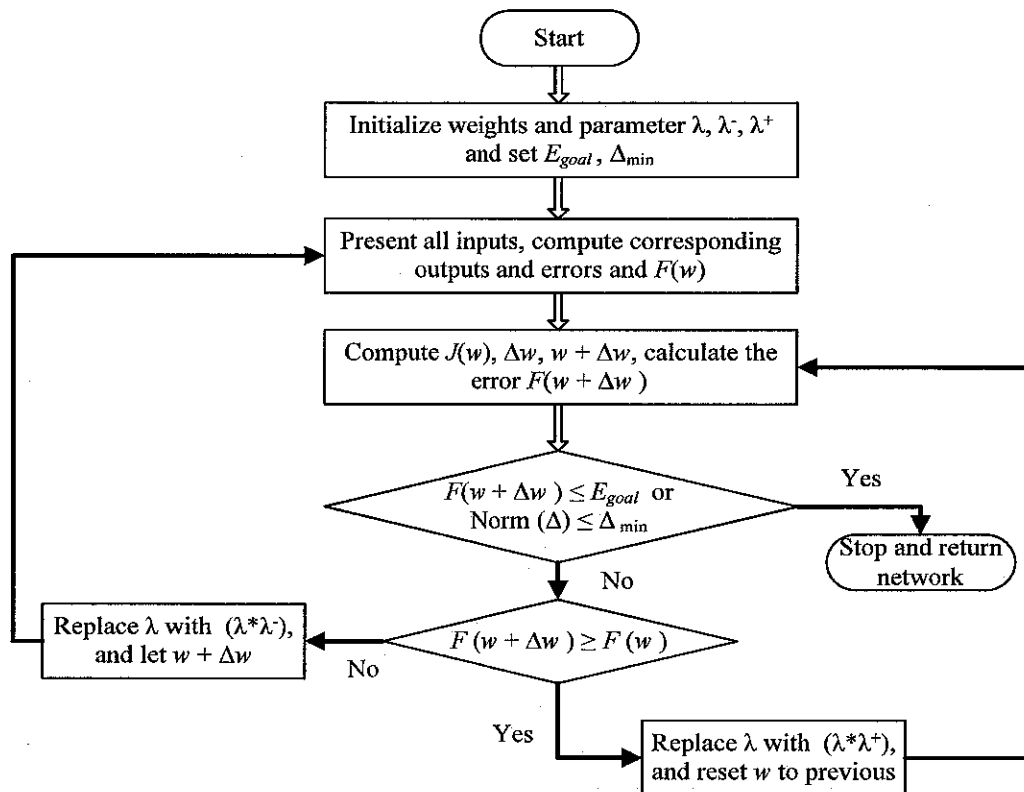


Figure 3.5: Training flowchart of LM algorithm

The steps involved in the training, which can also be inferred from Figure 3.5, are summarized as follows:

- Initialize the weights and parameter λ .
- Present all inputs to the network and compute the corresponding network outputs and errors. Compute the mean square error over all inputs as in Equation (3.16).
- Compute the Jacobian matrix, $J(w)$ where w represents the weights and biases of the network.
- Solve the Levenberg-Marquardt weight update equation (Equation 3.17) to obtain Δw .

- Recompute the weight update using Equations (3.19) and (3.20), and evaluate the error at the new weight vector. If the error has increased as a result of the update, then retract the step (i.e. reset the weights to their previous values) and increase λ by a factor of λ^+ (usually taken to be 10). Then go to step 3 and try an update again. If the error has decreased as a result of the update i.e. if this new error is smaller than that computed in step 2, then accept the step and keep the weights at their new values, reduce λ by a factor of λ^- and go back to step 2. Note: the parameters λ^- and λ^+ are called decrement and increment factors respectively, are predefined values set by the user.
- The algorithm is assumed to have converged when the norm of the gradient is less than some predetermined value, or when the error has been reduced to some error goal.

Alternatively, the following lines of steps are also equally practiced by many scholars for training an artificial neural network using LM algorithm. The idea is similar to the steps mentioned earlier, except that a new parameter called decay rate β is introduced here. In particular, λ is multiplied by decay rate β ($0 < \beta < 1$) whenever $F(w)$ decreases, whereas λ is divided by β whenever $F(w)$ increases in a new step. In short, the steps followed by this method are shown below.

- Initialize the weights and parameter λ ;
- Compute the sum of the squared errors over all inputs $F(w)$;
- Obtain the increment of weights Δw ;
- Recompute the sum of squared errors $F(w)$; using $w + \Delta w$ as the trial w , and evaluate
IF {trial $F(w) < F(w)$ in step 2} THEN:

$$\{w = w + \Delta w ;$$

$$\lambda = \lambda * \beta (0 < \beta < 1); \text{ Go back to step 2}\}$$
ELSE: $\{\lambda = \lambda / \beta; \text{ Go back to step 4}\}$ END IF

The first approach has been followed in this thesis for training the neural network.

3.2.6. Advantages and Applications of ANN in Power Systems

In order to find a relationship between input and output data derived from a system, a more powerful method than the traditional ones are necessary. ANN is an especially efficient algorithm to approximate any function with finite number of discontinuities by learning the relationships between input and output vectors [Bozorgmehry *et al.*, 2005] and [Hagan *et al.*, 1996]. These algorithms can learn from the experiments, and also are fault tolerant in the sense that they are able to handle noisy and incomplete data. The ANNs are able to deal with non-linear problems, and once trained can perform estimation and generalization rapidly [Sozen *et al.*, 2004]. They have been used to solve complex problems that are difficult to be solved if not impossible by the conventional approaches, such as control, optimization, pattern recognition, classification, and so on, specially it is desired to have the minimum difference between the predicted and observed (actual) outputs [Richon and Laugier, 2003].

The main advantages of ANN are summarized as follows:

- Neural networks are generally fast processing units. Though the neural network training is generally computationally expensive, it takes negligible time to take decision based on the training.
- Neural Networks possess learning ability, and represent a complex input-output relationship in a simple, yet efficient way.
- Neural networks adapt to certain data and do not need to be reprogrammed.
- Neural networks are by and large robust –insensitive to noise factors.
- Neural networks are appropriate for non-linear modeling.
- A neural network can perform tasks that a linear program cannot.
- When an element of the neural network fails, it can continue without any problem by their parallel nature.
- Neural networks can be implemented in any application without any problem.

Neural networks now operate well with modest computer hardware. Although neural networks are computationally intensive, the routines have been optimized to the point that they can now run in reasonable time on personal computers. Neural networks build informative models while the more conventional models fail to do so. Basically,

an ANN is configured for a specific application, such as forecasting and prediction or reconstruction/recognition through learning process that involves adjustments to the synaptic connections that exist between neurons, hence, can handle complex interactions. Because of handling very complex interactions, the neural networks can easily model data, which are too difficult to model traditionally [Osman and Al-Marhoun, 2002]. The neural networks built models are more reflective of the data structure and are significantly faster.

In power system, mathematical optimization (algorithmic) methods have been used over the years for many power systems planning, operation, and control problems. Mathematical formulations of real-world problems are derived under certain assumptions, and even with these assumptions; the solution of large-scale power systems is not simple. On the other hand, there are many uncertainties in power system problems because power systems are large, complex, and geographically widely distributed. More recently deregulation of power utilities has introduced new issues into the existing problems. It is desirable that solution of power system problems should be optimum globally, but solution searched by mathematical optimization is normally optimal locally. These facts make it difficult to deal effectively with many power system problems through strict mathematical formulation alone.

The electric power industry is currently undergoing an unprecedented reform. One of the most exciting and potentially profitable recent developments is increasing usage of artificial intelligence techniques. Networks have been used in a board range of applications including: pattern classification, pattern recognition, optimization, prediction and automatic control. Consequently, the application of ANNs in different power system operation and control strategies has led to acceptable results [K. Warwick, et al., 1997], [G. Rolim, et al., 2003] and [R. Lukomski, et al., 2003]. Recent developments in the area of AI applications to power systems have showed that the following fields have attracted the most attention in the past five years: fault diagnosis/fault location, transient stability, security assessment, load forecasting, economic dispatch and harmonic analyzing. In general, it has been repeatedly verified

by a number of scholars that neural networks can solve complex power system problems in the easiest and most attractive way.

3.3. OPTIMIZATION METHOD -TAGUCHI'S METHODOLOGY

Taguchi's method, pioneered by Dr. Genichi Taguchi and developed as a standardized optimization technique of control parameters in process, is based on the statistical analysis of data and offers a simple means of analysis and optimization of complex systems. Taguchi method is a scientifically disciplined mechanism for evaluating and implementing improvements in products, processes, materials, equipment, and facilities. These improvements are aimed at improving the desired characteristics and simultaneously reducing the number of defects by studying the key variables controlling the process and optimizing the procedures or design to yield the best results.

TM is a statistical method for analyzing experimental data for determining and optimizing the effects and levels of the various factors (parameters) involved in a system, allowing this to be done within less experimentation than in traditional methods. It merges statistical and engineering techniques to increase efficiency and productivity, and minimize costs of products, and manufacturing processes. TM further incorporates a method called parameter design for deciding the best optimal values (levels) of variable control factors which effect final product quality or cost. TM achieves this by experimenting on orthogonal arrays of the control factors of the system, and considering the variation of various noise sources. Basically, selection of an optimal set of values can reduce or minimize the effects of factor errors.

The method is applicable over a wide range of engineering fields that include processes that manufacture raw materials, sub systems, products for professional and consumer markets. In fact, the method can be applied to any process be it engineering fabrication, computer-aided-design, banking and service sectors etc. It has been verified that it greatly improves engineering productivity [H. R. Lochner, 1990].

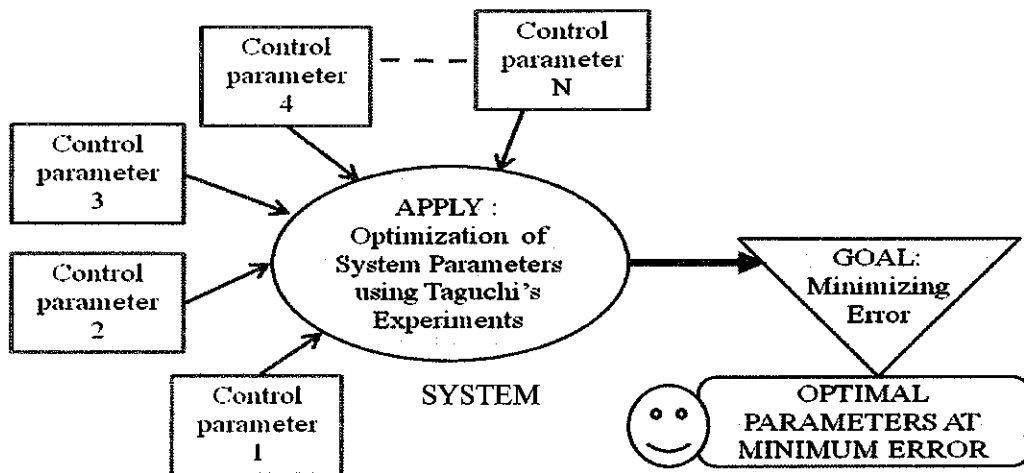


Figure 3.6: A schematic diagram demonstrating the use of Taguchi's experiment on various control parameters to minimize the error.

Taguchi method is useful for tuning factors in a given process, that significantly influence the quality of output/product of the process, for best results with minimum error. Figure 3.6 is a schematic diagram demonstrating the use of Taguchi's experiment on various control parameters to minimize the overall error of a system or process. The diagram signifies that the various control parameters are considered to greatly affect the output/product of the system or process. Hence, by fine-tuning the values of these parameters by applying Taguchi's method, an optimal combination from a set of their pre-determined levels, which offers minimum error, is selected.

In general, the total number of combinations is given as in Equation (3.21).

$$N_c = L^P \quad (3.21)$$

where N_c = total number of experiments (combinations)

L = number of levels for each factor

P = number of factors (parameters).

If, for example, there is an experiment requiring 21 factors at 4 different levels, it would require 4^{21} experiments ($= 4.3 \times 10^{12}$) to investigate all the possible combinations. Using Taguchi methods, however, only 64 experiments are required. For this reason, such an array is called a L_{64} orthogonal array, a type of experiment

where the columns for the independent variables are “orthogonal” to one another. The benefits of such experimentation include:

- Conclusions valid over the entire region spanned by the control factors and their settings;
- Large saving in the experimental effort; and
- Easy analysis.

TM is a handy tool to optimize some decisive parameters in neural networks to effectively hit the target. For instance, the usual practice to set the number of hidden layer neurons is ‘trial and error’. This practice, however; is inefficient and may not deliver the optimal solution. In the content of this work, Taguchi’s method is used to optimize the neural network’s control parameters of each training algorithm used. Specifically, the control parameters used in EBP algorithm are number of hidden neurons (h), learning rate (η) and momentum term (α). Whereas, number of hidden layer neurons (h), decay rate (β), and learning parameter (λ) are used in LM algorithm. And, the control parameters used in RPROP algorithm are initial update value (Δ_0), increase factor (η^+), decrease factor (η^-), decay factor (α) and number of hidden layer neurons (h). Among combinations of certain levels of the control parameters, the one with the smallest output error is selected after the Taguchi’s experiments.

The standard eight step procedures which Taguchi proposed to apply his method for optimizing any process are as follows:

- Identify the main function, side effects, and failure mode
- Identify the noise factors, testing conditions, and quality characteristics
- Identify the objective function to be optimized
- Identify the control factors and their levels
- Select the orthogonal array matrix experiment
- Conduct the matrix experiment
- Analyze the data; predict the optimum levels and performance, and
- Perform the verification experiment and plan the future action.

3.4. SUMMARY

In this Chapter, a review of artificial neural networks fundamental network elements topology, their applications in power system areas have been discussed. And, some of the main training methodologies specifically employed in this study, and data pre-processing and post-processing approaches, that help obtain required results from the neural network, have been described in detail. In addition, in depth analyses of information on Taguchi's methodology, the procedures followed and its application in our study have been also discussed.

CHAPTER FOUR

MODEL POWER SYSTEM SIMULATIONS AND DATA GATHERING

4.1. INTRODUCTION

As explained in the previous Chapters, the study is exclusively based on simulation of model power system network while due attention is given for validation of the work with IEEE benchmark electric system network. The simulation process encompasses simulations of model power system network and neural network. The latter is discussed in the next Chapter. The overall flow of the simulation work is shown in Figure 4.1.

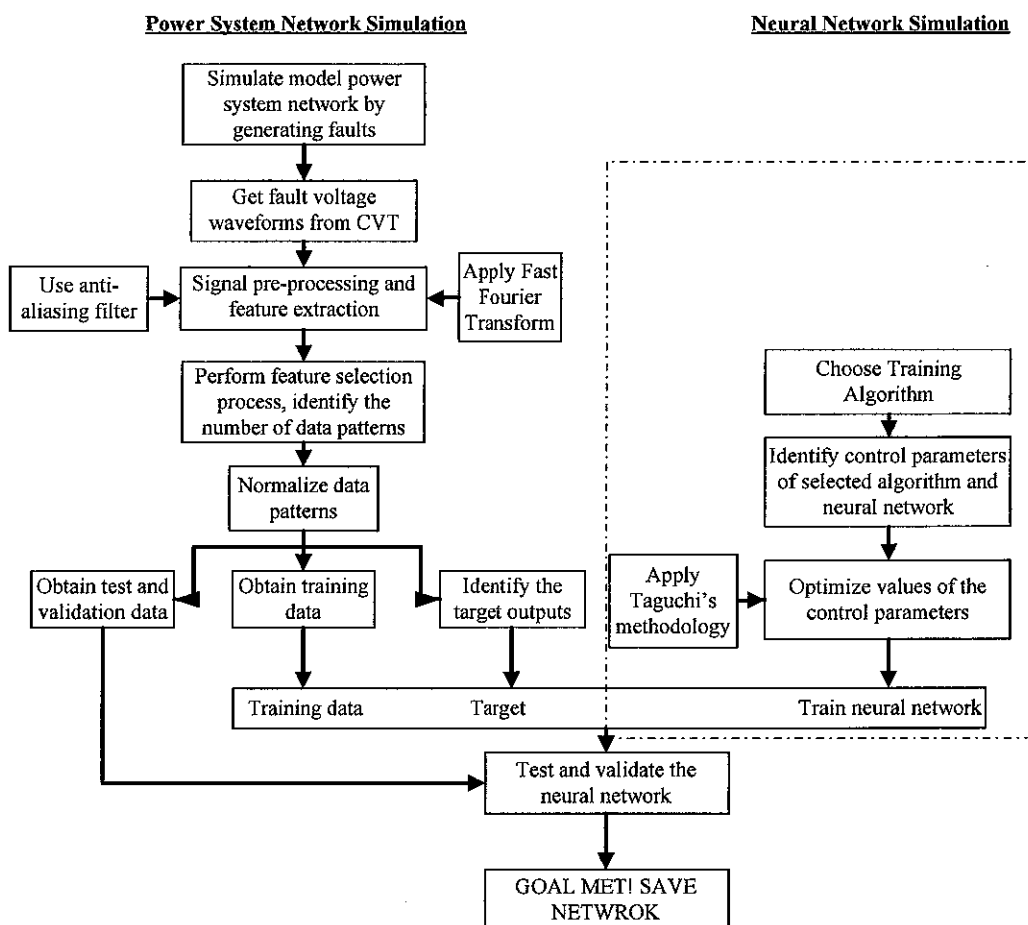


Figure 4.1: Schematic outline of the simulation work

Figure 4.1 illustrates an insight of the system simulation and other intermediate processes. To generate sufficient number of data patterns for training the neural network, simulation of a single machine infinite bus (SMIB) power system model by generating a number of faults on the transmission line followed by capturing signal from Capacitor Voltage Transformer (CVT) are performed. The signal conditioning and feature extraction processes are carried out by applying anti-aliasing filter and Fast Fourier Transform respectively. However, anti-aliasing filter, commonly used in practical digital sampling systems to avoid acquiring bad data due to noise factors, has been skipped; yet, many technical articles advised using anti-aliasing filters in practical implementation [Math H. J. Bollen, et al. 2006].

Following the feature extraction, selection of decisive features which are adequate for the neural network to identify one fault from the other, and deciding the number of data patterns required for sufficiently training the neural network are done. Then, the data pass through normalization process (which is discussed later in next Chapter), and get break up into sets of training, testing and validation data.

On the other hand, the selection of suitable algorithm for training the neural network is mandatory. To get the neural network effectively trained, and obtain reasonable outcome with high accuracy, optimization of key parameters of the algorithm and neural network is required which is met by using a robust system parameters design methodology –Taguchi’s method (Details are discussed in the previous Chapters). The final steps in the whole process are training, testing and validating the neural network for perfection, the return being a fully functional neural network which can make accurate decisions whenever is required.

The simulation results based on SMIB model are validated by following the same process using benchmark IEEE 9-bus and 14-bus electric power systems. This Chapter addresses the major power system simulation case studies on SMIB and IEEE 9-bus system models, particularly, for obtaining data patterns for effectively training the neural network. Moreover, a number of faults are also generated on IEEE 14-bus

electric power system model for testing the robustness and effectiveness of the trained neural networks in the previous models.

4.2. CASE STUDY I: A SINGLE MACHINE - INFINITE BUS SYSTEM

4.2.1. Introduction

In the first stage of the research work, a single machine connected via an EHV transmission line to an infinite bus system was considered for simulation purpose. Before the details of simulation results of the considered system are discussed, it is important that the concept of infinite bus be understood.

In solving power system problems, it is common practice to assume one bus, usually the receiver bus, as an infinite bus, as shown in Figure 4.2. An infinite bus is characterized by the following properties [Atif Zaman Khan, 1998].

- *It has infinite capacity.* The capacity of the generators directly connected to the infinite bus is so large compared to the amount of power supplied by a transmission system so that a fault at any point on the transmission system will not cause the receiver end bus voltage to decrease appreciably.
- *It is not affected by external fault.* Any fault on the transmission system changes the loading on the generators at the receiver end to a very small percentage; thus, the change in rotor speed above or below synchronous speed is negligible. Rotor positions of the synchronous machines directly connected to the infinite bus are considered to change insignificantly. Under such circumstances, the fault causes a change in operating angle of the generator rotors at the sending end of the transmission system only.
- *It has constant bus voltage and frequency.* All generators, when loaded onto a power system, will to some degree alter the system's voltage and frequency. However, when a small generator is loaded on a large system, it will have negligible effects on the voltage and frequency. Thus, an infinite bus absorbs or supplies any amount of real and reactive power from or to the transmission

system without change in bus voltage. As a result, an infinite bus is considered as an ideal voltage source.

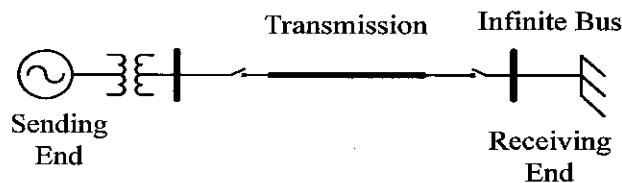


Figure 4.2: Single machine infinite bus (SMIB) power system

The concept seems to be ideal. However, the simplicity and overall usefulness of SMIB model continues to find wide use by scholars in power system studies [H.F. Wang, et al. 1997]. It has been repeatedly proven that this model is capable of providing reliable results and outstanding approximations while dealing with a complex power system grid [Sidhartha Panda, et al. 2007].

4.2.2. Fault Simulations on SMIB Electric Power System Model

As mentioned before, Figure 4.3 shows SMIB model with a 400 kV transmission line connecting the generator and the infinite bus. This model is primarily considered in the simulation. Since transmission lines are currently series-compensated to boost their loading capacity, it was essential to take a series and parallel compensated transmission line for the intended research work. A standard flat transmission line tower configuration, whose details of all parameters are given in Appendix A, is set up for simulation. Added to this is that the frequency-dependent distributed model is used to represent the line, and for computing the transmission line parameters. The physical configurations of transmission line conductors and towers are described to the simulation software, and the frequency-dependent parameters of the line are calculated via MATLAB SimPowerSystems from the constant line parameters.

The model shown in Figure 4.4 is set up in MATLAB Simulink with a generator, rated at 1200 MVA and 13.8 kV with reactance to resistance (X/R) ratio of 20. The sending end is connected via a 400 kV transmission line to the receiving end with surge impedance loading (SIL) of 15000 MVA [Kimbark, et al. 1998]. The model is simulated by generating several faults (including line to ground and line to line) using

MATLAB SimPowerSystems simulation software. The faults are generated at different locations with variable fault resistance and fault duration. Throughout the simulation, the ground resistivity is taken to be $100 \Omega\text{m}$ which is practically acceptable.

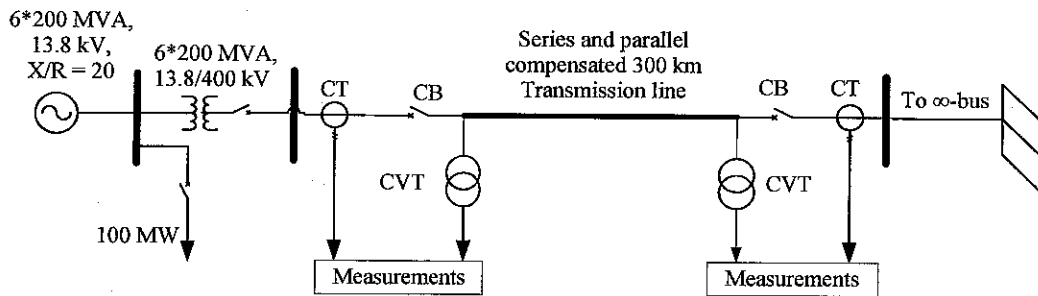


Figure 4.3: Single line diagram of line model used in the study

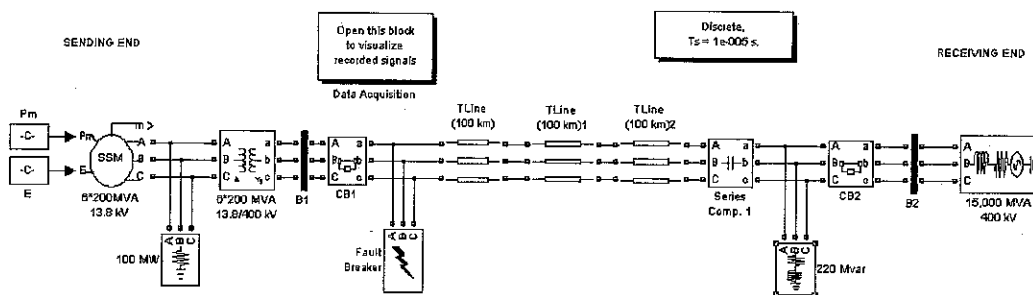


Figure 4.4: A setup of SMIB model in Simulink

The simulation of faults is based on realistic faults model described in [A. T. Johns, et al. 1994], where a time dependent dynamic resistance representation of a primary arc and improvements to the dynamic conducting characteristics of secondary arc models are adopted with emphasis on an empirical approach which is used to determine the parameters of the models. Fault voltage and current signals are taken from measurements as shown in Figure 4.3. A typical single phase-to-ground temporary fault generated at 50 km away from the sending end is shown in Figure 4.5. Figure 4.6 demonstrates the permanent fault voltage waveform for three phases to ground fault generated at midpoint in the transmission line. Extensive study on various fault waveforms are conducted by taking in to consideration different factors that have

significant influence on faults; typically, fault inception, fault resistance, fault duration and location.

Fault Distance –Different types of faults are applied at 10 km intervals on the 300 km long transmission line. As far as the location is concerned, the faults are observed to have more total harmonic distortion near the sending end than those near the receiving end.

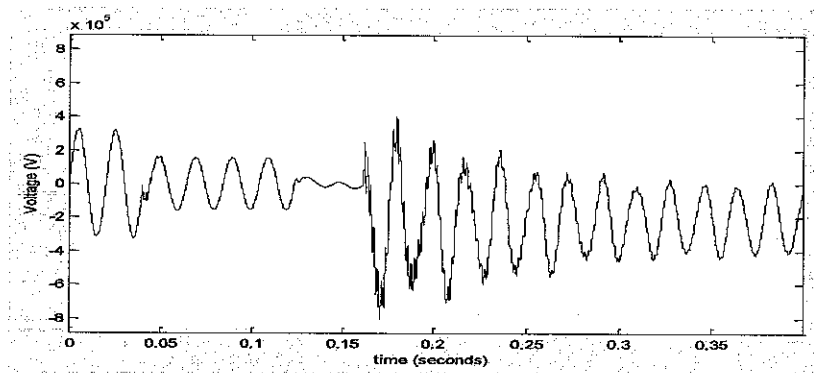


Figure 4.5: Temporary a-phase-to-ground fault voltage waveform

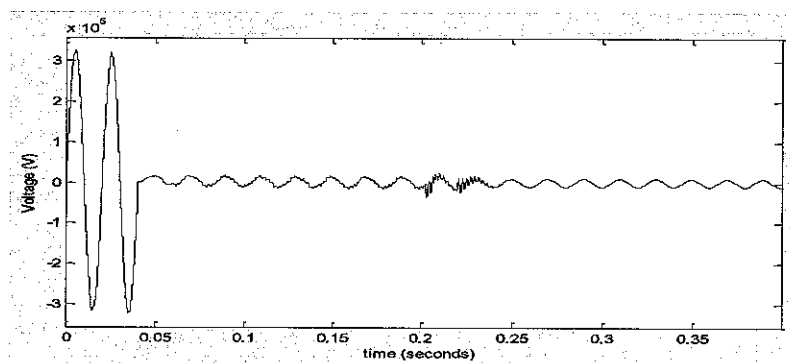


Figure 4.6: Permanent three-phase-to-ground fault voltage waveform

Fault Types –The types of faults applied on the transmission lines are:

- Single phase to ground fault,
- Double phase fault,
- Double phase to ground fault, and
- Three phase fault.

Fault Resistance –The intensity of the fault decreases with the increase in the value of fault resistance. The cases were simulated by assuming dynamic representation of fault resistance as based on the reference [A. T. Johns, et al. 1994].

Fault Inception Angle – Fault cases are developed with the fault inception angle equal to 90° and 0° .

In general, this study endeavored a lot to represent the possible faults that potentially occur in a power transmission system.

4.2.3. Feature Extraction and Selection

ANN solutions often employ a pre-processing stage of feature extraction. The aim of feature extraction is to extract valuable information from certain data, in this case the simulated fault voltage waveforms, which can be used to identify and classify the input data with sufficient accuracy. In general, feature extraction is an important pre-processing step as selected features must characterize properly a variety of power systems fault conditions.

For obvious reasons, the simulated fault voltage waveforms should undergo some form of transformation so as to help extraction of important features of temporary and permanent faults. Most of the earlier approaches using ANN were based on comparing voltage or current values with a preset threshold, measuring total harmonic distortion or peak voltage, etc. and features were taken from the time domain analysis of fault voltages or currents (for more details, please refer to Section 2.10 of Chapter 2). A closer investigation of all sorts of fault waveforms showed that time domain analysis is not viable to use it as feature extracting method; nor are the time-domain waveforms convenient to feed directly as input to a neural network. The faults generated on a system contain a wide range of frequency components. Hence, certain parameters of the identified characteristics must be extracted to fully represent the state of the transmission line. From an analysis point of view, the most distinct characteristics of the waveforms are those associated with the variation of the frequency components over time. Thus, the frequency domain decomposition of features is adopted. The sequential spectral analysis of the fault voltage waveforms is

made by Fast Fourier Transform (FFT). FFT processing has been adopted in this work because of its faster, efficient and more reliable signal processing ability over Discrete Fourier Transform. Hence, FFT is used to examine the simulated fault voltage waveforms in frequency model for the feature extraction scheme.

The other challenge here is feature selection process. This is a process of finding the most significant variables (in this case, the harmonic components), eliminating redundancy (from the simulated faults) and reducing the dimension of the pattern vector which simplify the amount of resources required to describe a large set of data accurately. When performing analysis of complex data, one of the major problems stems from the number of variables involved. Analysis with a large number of variables generally requires a large amount of memory, and computation power or a classification algorithm which overfits the training sample, and generalizes poorly to new samples. This means when the number of inputs is large, but the number of training examples is relatively small, it may result in poor generalization performance.

In any way, the data should be rendered into a form which makes the ANN more effective at making decisions and making computation easier and faster. To facilitate the decision making process of the proposed adaptive auto-reclosure scheme, the fault voltage waveforms are separated into sets of one cycle windows. An extensive series of studies using spectrum analysis has shown that for each cycle, certain frequency components can be selected as the potential features. This process is carried out by taking information from the energy of the harmonics of the fault voltages. In this study, the following six parameters of the fault voltage have been clearly identified as those representing the most significant features of the state of the transmission lines:

- DC component,
- Fundamental component,
- Second harmonic component,
- Third harmonic component,
- Fourth harmonic component,
- Fifth harmonic component.

These features are selected because of their importance in the overall fault voltage waveforms. The features are then used as inputs to the neural network. An extensive

series of test results have clearly shown the effectiveness of selecting these specific features.

Typical FFT signals for corresponding temporary single-phase-to-ground and permanent three-phases-to-ground fault voltages are shown in Figures 4.7 and 4.8 respectively.

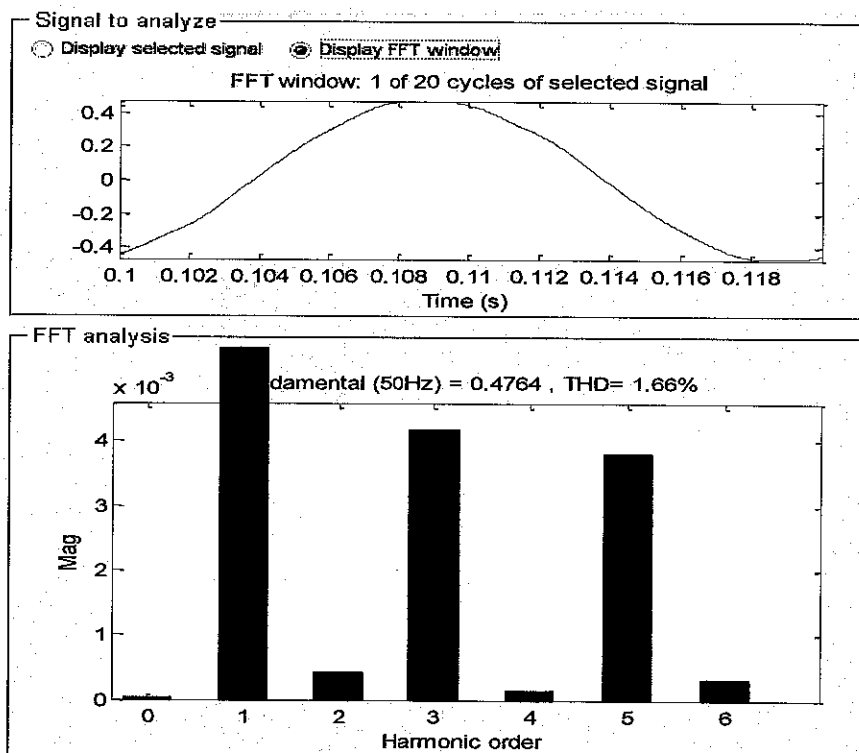


Figure 4.7: FFT of voltage signal for single-phase-to-ground temporary fault

Table 4.1 represents some of the data patterns extracted from the FFT spectra of the fault voltage signals.

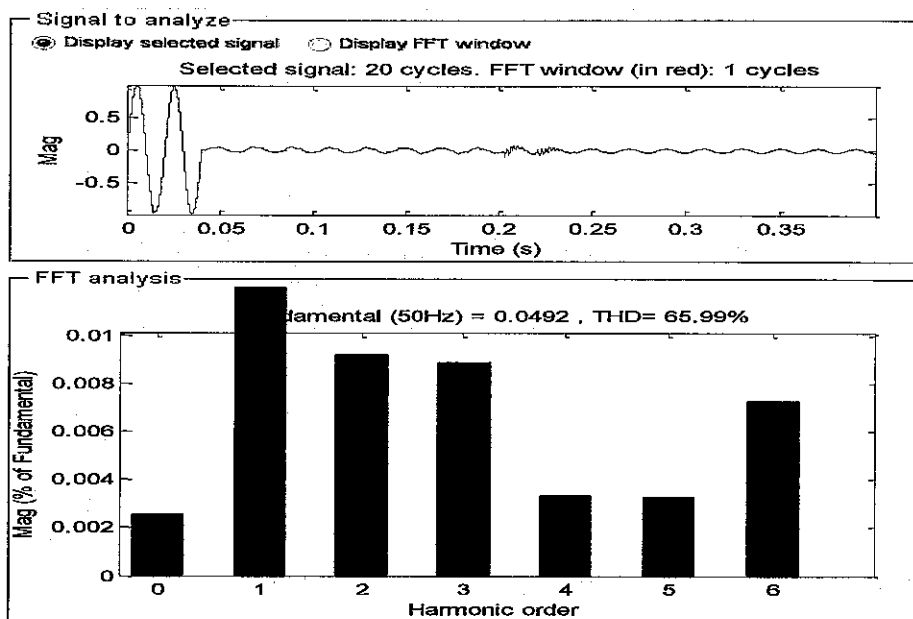


Figure 4.8: FFT of voltage signal for three-phases-to-ground permanent fault

Table 4.1: Some simulated data patterns for training ANN and the target values

DC	50 Hz	100 Hz	150 Hz	200 Hz	250 Hz	Target
Temporary fault data pattern						
0.537762	6.090184	1.166236	2.624032	0.157442	1.749355	1
1.986682	10.81445	1.985379	4.467102	0.268026	2.978068	1
4.014074	18.54088	0.594530	1.337692	0.080262	0.891795	1
2.339997	16.76247	0.209368	0.471079	0.028265	0.314053	1
Fault free (cleared fault) data patterns						
6.847229	16.15522	0.041376	0.093095	0.005586	0.062063	0
5.925262	16.21791	0.007813	0.017579	0.001055	0.011719	0
4.770965	16.22556	0.006001	0.013502	0.000810	0.009001	0
4.523346	16.22684	0.005688	0.012798	0.000768	0.008532	0
Permanent fault data patterns						
0.008609	0.279653	0.064918	0.146066	0.008764	0.097377	1
0.054321	0.150095	0.000888	0.001998	0.000120	0.001332	1
0.027465	0.150511	0.000448	0.001008	0.000060	0.000672	1
0.013359	0.150602	0.000240	0.000539	0.000032	0.000359	1

The FFT output features clearly showed the differences in the spectra of both types of faults, and are useful features for the ANN to recognize the fault type. When the frequency spectra for different waveforms of data were examined, some important differences were noticed. For instance, there is more high frequency energy while a temporary fault exists than when the fault has been extinguished (or while system is healthy). Higher harmonic components of temporary faults are higher in magnitude than those of permanent and cleared faults while the DC and fundamental components in temporary fault samples are mostly lower than that of their consequent extinguished samples i.e. cleared fault cases contain higher system frequency component and smaller harmonic components. Figure 4.9 shows the energy contained in each harmonic component for seven temporary fault samples (taken immediately after fault inception) and corresponding seven cleared fault samples (taken one cycle after the fault has been extinguished). The stacked column representation of temporary and cleared fault patterns as shown in Figure 4.9 and the data patterns in Table 4.1 clearly illustrate the differences previously mentioned.

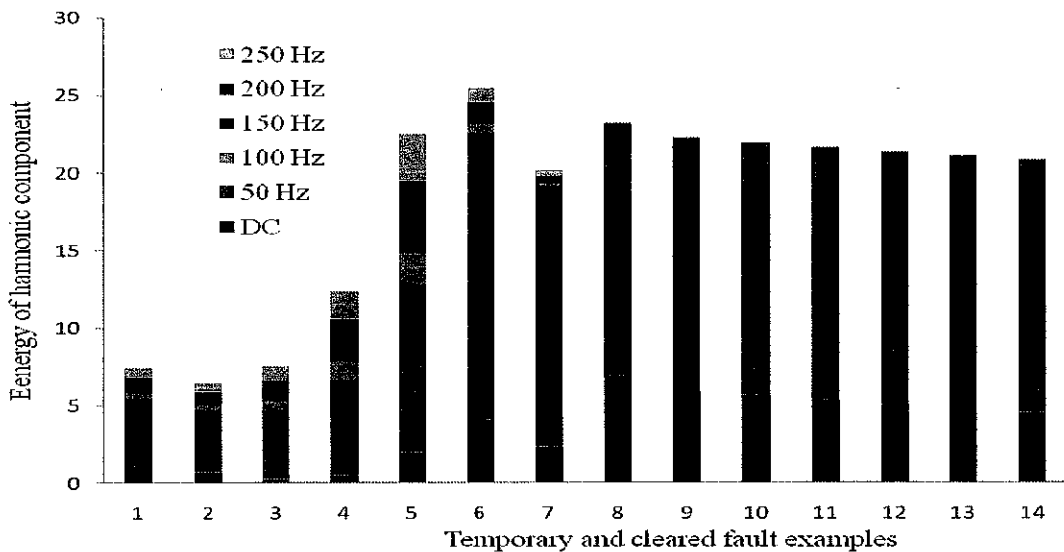


Figure 4.9: A stacked column representation of temporary and cleared fault patterns

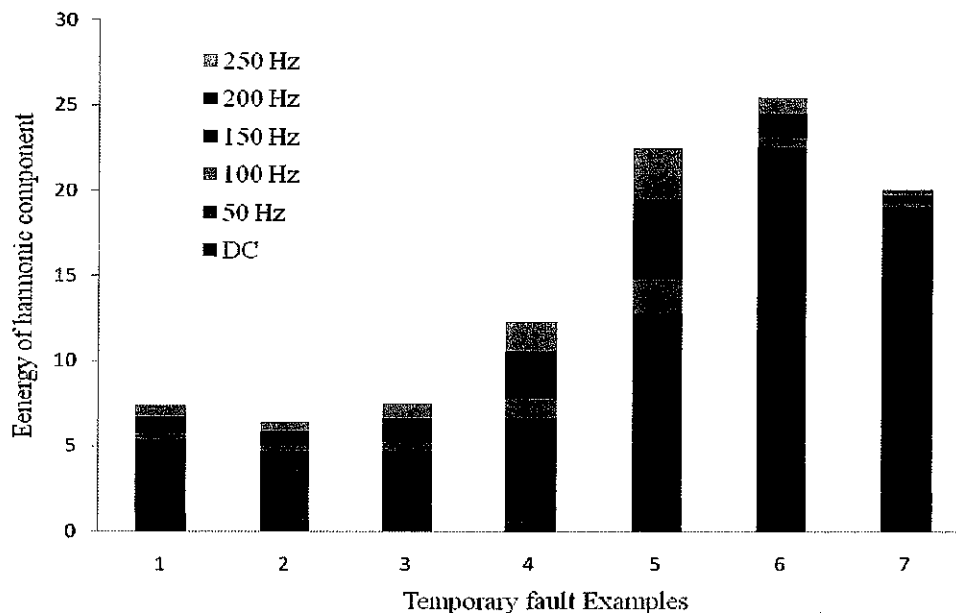


Figure 4.10: A stacked column representation of temporary fault patterns

On the other hand, the permanent fault waveforms contain smaller fundamental frequency component and harmonic components than their temporary counterparts. To have a closer investigation of the variations of harmonic components and to easily identify the differences, the data patterns are separately plotted with stacked column representation as shown in Figures 4.10 through 4.12.

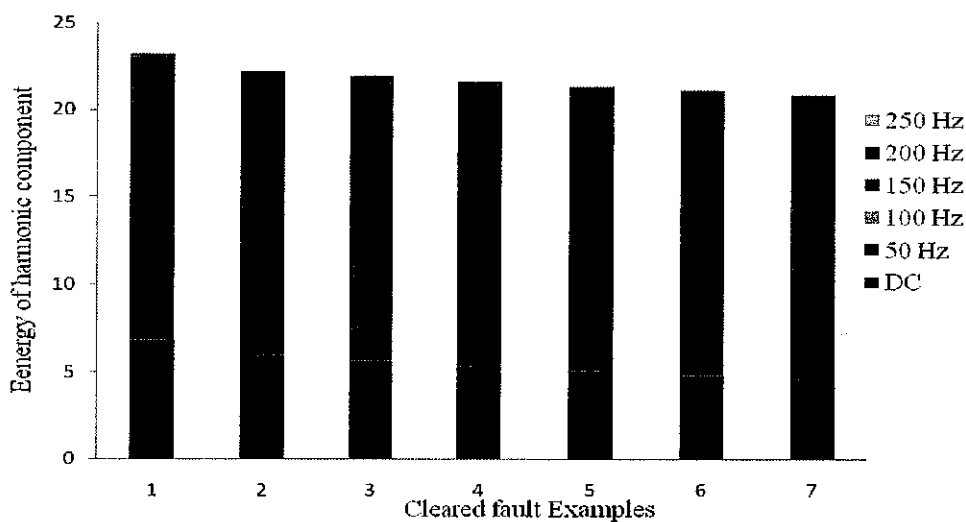


Figure 4.11: A stacked column representation of cleared fault patterns

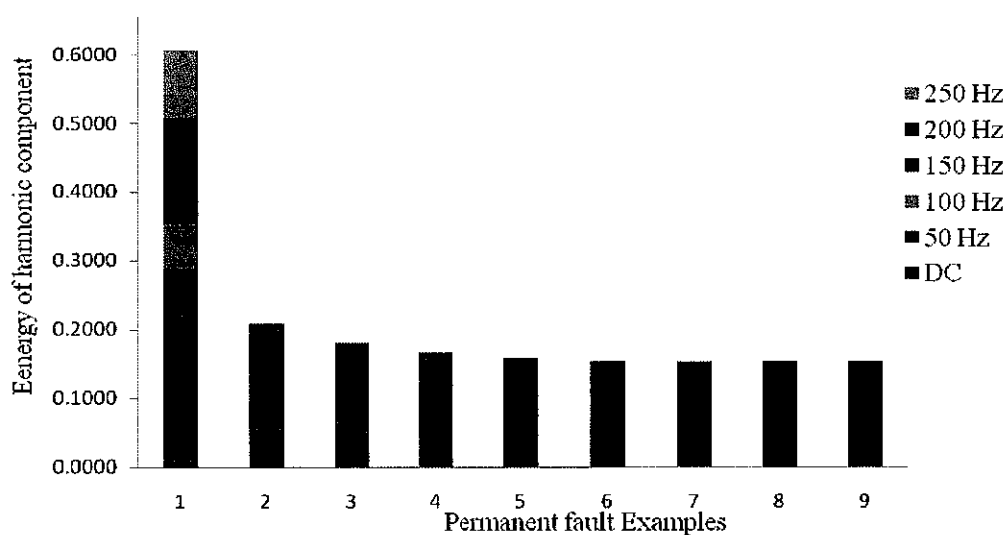


Figure 4.12: Stacked column representation of permanent fault patterns

A total of 43 patterns have been readied for training the neural network. Among these patterns, 13 are taken from temporary faults, 13 are taken when the temporary faults extinguish, and the rest 17 are from permanent faults. In addition to this, 23 different data has been reserved for testing the neural network after it has been fully optimized through training. The following Chapter discusses about the issues in the neural network simulation (optimization + learning) phase.

4.3. CASE STUDY II: IEEE 9-BUS ELECTRIC POWER SYSTEM

4.3.1. Introduction

Figure 4.13 shows the benchmark IEEE 9-bus electric power system model whose data are taken from [Anderson and Fouad, 2003]. This model has been previously successfully used in wide range of power system analysis. The model consists of three generators, six transmission lines, three transformers and three loads. The transmission line extending from busbar 8 to busbar 7 is the line of interest for simulations during the study. For more generality, it is empirical to consider the transmission line as series and parallel compensated. Moreover, a standard flat transmission line tower configuration is considered during the simulation and the

frequency dependent distributed model is used to represent the line.

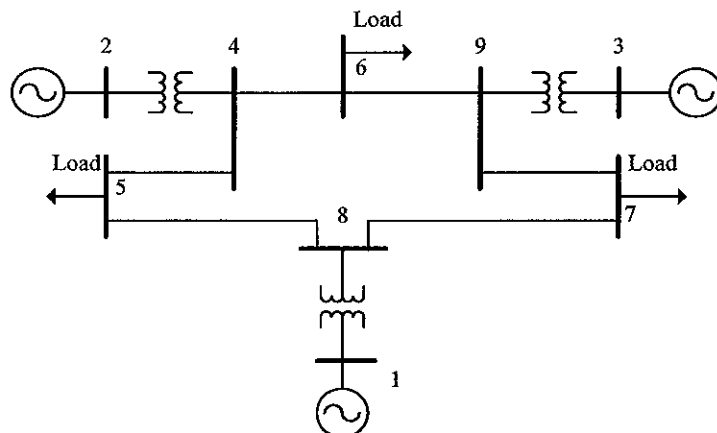


Figure 4.13: Single line diagram of an IEEE 9-bus system used in the study

4.3.2. Fault Simulations on IEEE 9-Bus Electric Power System Model

Before the ANN implementation, time domain simulations considering several contingencies are carried out for the purpose of gathering the training data sets. Simulations are carried out by using MATLAB-based SimPowerSystems software package. The model is set up in Simulink as in Appendix D, and is simulated by generating several faults in the 240 km long transmission line extending from busbar 8 to busbar 7. Certain parameters including fault models are kept the same as that of SMIB model. An extensive study on various fault waveforms is conducted by taking into consideration factors that have significant influence on the faults –fault inception, fault resistance, fault duration and location. Fault voltages are taken from measurements at busbar B8 and line capacitor voltage transformer (CVT) as shown in Simulink setup in Appendix D.

A typical single-phase-to-ground temporary fault voltage signal generated at mid way from the sending end is shown in Figure 4.14. And, Figure 4.15 demonstrates permanent fault voltage waveform for three-phases-to-ground fault generated at midpoint of the line.

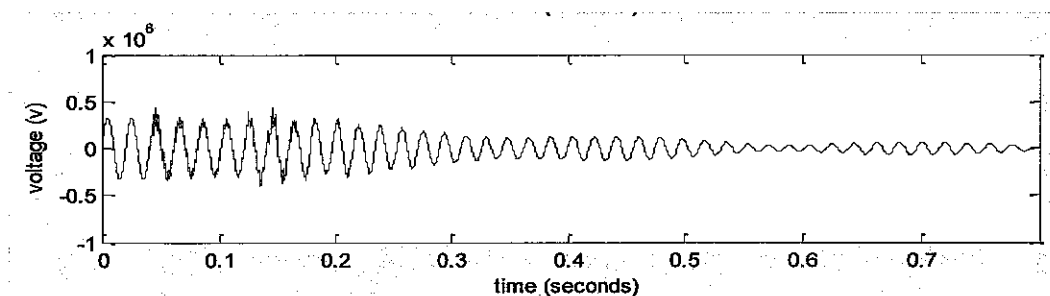


Figure 4.14: A temporary single-phase-to-ground fault voltage

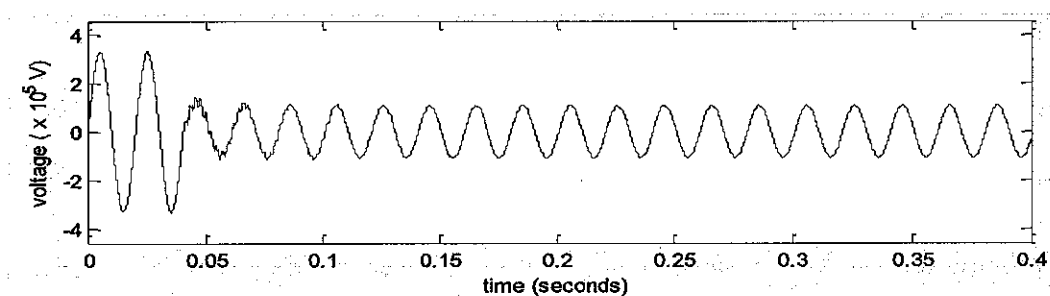


Figure 4.15: A permanent three-phase-to-ground fault voltage

4.3.3. Feature Extraction

Before the ANN implementation, time domain simulations considering several contingencies are carried out for the purpose of gathering the training data sets, which is termed as feature extraction. The feature extraction process is done in the same way as in SMIB model. A total of 100 different data patterns are extracted from 70 faults, 30 of which are temporary and the remaining 40 are of permanent type. The other 30 data patterns have been extracted from sample voltage waveforms when the fault has been extinguished. As mentioned previously (refer to SMIB simulations), the extraction of features is carried out by taking information from energies of harmonics of the fault voltages which is handled with Fast Fourier Transform (FFT). FFT is employed to examine the simulated fault voltage waveforms for feature extraction scheme. A typical FFT signal analyzed from a single cycle of a temporary fault voltage waveform is shown in Figure 4.16.

Similar to the previous case study, the following six parameters of faulted voltage waveform have been clearly identified as those representing the most significant features of the state of the fault for further investigation:

- DC component,
- Fundamental component
- Second harmonic component,
- Third harmonic component,
- Fourth harmonic component,
- Fifth harmonic component.

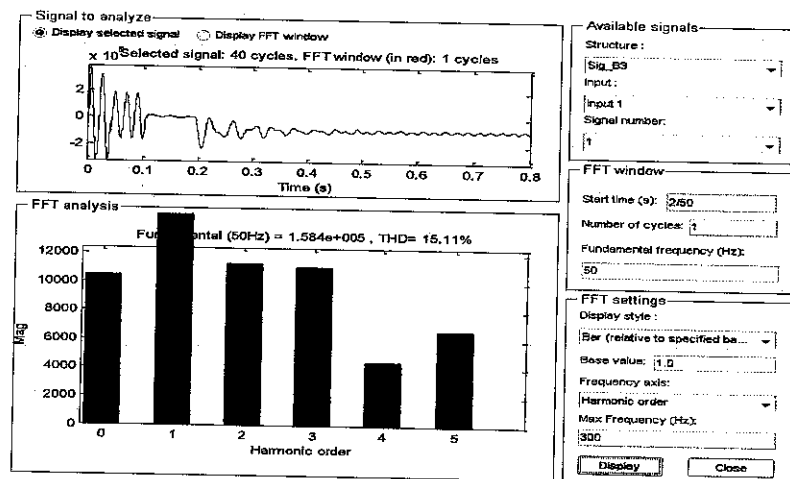


Figure 4.16: FFT analysis of a sample taken from temporary 2-phase-to-ground fault

The FFT analyses, like that of previous model –SMIB, show the differences in the spectra of the faults in consideration. The differences in magnitude of the energies of harmonic components were crucial in the overall feature extraction and selection of key features. From the spectral (FFT) analysis of the fault voltage waveforms, the following conclusions can be drawn:

- There is more high frequency energy while a temporary fault exists than when the fault has extinguished. A stacked column plot of energies of harmonic components versus sample data patterns is shown in Figure 4.17. This strengthens the fact that there are higher harmonic components in temporary faults before they vanish out.

- Cleared faults mostly contain higher system (fundamental) frequency component and DC component than temporary faults. This can be best understood from Figures 4.17 and 4.18.
- Permanent faults contain smaller fundamental component and harmonic components than temporary ones. This is illustrated by Figures 4.18 and 4.19.

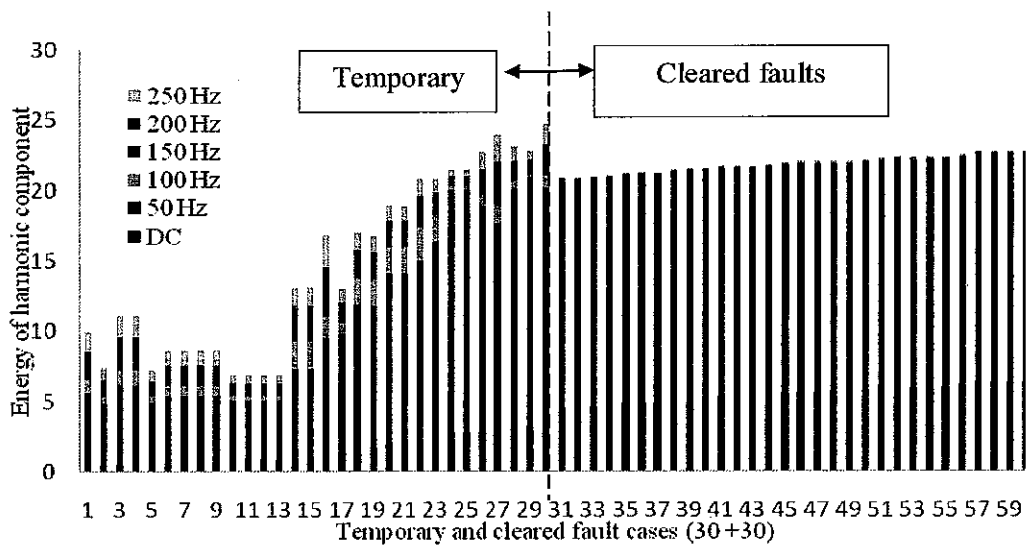


Figure 4.17: Stacked column representation of temporary and cleared fault data

Figure 4.18 shows the energy contained in each harmonic component for 60 different temporary fault samples from which 30 of the sample data are obtained by immediately examining the first cycle after the fault inception and the remaining 30 data are taken from the 10th cycles where the faults fully extinguish. In other words, each of the temporary faults starts 2 cycles after initiation of simulation, lasts for about 3 to 5 cycles, and fully extinguishes after 8th cycle. The 3rd and 10th or 11th cycles of voltage waveforms are taken as samples for training ANN. Some of the extracted features for all types of faults (temporary, cleared and permanent) are shown in Appendix C. As mentioned earlier, (For FFT results of temporary fault before and after extinction, refer to Appendix E). Both temporary and cleared fault sample data are also plotted individually in Figures 4.19 and 4.20.

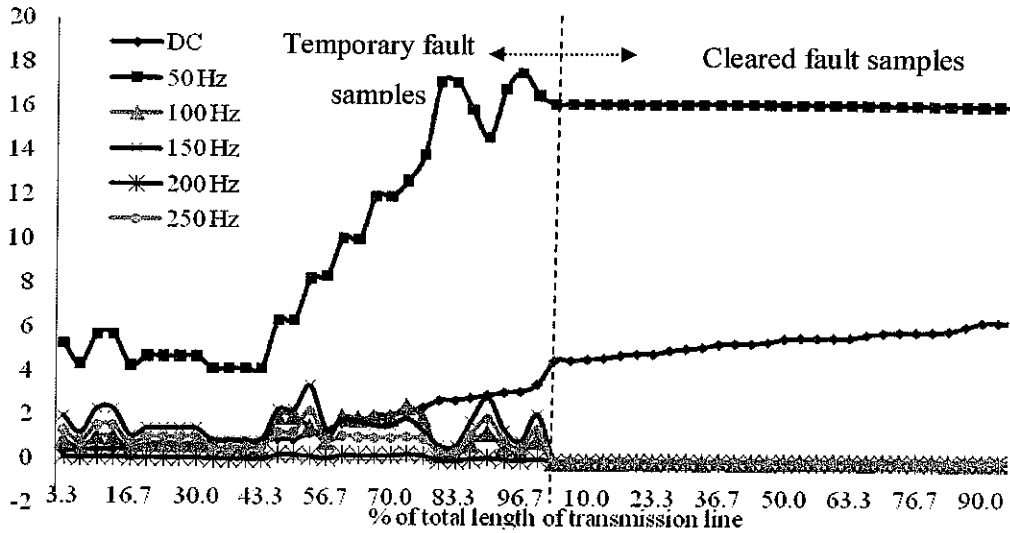


Figure 4.18: Energies of temporary and cleared fault samples vs. location of fault

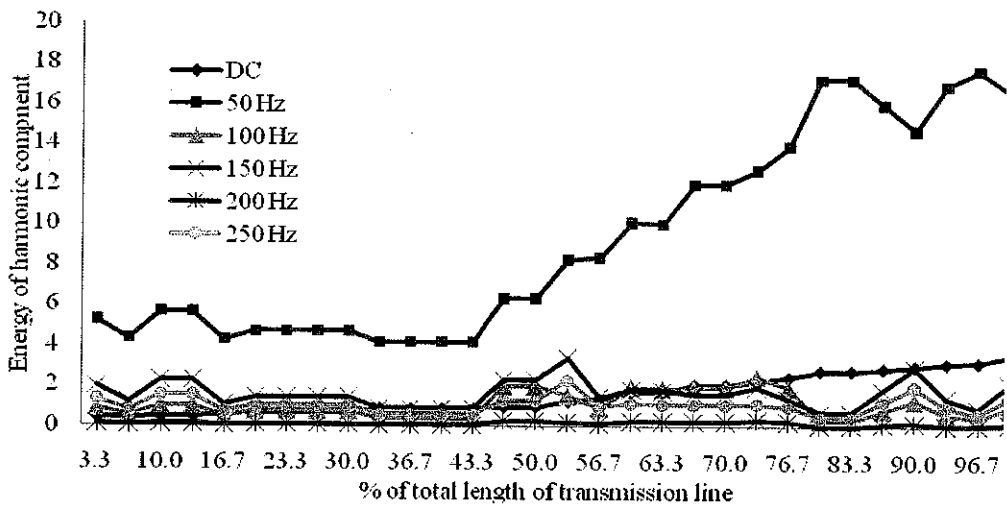


Figure 4.19: Energies of harmonic components of temporary fault patterns vs. location of a fault (% of total length)

On the other hand, Figure 4.21 illustrates a plot of the energy contained in each harmonic component for permanent fault samples with increasing fault location from the sending end. Similar to the case of temporary faults, permanent fault data have been taken twice –immediately after the fault inception and ten cycles after the fault

inception. Unlike to the temporary fault case, the two cases more or less have the same features. This is due to the fact that a permanent fault persists for a longer time as opposed to the transient fault case which usually vanishes shortly following a trip.

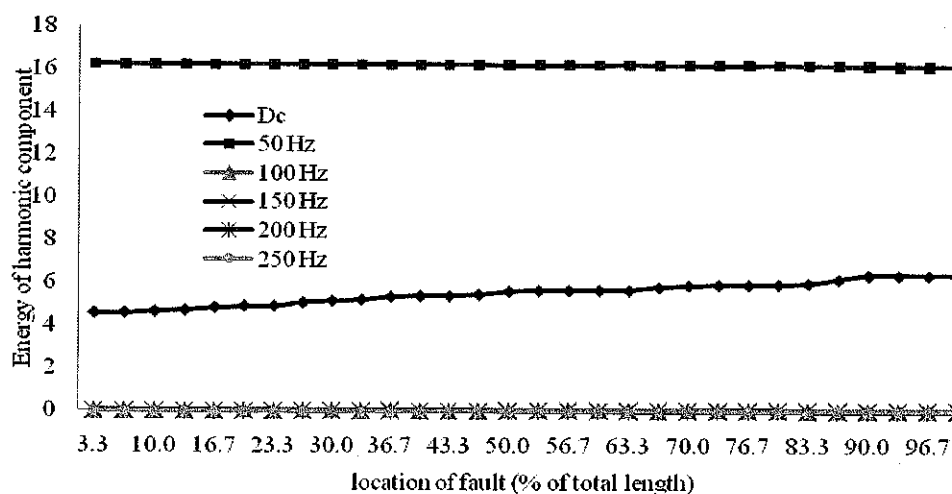


Figure 4.20: Cleared fault cases with increasing location of fault (in % of total length)

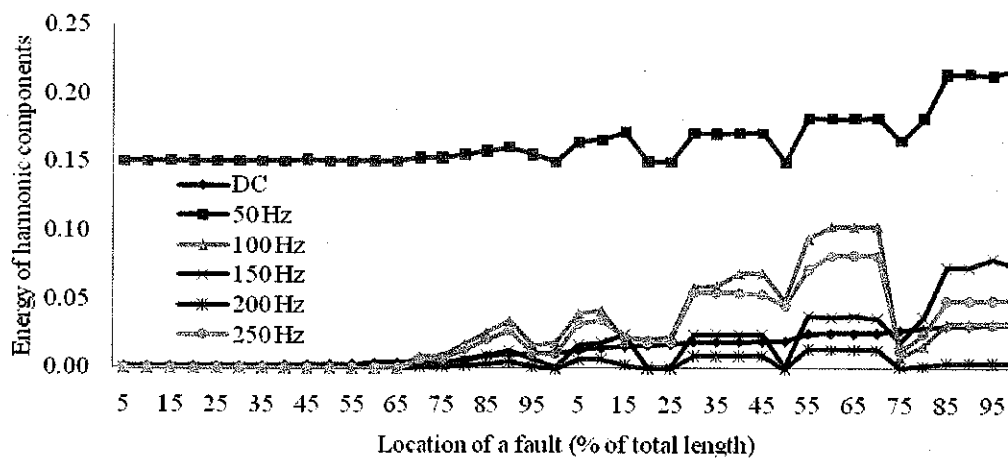


Figure 4.21: Energies of harmonic components of permanent fault patterns vs. location of fault (% of total length)

The variations in spectra of the sample waveforms of all sorts of faults (temporary, cleared and permanent) manifest the need for efficient way of training the neural

network. Table 4.2 tabularizes the maximum and minimum values of the selected 6 input features.

Table 4.2: Maximum and minimum values of features extracted

	DC	50 Hz	100 Hz	150 Hz	200 Hz	250 Hz
Maximum	6.391146	17.651679	2.466465	3.380952	0.332973	2.253968
Minimum	0.001266	0.150557	0.000010	0.000022	0.000001	0.000015

4.4. CASE STUDY III: IEEE 14-BUS ELECTRIC POWER SYSTEM

4.4.1. Introduction

As a means of validation to the previous works, the research work was continued with an IEEE 14-bus electric power system model. This benchmark model has been used extensively by scholars to investigate wide range power system problems [Anderson and Fouad, 2003]. As shown in Figure 4.22, the system has 2 generators and 3 synchronous compensators and 9 loads connected at its 14 buses.

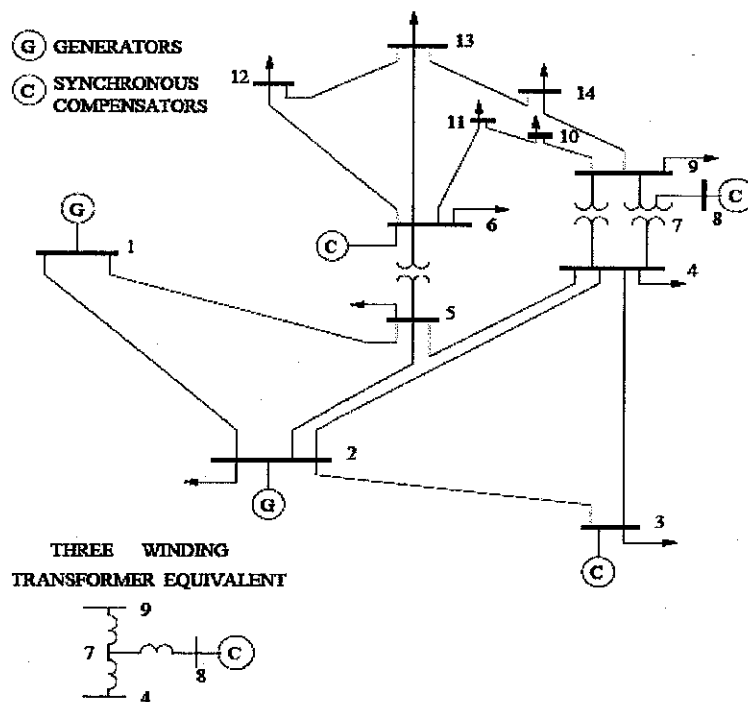


Figure 4.22: IEEE 14-bus system

The data for this model are taken from [M.A. Pai, 2005] for simulation purposes. And, the line under consideration is the 200 km long transmission line connecting bus 1 to bus 5.

4.4.2. Fault Simulations on IEEE 14-Bus Electric Power System

The IEEE 14-bus model is further investigated by generating 12 distinct faults which are recorded by varying the location of fault, measured from bus 1, and fault inception angle as shown in Table 4.3. Simulink setup of this model is presented in Appendix F. The models of the faults utilized here are as per the models reported in [A. T. Johns, et al. 1994], where a time dependent dynamic resistance representation of a primary arc and improvements to the dynamic conducting characteristics of secondary arc models are adopted with emphasis on an empirical approach which is used to determine the parameters of the models. Unlike to the previous reported case studies, high impedance faults (HIFs) are included in this study, just to find out how the developed algorithm responds to these types of faults. The results are discussed later.

Table 4.3: Generated faults and their variable parameter settings

Case	Fault type	Fault location (km)	Inception angle (°)	Ground resistivity ($\Omega.m$)
1	AG (phase A to Ground - temporary)	10	0	100
2	AG HIF (phase A to Ground High Impedance Fault - permanent)	10	0	100
3	ABG (Phases A and B to Ground - temporary)	10	0	100
4	AG (phase A to Ground - temporary)	50	90	100
5	ABG (phases A and B to Ground - temporary)	50	90	100
6	ABCG (phases A, B and C to Ground - permanent)	50	90	100
7	AG (phase A to Ground - permanent)	100	0	100
8	AG HIF (phase A to Ground High Impedance Fault - permanent)	100	0	100
9	AB (phase A, B and C shot-circuited - permanent)	100	0	100
10	AG (Phase A to Ground - temporary)	150	90	100

11	ABG HIF(phases A and B to Ground High Impedance Fault - permanent)	150	90	100
12	ABG (phases A and B to Ground - temporary)	150	90	100

High impedance faults are kind of faults that do not draw enough current to cause conventional protective devices to operate; therefore, high impedance faults represent one of the most difficult protection problems in power system today [A. F. Sultan, et al. 1992]. These faults often occur when an overhead conductor breaks and falls on high impedance surface such as asphalt road, sand, cement, grass or tree. When these types of faults happen, energized high-voltage conductors may fall within reach of personnel; yet may remain undetected and pose fire hazard. A sample high impedance single phase to ground fault is illustrated in Figure 4.23.

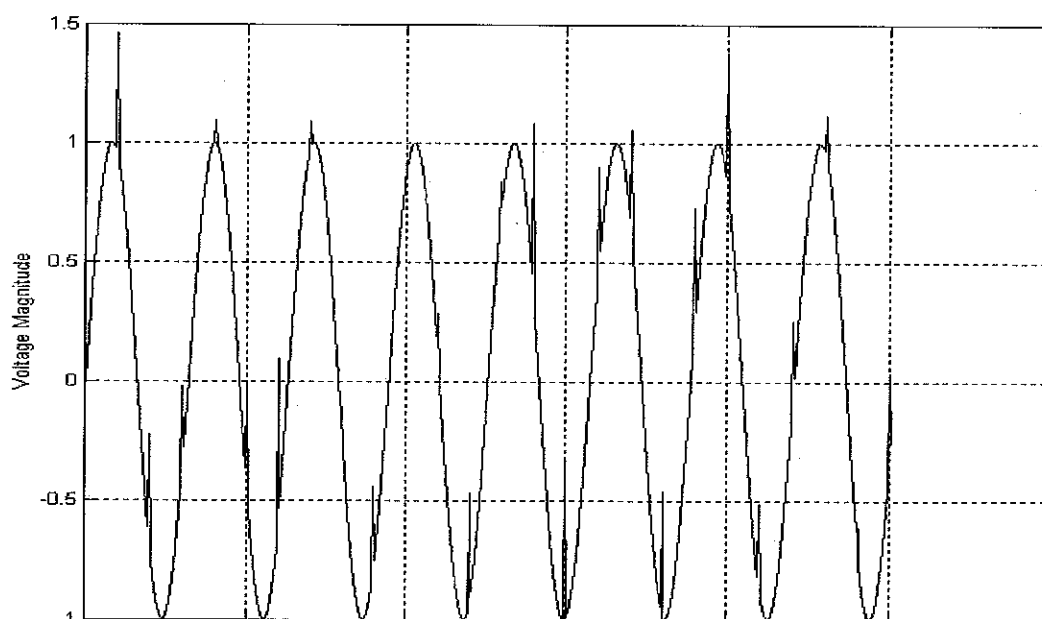


Figure 4.23: Recorded temporary ABG-HIF fault (at 100 km) – IEEE 14-bus system

4.4.3. Feature Extraction and Selection

The feature extraction and selection processes are carried out in the same way as in the previously reported models. That is, the fault voltage waveforms are fed into FFT module for spectral analysis and energy contained in the DC, fundamental and the

first four low frequency harmonics are utilized as inputs to a neural network. Each generated fault has been analyzed twice (immediately after the fault inception and after 8 cycles). This means 24 data (2x12 fault cases) have been prepared for further analysis. For example, the generated temporary fault, shown in Figure 4.24 has been examined at its 3rd and 10th cycles in which, for the latter case, the fault fully extinguishes. Table 4.4 shows the data patterns collected by the feature extraction and selection processes and their corresponding targets (where '0' represents cleared fault while '1' does mean either permanent or uncleared temporary fault case). In this table, the corresponding data taken at the 10th cycle of each fault cases are primed (i.e. x' where x implies the fault case number) to differentiate them from those taken from 3rd cycle of respective fault case. Table 4.4 presents only 21 data patterns. The reason is that the fault samples taken from the 10th cycle of each of the fault cases 7, 8 and 9 have been disregarded to avoid redundancy, i.e. the patterns obtained from the 10th cycles of the fault cases have been much more similar to those taken from the 3rd cycles.

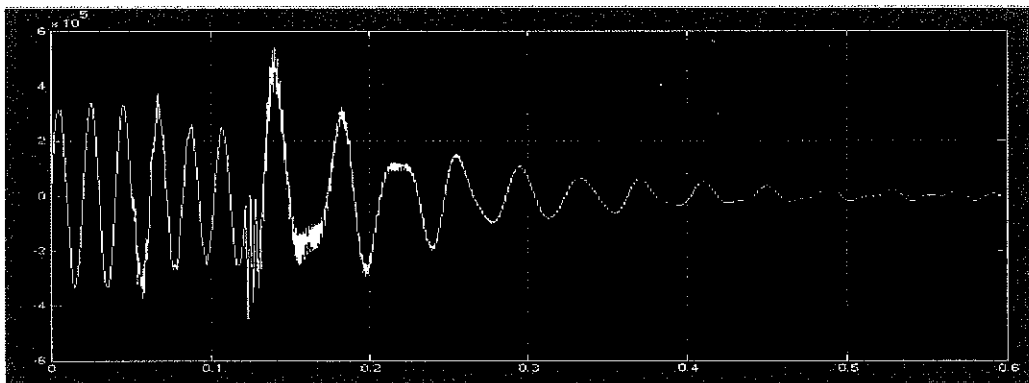


Figure 4.24: Recorded temporary ABG fault (at 50 km) – IEEE 14-bus system

Table 4.4: Extracted data patterns (immediately after fault inception and 10th cycles)

Case	Features						Neural output
	DC	50 Hz	100 Hz	150 Hz	200 Hz	250 Hz	
1	0.543451	6.132426	1.201243	2.589324	0.145265	1.842311	1
1'	4.770965	16.22556	0.006001	0.013502	0.000810	0.009001	0
2	1.243620	10.43259	0.114500	0.154326	0.009260	0.102884	1
2'	1.199520	11.03224	0.124321	0.142657	0.010433	0.104533	1
3	0.702544	4.025434	0.364326	0.804365	0.050254	0.542546	1

3'	5.032634	16.22413	0.006353	0.014295	0.000858	0.009530	0
4	1.104321	4.265762	0.432254	0.940436	0.054353	0.625435	1
4'	5.310360	16.22248	0.006762	0.015214	0.000913	0.010143	0
5	2.012453	9.998432	2.013432	3.992435	0.239546	2.661623	1
5'	5.606986	16.22053	0.007248	0.016308	0.000978	0.010872	0
6	0.000243	0.195432	0.000004	0.000069	0.000004	0.000046	1
6'	0.006010	0.163493	0.000335	0.000542	0.000033	0.000361	1
7	0.007943	0.302546	0.070453	0.163484	0.009809	0.108989	1
8	0.030154	0.160254	0.000501	0.001016	0.000061	0.000677	1
9	0.015465	0.148974	0.000302	0.000493	0.000030	0.000328	1
10	2.414311	16.43243	0.211532	0.462433	0.030143	0.308288	1
10'	5.925262	16.21791	0.007813	0.017579	0.001055	0.011719	0
11	1.105239	15.00868	0.104325	0.203146	0.012189	0.135430	1
11'	1.053925	14.14982	0.150010	0.210156	0.000116	0.140104	1
12	4.143260	17.42615	0.612623	1.421363	0.081321	0.947575	1
12'	6.847229	16.15522	0.041376	0.093095	0.005586	0.062063	0

4.5. SUMMARY

This Chapter discussed about fault simulations on three different power system models. And, aspects of the waveform capturing methods (from fault voltage signals generated on a specified transmission line of each model), feature extraction and selection have been explained plainly in separate sections of this Chapter. Ways of gathering a number of data patterns each of them possessing painstakingly and reasonably selected features have been also reported. The features (including the DC, fundamental, 2nd, 3rd, 4th and 5th harmonic components), which sufficiently and uniquely represent the condition of each fault, have been extracted using Fast Fourier Transform. A total of 43 data patterns plus 23 dedicated testing data, obtained from generating a number of faults on SMIB system model, have been prepared for further processing. From the IEEE 9-Bus system model fault simulations, 100 fault data patterns have been extracted and readied for training, testing and validating the neural network at hand. On the other hand, the fault data patterns including high impedance faults (HIFs) acquired from IEEE 14-bus electric power system model are exclusively employed for testing the trained and optimized neural network in both SMIB and IEEE 9-bus electric power system models. The neural network related simulations, optimization and analysis are discussed in the next Chapter (Chapter 5).

CHAPTER FIVE

DESIGN AND OPTIMIZATION OF ANN USING TAGUCHI'S METHODOLOGY AND TEST RESULTS

5.1. INTRODUCTION

Ways of obtaining fault data patterns (a total of 43 training and 23 testing from SMIB power system model, and 100 patterns from IEEE 9-bus model) for effectively training, testing and validating the neural networks under consideration have been shown in Chapter 4. In addition, 21 fault data patterns including high impedance faults, generated on IEEE 14-bus model, have been made ready for testing purpose. Following this is neural network simulation that encompasses training, optimization, testing, validation and other neural network related works.

The process followed in the optimization of key parameters of training algorithms (EBP, LM and RPROP) with the help of Taguchi's methodology on both power system models is thoroughly discussed in this Chapter. In the end, testing results of the optimized neural network in SMIB system model and a means on how to accurately determine the fault extinction time are reported.

5.2. ANN SIMULATION AND TAGUCHI'S EXPERIMENTS WITH DATA FROM SMIB MODEL –CASE STUDY I

5.2.1. Method of Training Neural Network

During training, the performance of ANN models does not depend only on the size of the neural network that is chosen for the problem in hand, but it also depends on the problem complexity. The problem complexity in turn depends on the type of functional mapping, accurate and sufficient training data acquired and their effective way of presentation to ANN during training. During the training phase of ANN, unknown neural network weights are to be determined.

The training process is carried out based on the fact that the target or the output of the neural network is considered to be '1' whenever there is a fault and '0' when the fault is cleared i.e. temporary and permanent fault sample patterns are mapped to ANN output of '1' and cleared fault patterns to ANN output of '0' as shown in Figure 5.1.

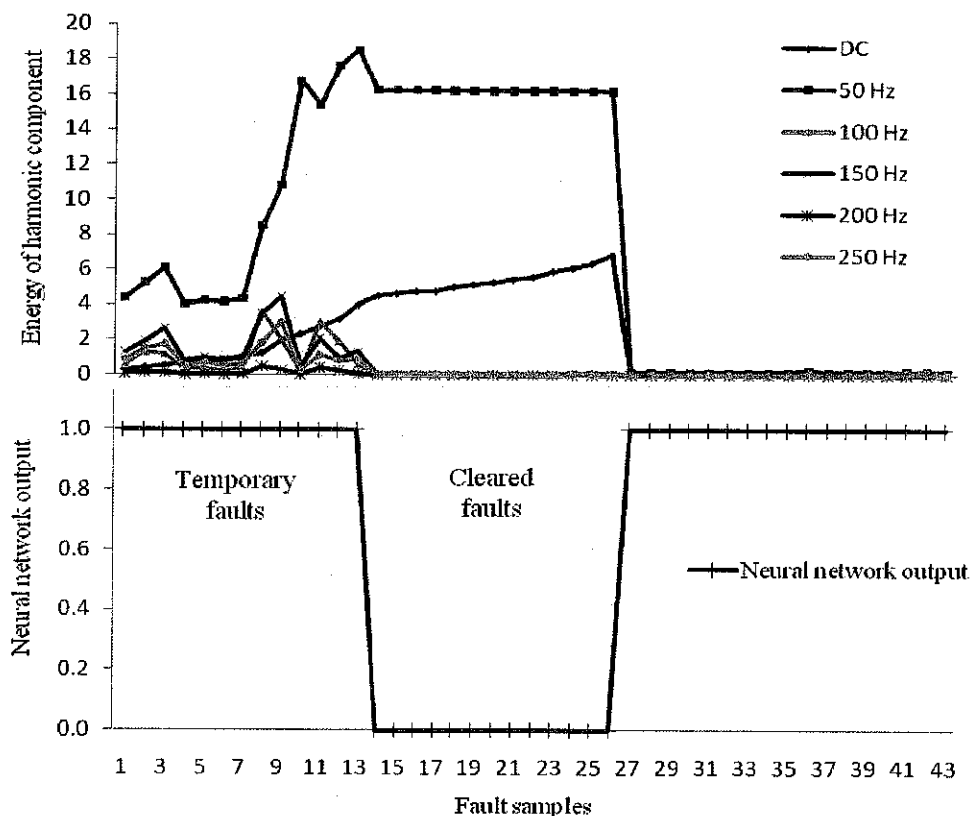


Figure 5.1: A plot of harmonic components of data patterns and their corresponding neural network outputs

Three algorithms have been used for accurately mapping the input data patterns to their corresponding output patterns which allows the neural network generate efficient mappings, make reasonable inference and classification work based on its knowledge. To facilitate this process, each of the algorithms are coded in MATLAB software with a graphical user interface (GUI) as in Figures 5.2 and 5.3, from which most of the important parameters are varied.

Figure 5.2 is specifically designed to handle the learning process using error back propagation algorithm. This user friendly GUI gives options for varying the learning rate, momentum term and number of hidden neurons which are the most important parameters for effective training process. Additionally, tolerance and speed of simulation can also be varied to convenient values by a user.

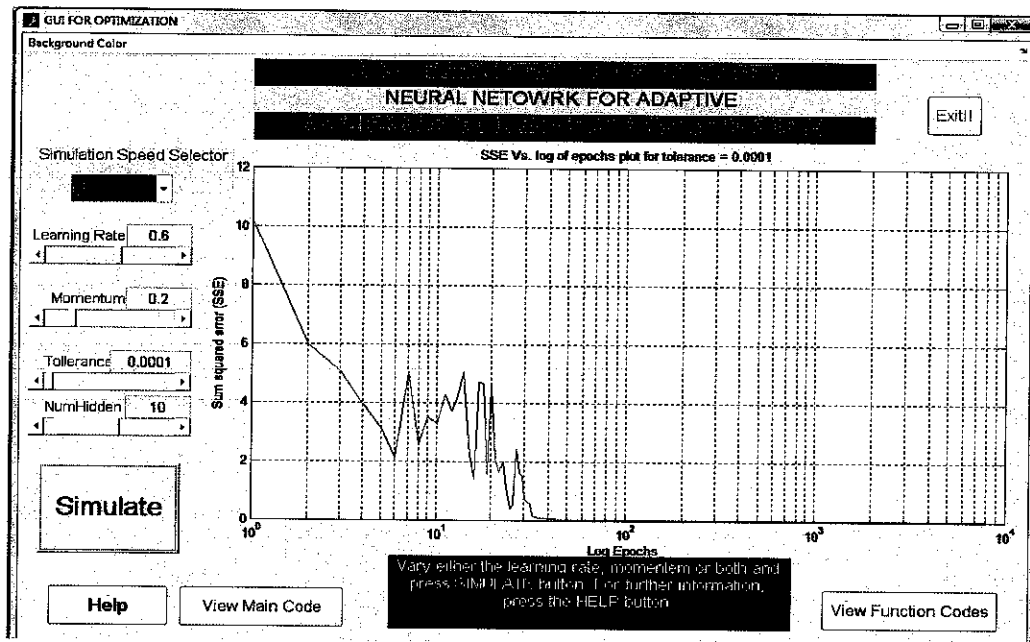


Figure 5.2: A GUI for training neural network

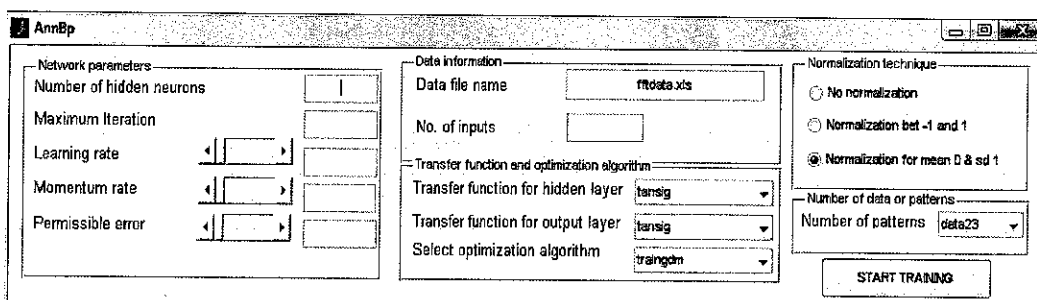


Figure 5.3: A generalized GUI for training neural network

The GUI in Figure 5.3 is, however, well suitable to all of the algorithms. Almost all the parameters in each algorithm can be controlled from this GUI including dropdown

buttons for transfer function and optimization algorithm selection, and normalization technique. Besides, the GUI reads input patterns from a specified excel file and allows user to select number of inputs.

5.2.2. Normalization of Input Data

Normalization is a process of scaling the numbers in a data set into a specified range, to improve the accuracy of the subsequent numeric computations. Normalization of input and output data is very critical. The values in the external data files are not always well suited for directly copying to network activities. This is because the activities in the network are normally in the range $[-1, 1]$, and if some activities differ significantly from this behavior, training performance is often degraded. Hence, without normalization, there is a tendency that the signal or value of large magnitude will be too dominating. Proper normalization of particularly input data makes training algorithms numerically robust and leads to a faster convergence. The training performance also depends on the effective way of presentation of data, in which normalization has to be considered. The common normalization method is to normalize each pattern in such a way that the minimum value is mapped to -1 and the maximum value is mapped to $+1$. Equation (5.1) suggests a method for scaling a dataset.

$$x_{ki} = \frac{(H_i - L_o)(X_{ki} - X_{k\min})}{(X_{k\max} - X_{k\min})} + L_o \quad (5.1)$$

Here, x_{ki} is the i^{th} element of the k^{th} scaled input data vector; X_{ki} is the i^{th} element of the raw data vector; $X_{k\min}$ is the minimum raw data value; $X_{k\max}$ is the maximum raw data value; $(X_{k\max} - X_{k\min})$ is the divisor, normalizing the raw input vector to user-defined range; H_i is the highest desired input value; L_o is the lowest desired input value, defining the minimum value to be presented to the neural network; and $(H_i - L_o)$ is the scaling factor mapping the raw data into the desired input range. For example, to scale raw data patterns in the range 0 to 1, we set $H_i = 1$, and $L_o = 0$. To scale raw data patterns in the range -1 to $+1$, we set $H_i = 1$, and $L_o = -1$.

Equation (5.1) is adopted in this thesis so that the input data patterns are normalized between -1 and $+1$.

5.2.3. Choice of Transfer Function

One more big concern that has to be taken into consideration before starting training the neural network is the choice of transfer (also known as activation) function. As stated in Chapter 3, if the right transfer functions are not selected, the training process may be affected, hence, proper mapping of the input with the target outputs may be degraded. After closely studying the effects of each transfer function (one or hybrid) on the overall training performance, ‘tansig - tansig’ transfer function combination, adopted in this thesis, has given the best results, and worst training performance have been observed when the hybrid ‘purlin – tansig’ transfer functions have been utilized in the hidden and output layers of the neural network (For details of transfer functions, refer to Chapter 3).

5.2.4. Application of Taguchi’s Methodology for Optimization

As comprehensively explained in Chapter 3, Taguchi’s method has been extensively used in optimizing the parameters which strongly influence the training performance of a neural network. Most of these parameters are stated earlier in the same Section. The basic interest here is, however, to present the detailed optimization procedures followed to tune up the training parameters by employing Taguchi’s methodology (For detail description, refer to previous Chapters).

To setup Taguchi’s experiments, certain levels of each parameters are considered. The choice of these levels does not stand from scratch but it is based on recommended range of values for each control parameter in each algorithm. The performance can be measured by several ways such as tracking root mean square error (*RMSE*), percent error index (% *EI*), accuracy, etc. The first two are shown as in Equations (5.2) and (5.3).

$$RMSE = \sqrt{\frac{2 * E}{P * K}}$$

Root mean square error,

(5.2)

where *E* is the system error; *P* is number of patterns, and *K* is number of network outputs.

$$\text{Error Index (EI), } \%EI = \frac{\sum_{p=1}^P \sum_{k=1}^K \|T_{kp} - A_{kp}\|}{\sum_{p=1}^P \sum_{k=1}^K \|T_{kp}\|} * 100\% \quad (5.3)$$

where T_{kp} and A_{kp} are target and actual values for p^{th} pattern and k^{th} output respectively; P is number of patterns; and K is number of network outputs.

None of the above approaches takes the speed of training process into account. Time is an important factor in training. As a matter of fact, fast convergence is required during training. For this reason, it is required that the training process time (or equivalently saying the number of epochs) be small while maintaining minimum overall error. A new performance measuring index obtained by multiplying the percent EI by the number of epochs, as in Equation (5.4), is used in this report. This approach considers the combined effect of both $\% EI$ and time by effectively assessing the error index over time.

$$\varepsilon = n \times \%EI \quad (5.4)$$

where ε is the modified error index over time, n is the number of epochs (or iterations) a neural network took for training, and EI is the overall error index after training.

In this report, Equation (5.4) is adopted to measure the performance of each combination in Taguchi's experiments. Combinations of factors and levels identical to the number of Taguchi's orthogonal arrays [Lochner, 1990] are set up and the corresponding error index (EI) is obtained for each of them. After all, the objective of Taguchi's experiment is to find parameter combinations with minimum error index based on the notion of Taguchi - "smaller-the-better - SB". This is to mean the smaller the mean square error, the better the classification performance of the neural network used in the study. For clarification purpose, Taguchi's experiment of LM algorithm is presented in this thesis. The control parameters for this algorithm are initial learning parameter (λ_0), increment factor (λ^+), decrement factor (λ^-) and number of hidden units (h). The corresponding levels are shown in Table 5.1. With number of levels L and control parameters P , there are L^P number of combinations; in

this case, $4^4 = 256$ possible combinations. There are two ways in which the optimal combination which gives the least error (out of these 256 different combinations) is determined. One way is to conduct experiment on each and every combination, compare the errors and pick up the one with the least error. It is probably cumbersome to check all the combinations to come up with the optimal values of the parameters (especially when the number of all combinations is too big).

The second way is by using a systematic approach that reduces the number of experiments to be carried out, largely saves the experimental effort and eases overall analysis. Taguchi's proposal reasonably reduces the number of experiments, yet sufficient to make valid conclusions over the entire region spanned by the control factors and their levels. Taguchi's experiments reduce the number of experiments required to find the best level for each factor [Lochner H.R., 1990]. The method works by calculating the statistical properties of orthogonal arrays. For instance, in this study, it is required to perform experiments on only 16 orthogonal arrays as in Table 5.2 based on Taguchi's proposal.

As stated earlier, the detailed steps of Taguchi's experiment for LM algorithm are presented in this report. Four levels, corresponding to the four control parameters: λ_0 , λ^+ , λ^- and h , have been selected as shown in Figure 5.4, and the corresponding values set for the levels of each of the four control parameters are depicted in Table 5.1. The challenge here is to obtain a set of values of each of the parameters, out of their four level settings, that gives the minimum error. In Table 5.2, the modified error indices (ε) for each experimental run are shown in its last column.

Table 5.1: Control parameters and their corresponding levels for LMA

level	Control parameters			
	λ_0	λ^+	λ^-	h
1	0.001	2	0.5	4
2	0.01	5	0.2	6
3	0.1	10	0.1	8
4	1.0	20	0.05	10

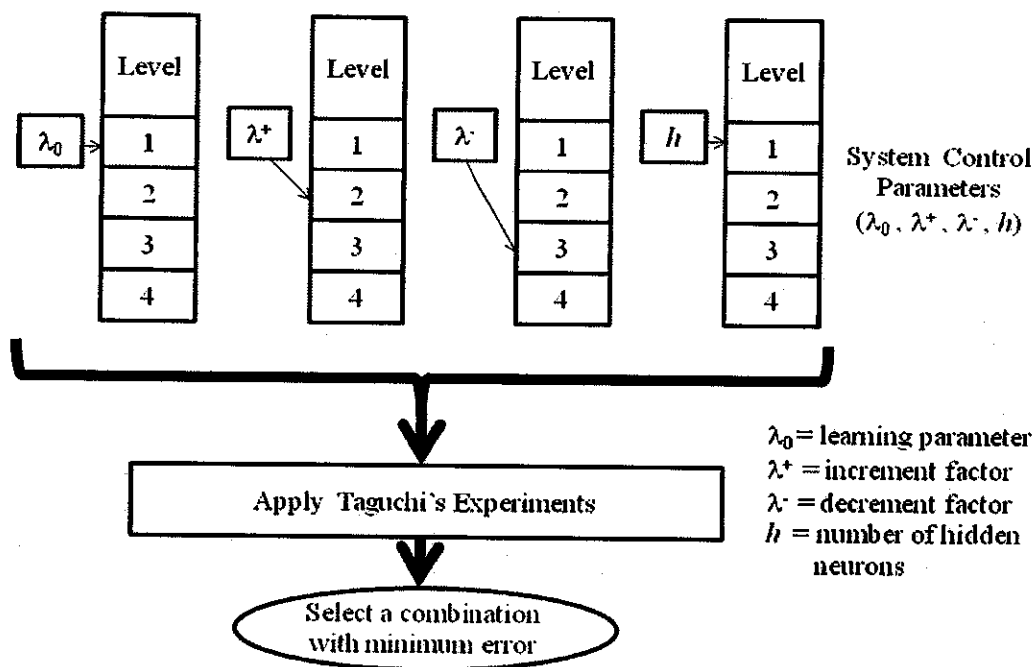


Figure 5.4: Schematic of Taguchi's experimentation on selected parameters of LM

Table 5.2: L_{16} Orthogonal arrays for 4 parameters each with 4 Levels and their corresponding error index and epochs for LM algorithm

Experiment	Control Parameters				% Error Index, EI (%)	Epoch (n)	ε
	λ_0	λ^+	λ^-	h			
1	1	1	1	1	0.0126	11	0.1386
2	1	2	2	2	0.0197	16	0.3152
3	1	3	3	3	0.0981	16	1.5696
4	1	4	4	4	0.0198	10	0.1980
5	2	1	2	3	0.0123	16	0.1968
6	2	2	1	4	0.0169	34	0.5746
7	2	3	4	1	0.0139	9	0.1251
8	2	4	3	2	0.0163	11	0.1793
9	3	1	3	4	0.0468	23	1.0764
10	3	2	4	3	0.0136	16	0.2176
11	3	3	1	2	0.0549	48	2.6352
12	3	4	2	1	0.0472	16	0.7552
13	4	1	4	2	0.0167	10	0.1670
14	4	2	3	1	0.2795	24	6.7080
15	4	3	2	4	0.1347	27	3.6369
16	4	4	1	3	0.2520	58	14.616

To find the optimal combination of levels, the effect of each level in each factor is obtained by averaging the resulting error indices which contain the same level and factor. For example, the net percent error indices (equivalently saying, the net contribution of that level to the error index) for level 2 of λ_0 and level 2 of h are calculated in the following ways:

$$\varepsilon \rightarrow (\lambda_0)_{level2} = \frac{(0.0123 + 0.0169 + 0.0139 + 0.0163)}{4} = 0.01485$$

$$\varepsilon \rightarrow (h)_{level2} = \frac{(0.0197 + 0.0163 + 0.0549 + 0.0167)}{4} = 0.0269$$

Table 5.3 shows the effective error indices for all the levels in each factor, calculated in the same way as demonstrated earlier. From this table, it is inferred that the optimal combination of parameters with smallest effective EI is $\lambda_0 \lambda^+ \lambda^- h = \{2 \ 1 \ 4 \ 2\}$. This means the optimal combinations of parameters is achieved when the parameters are set as: $\lambda_0 = 0.01$, $\lambda^+ = 2$, $\lambda^- = 0.05$ and $h = 6$. The optimization is not still over. As stated earlier, in addition to % EI , the number of epochs (iterations) is a decisive factor in the overall training process. It is required that training be achieved after a few iterations. Thus, considering the number of iteration as an objective function, the combination of parameters which gives less numerical iterations to yield the output is $\lambda_0 \lambda^+ \lambda^- h = \{1 \ 1 \ 4 \ 1\}$ as shown in Table 5.4. Equivalently saying, a network whose parameters are set as $\lambda_0 = 0.001$, $\lambda^+ = 2$, $\lambda^- = 0.05$ and $h = 4$ converges more quickly than any other combination, hence, the best combination of parameters.

As stated in the preceeding Chapter, an objective function to get a compromise of the % EI and number of iterations (n) is proposed as in Table 5.2. A column of simple geometric product % EI and n (which is the modified error index, ε) is formed as in Table 5.2. This product is used to find the optimal combination of parameters which takes care of the effects of % EI and n . Table 5.5 shows the effect of each level in each parameter for the error index ε calculated in the same way as in Table 5.3. Following this step, the optimal combination of parameters is $\{2 \ 1 \ 4 \ 2\}$ which corresponds to $\lambda_0 = 0.01$, $\lambda^+ = 2$, $\lambda^- = 0.05$ and $h = 6$.

Table 5.3: Average % EI for each factor and level in LM

levels	Control Parameters			
	λ_0	λ^+	λ^-	h
1	0.037550	0.022100	0.084100	0.088300
2	0.014850	0.082425	0.053475	0.026900
3	0.040625	0.075400	0.110175	0.094000
4	0.170725	0.083825	0.016000	0.054550

Table 5.4: Average epochs (n) for each factor and level in LM

levels	Control Parameters			
	λ_0	λ^+	λ^-	h
1	13.25	15.00	37.75	15.00
2	17.50	22.50	18.75	21.25
3	25.75	25.00	18.50	26.50
4	29.75	23.75	11.25	23.50

Table 5.5: Average ε for each factor and each level in LM

lev els	Control Parameters			
	λ_0	λ^+	λ^-	h
1	0.5553	0.3947	4.4911	1.931
2	0.2689	1.9538	1.2260	0.824
3	1.1711	1.9917	2.3833	4.150
4	6.2819	3.9371	0.1769	1.371

In a similar way, parameters for Resilient Back-Propagation (RPROP) algorithm (Δ_0 , η^- , η^+ , α and h) are optimized by conducting Taguchi's experiments on 16 orthogonal arrays, L_{16} . Table 5.6 shows the five control parameters of RPROP training algorithm, each with four levels. When Taguchi's methodology is applied to this case, the results are obtained as shown in Table 5.7 from which it can be observed that $\Delta_0 \eta^- \eta^+ \alpha h = \{2 \ 2 \ 3 \ 2 \ 3\}$ makes the optimal combination vector with minimal error index ε .

Table 5.6: Control parameters and their corresponding levels for RPROP

levels	Control Parameters				
	Δ_0	η^-	η^+	α	h
1	0.01	0.4	1.2	0.001	4
2	0.07	0.5	1.5	0.01	6
3	0.13	0.6	1.8	0.1	8
4	0.20	0.8	2.0	1.0	10

Table 5.7: Average ε for each factor and each level for RPROP

levels	Control Parameters				
	Δ_0	η^-	η^+	α	h
1	0.13093	0.17195	0.26005	0.11878	0.14198
2	0.06123	0.04370	0.09113	0.07893	0.11990
3	0.07858	0.10173	0.04245	0.14498	0.07210
4	0.16685	0.12020	0.04395	0.09490	0.10360

Like the other two algorithms, Error Back-Propagation (EBP) algorithm parameters (η , α and h) each with four levels, as in Table 5.8, are optimized by setting up L_{16} Taguchi's orthogonal arrays and experimenting on them. The results from the experiment, as in Table 5.9, show that $\eta_4 \alpha_2 h_3$ or simply 4 2 3, which corresponds to a learning rate, $\eta = 0.4$, momentum term, $\alpha = 0.2$ and $h = 8$ hidden neurons, gives the optimal solution.

Table 5.8: Control parameters and their corresponding levels for EBP

levels	Control Parameters		
	η	α	h
1	1.0	0.1	4
2	0.8	0.2	6
3	0.6	0.4	8
4	0.4	0.6	10

Table 5.9: Average ε for each factor and each level for EBP

levels	Control Parameters		
	η	α	h
1	3.7944	3.0456	3.4429
2	4.1783	2.7493	3.7054
3	3.3530	5.0026	2.0677
4	3.0869	3.6151	5.1966

A comparison of the three algorithms shows that both LM and RPROP yield accuracy greater than 99 % and guarantee fast convergence. Whereas, EBP is by far substandard to the other two algorithms as far as accuracy and fast convergence are concerned. This is clearly shown in Table 5.10. An accuracy of 96.8699 % is attained after 10,000 iterations when EBP is used. Whereas, the network required only 2 iterations to converge during the training process by using LM algorithm. Figure 5.5 illustrates how the training performance has been improved after optimization of parameters with Taguchi's method. The convergence criteria were met after 2 iterations with mean square error of 0.0000001.

Table 5.10: Accuracy and convergence rate of the three algorithms

Algorithm	Optimal combination	Tuned Values	Iterations	Accuracy (%)
EBP	4 2 3	$\eta = 0.4, \alpha = 0.2, h = 8$	10000	96.8699
LM	2 1 4 2	$\lambda_0 = 0.01, \lambda^+ = 2, \lambda^- = 0.05, h = 6$	2	99.9999
RPROP	2 2 3 2 3	$\Delta_0 = 0.07, \eta^- = 0.5, \eta^+ = 1.8, \alpha = 0.01, h = 8$	10	99.9989

The optimally trained neural network is tested with a separate 23 testing data set. The responses (results) to the testing data of each training algorithm are shown in Appendix B. A maximum of 0.0028 % error has been noticed, which is quite a small figure for practical reasons.

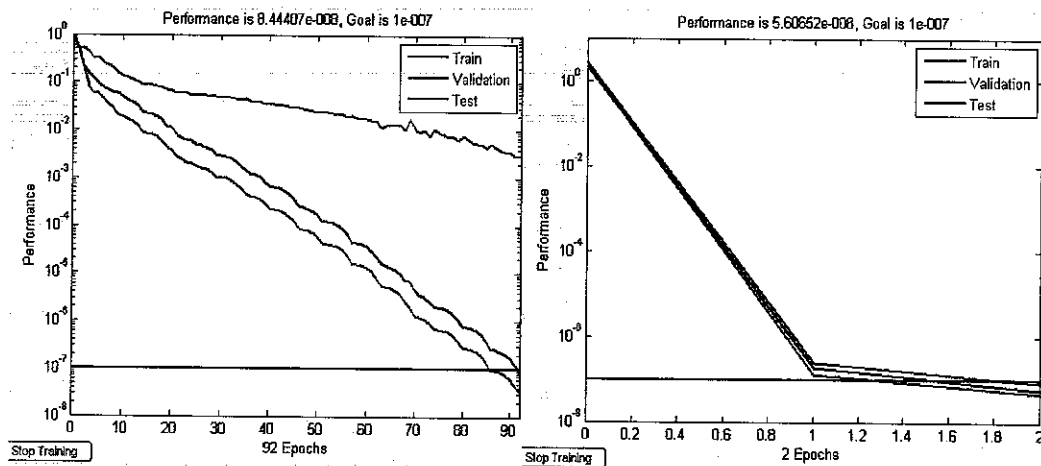


Figure 5.5: Training Performance before and after optimization

5.3. ANN SIMULATION AND TAGUCHI'S EXPERIMENTS WITH DATA FROM IEEE 9-BUS POWER SYSTEM MODEL

5.3.1. Method of Training Neural Network and Normalization

In the previous work, the power system model used in the study of adaptive auto-reclosure was based on a single generator connected via an EHV transmission line to an infinite bus where the voltage is considered to be constant. The results obtained from the first case study vindicate the efficacy of the developed AR scheme.

However, the findings from the previous research works need to be verified with the consideration of real or benchmark networks. Owing to this fact, a standard IEEE 9-bus electric power system has been utilized to illustrate the capabilities and effectiveness of the tool developed in earlier works (refer to Section 5.2).

Similar to the previous case study, the target or the output of the neural network is considered to be '1' whenever there is a fault and '0' when the fault is cleared as depicted in Figure 5.6.

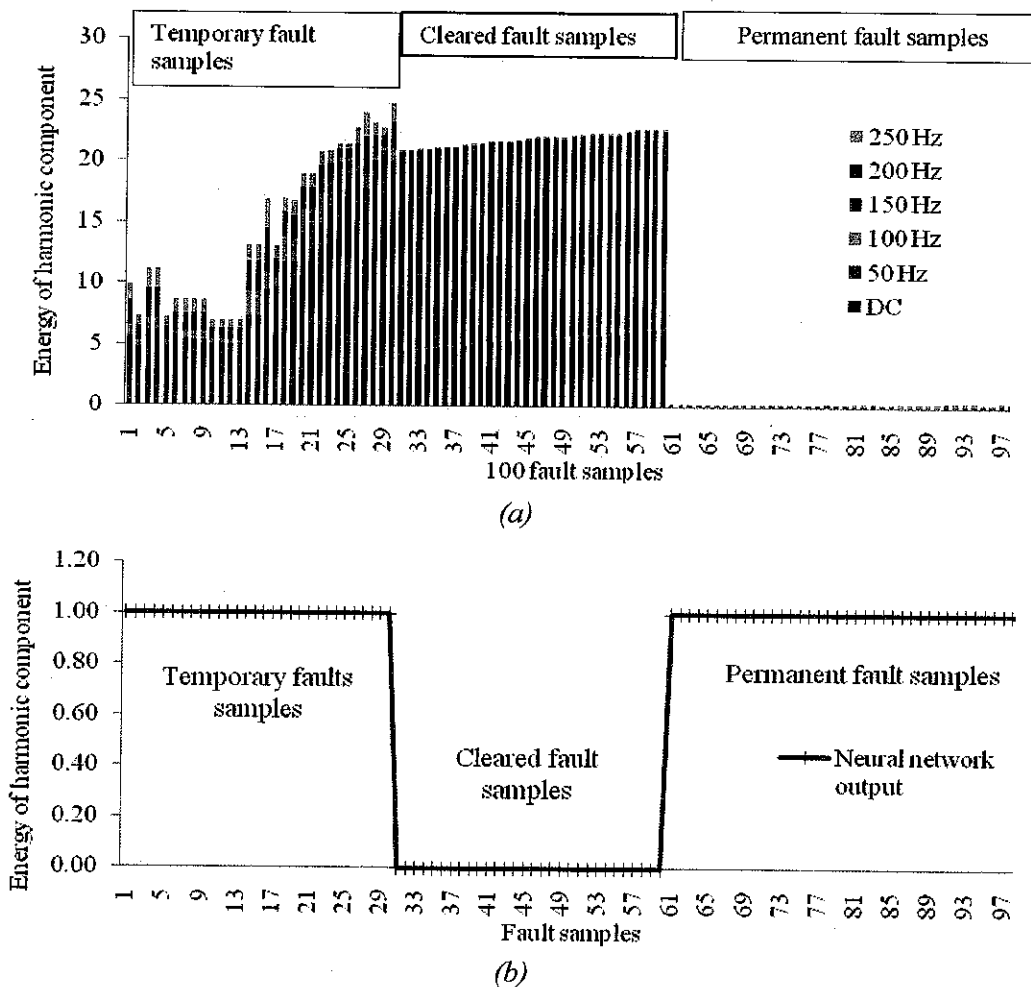


Figure 5.6: A stacked column representation of harmonic components of fault sample patterns (a), and their corresponding neural network output (b).

While training the ANN, the algorithms coded in MATLAB with interactive GUI's from which key parameters are varied, are utilized again in this case study. In connection to this, the hundred input data patterns are normalized between -1 and +1 for the reasons mentioned under Section 5.2 of this Chapter. They are also randomly segregated into training, testing and validation data sets. Accordingly, 80 % of them are dedicated for training purpose while the remaining 20 % are set for testing and validation. The 'tansig -- tansig' combination of transfer function have been utilized in this case study, similar to the previous SMIB case study.

5.3.2. Taguchi's Experimentation for Optimization

The next procedure is to setup Taguchi's experiments. To proceed further, there is a need to select key parameters which influence the overall performance of the neural network during or after training to a great extent. These parameters are identified and certain levels of values (within previously recommended range of each parameter) are selected for each of them. Specifically, four levels of values of each parameter are set and readied for Taguchi's experimentation.

As in the previous case study, the objective function, cited in Equation (5.4), is adopted in this Section to measure the performance of the ANN for each combination during the Taguchi's experiments. Combinations of control parameters and levels identical to the number of Taguchi's orthogonal arrays are set up and the corresponding percent error indices are determined accordingly [Lochner, 1990]. The objective of Taguchi's experiment is to find, out of selected control parameters with certain levels, as in Table 5.11, a combination of parameters which gives rise to minimum error index and minimum number of epochs after training the ANN. This is based on the notion of Taguchi –“Smaller-the-Better - SB”– which means the smaller the error, the better the classification performance of the ANN is.

The procedures followed during the Taguchi's experiments are the same for all algorithms. Hence, to avoid repetitions, Taguchi's experiment for LM algorithm is presented in this report. As mentioned in Section 5.2 earlier, the identified control parameters which have significant effect on the overall performance of the neural network are initial learning parameter (λ_0), increment factor (λ^+), decrement factor

(λ^-) and number of hidden units (h). And, the corresponding 4 levels for each of these 4 control parameters are shown in Table 5.11. In this case, the number of total combinations is $4^4 = 256$ combinations. However, based on Taguchi's proposed technique, it is required to conduct experiments only on 16 of the combinations which correspond to L_{16} orthogonal arrays in this study as in Table 5.12. The values of the control parameters considered during the Taguchi's experiments are shown in brackets, and the modified error indices (ε) for each Taguchi's experimental run are shown in the last column of Table 5.12.

Table 5.11: Control Parameters and Corresponding Levels

Algorithm	Control parameters	Levels			
		1	2	3	4
EBP	Momentum (α)	0.1	0.2	0.4	0.6
	Learning rate (η)	1.0	0.8	0.6	0.4
	# of hidden units (h)	2	3	4	5
LM	Learning factor (λ_0)	0.001	0.01	0.1	1.0
	Increment factor (λ^+)	2	5	10	20
	Decrement factor (λ^-)	0.5	0.2	0.1	0.05
	# of hidden units (h)	2	3	4	5
RPROP	Update value(Δ_0)	0.01	0.07	0.13	0.20
	Increment factor (η^+)	1.2	1.5	1.8	2.0
	Decrement factor (η^-)	0.4	0.5	0.6	0.8
	Learning rate (α)	0.001	0.01	0.1	1.0
	# of hidden units (h)	2	3	4	5

Table 5.12: Results of Taguchi's experiment for LM algorithm

Exp. #	Control Parameters (CPs)				ε
	λ_0	λ^+	λ^-	h	
1	1 (0.001)	1 (2)	1 (0.5)	1 (2)	0.45000
2	1 (0.001)	2 (5)	2 (0.2)	2 (3)	0.19350
3	1 (0.001)	3 (10)	3 (0.1)	3 (4)	0.30590
4	1 (0.001)	4 (20)	4 (0.05)	4 (5)	3.06000
5	2 (0.01)	1 (2)	2 (0.2)	3 (4)	0.10440
6	2 (0.01)	2 (5)	1 (0.5)	4 (5)	0.20200

7	2 (0.01)	3 (10)	4 (0.05)	1 (2)	4.91000
8	2 (0.01)	4 (20)	3 (0.1)	2 (3)	0.38930
9	3 (0.1)	1 (2)	3 (0.1)	4 (5)	0.18270
10	3 (0.1)	2 (5)	4 (0.05)	3 (4)	23.62000
11	3 (0.1)	3 (10)	1 (0.5)	2 (3)	0.22680
12	3 (0.1)	4 (20)	2 (0.2)	1 (2)	0.26400
13	4 (1.0)	1 (2)	4 (0.05)	2 (3)	27.63000
14	4 (1.0)	2 (5)	3 (0.1)	1 (2)	0.07810
15	4 (1.0)	3 (10)	2 (0.2)	4 (5)	0.06160
16	4 (1.0)	4 (20)	1 (0.5)	3 (4)	0.28500

The next step is to obtain the net effect of each level value in each factor which is carried out by averaging the results which contain the same level and factor. For example, λ_0 has its level set to 1 (where its value is 0.001) in the first four rows as shown in Table 5.12 while the experiments are carried out. Correspondingly, there are four different error indices, ε , for each row. To find the net contribution of level 1 of λ_0 , the effective error index is evaluated by averaging the error indices shown in bold in Table 5.12, i.e.

$$\varepsilon \rightarrow (\lambda_0)_{level1} = \frac{(0.4500 + 0.19350 + 0.30590 + 3.06000)}{4} = 1.00235$$

$$\varepsilon \rightarrow (h)_{level4} = \frac{(3.06000 + 0.2020 + 0.1827 + 0.06160)}{4} = 0.87658$$

The effective error indices for the remaining levels of each factor are calculated in a similar way as shown in Table 5.13. From Table 5.13, out of four levels of each parameter, the levels which contributed less amount of effective error (shown in bold) are selected. Hence, the optimal combination of parameters with smallest effective ε is $\{\lambda_0 \lambda^+ \lambda^- h\} = \{1 \ 4 \ 2 \ 4\}$. In other words, the optimal combination of parameters is achieved when the values are set as: $\lambda_0 = 0.001$, $\lambda^+ = 20$, $\lambda^- = 0.2$ and $h = 5$.

Table 5.13: Average ε for each CP and each level –LM

CPs	Levels of CPs			
	1	2	3	4
λ_0	1.00235	1.40143	6.07338	7.01368
λ^+	7.09178	6.02340	1.37608	0.99958
λ^-	0.29095	0.15588	0.23900	14.80500
h	1.42553	7.10990	6.07883	0.87658

Similarly, parameters of RPROP (Δ_0 , η^- , η^+ , α and h) are optimized by conducting Taguchi's experiments on 16 orthogonal arrays, L_{16} . Table 5.11 shows the five control parameters of RPROP algorithm each with four levels. When Taguchi's methodology is applied, the results are obtained as shown in Table 5.14 where $\{\Delta_0 \eta^- \eta^+ \alpha h\} = \{4 \ 3 \ 2 \ 1 \ 2\}$ makes the optimal combination vector with minimum ε outputs. This effectively means parameter values set $\Delta_0 = 0.2$, $\eta^- = 1.8$, $\eta^+ = 0.5$, $\alpha = 0.001$ and $h = 3$ give the best result compared to other sets of values.

Table 5.14: Average ε for each CP and each level –RPROP

CPs	Levels of CPs			
	1	2	3	4
Δ_0	7.04674	11.86737	5.18010	4.31863
η^-	4.10020	12.17211	0.59085	11.54968
η^+	6.79093	0.38456	6.12983	15.10752
α	0.72512	8.77551	5.86965	13.04255
h	10.09145	0.12296	10.58538	7.61305

With regard to EBP algorithm (whose parameters are η , α and h , each with four levels as in Table 5.11), experiments conducted on L_{16} Taguchi's orthogonal arrays has given rise to an optimal combination of $\eta_1 \alpha_2 h_4$ or simply $\{1 \ 2 \ 4\}$ as in Table 5.15 where the optimal combination corresponds to $\eta = 1.0$, $\alpha = 0.2$, and $h = 5$.

Table 5.16 summarizes the values of parameters optimized using Taguchi's experiments for each algorithm implemented to train the neural network.

Table 5.15: Average ε for each CP and each level –EBP

CPs	Levels of CPs			
	1	2	3	4
η	1.73255	2.07115	3.23330	3.73593
α	2.81043	2.39105	2.66540	2.90605
h	2.96128	2.99818	2.43473	2.37875

Figures 5.7 and 5.8 illustrate the differences in training performances of ANN with randomly selected parameters and with the optimized values of parameters, as in Table 4.18, for LM and RPROP algorithms, respectively. It is evident to observe the improvements to the training performance of the neural network achieved with the help of Taguchi's method.

Table 5.16: Optimized values of CPs and corresponding accuracies

Algorithm	Control parameters	Level	Tuned Values	Iterations	Accuracy
EBP	Learning rate (η)	1	1	10,000	94.79 %
	Momentum (α)	2	0.2		
	# of hidden units (h)	4	5		
LM	Learning factor (λ_0)	1	0.001	1	≈ 100 %
	Increment factor (λ^+)	4	20		
	Decrement factor (λ^-)	2	0.2		
	# of hidden units (h)	4	5		
RPROP	Update value (Δ_0)	4	0.2	5	≈ 100 %
	Decrement factor (η^-)	3	0.6		
	Increment factor (η^+)	2	1.5		
	Learning rate (α)	1	0.001		
	# of hidden units (h)	2	3		

On the other hand, a comparison of the three algorithms used in this case study also shows that both LM and RPROP yield accuracy greater than 99 % and guarantee fast convergence. Whereas, EBP is by far substandard to the rest as far as accuracy and fast convergence are concerned. An accuracy of 94.79 % is attained after 10,000 iterations when EBP is used. Whereas, using LM and RPROP algorithms, training process took only 1 and 5 iterations to converge, respectively.

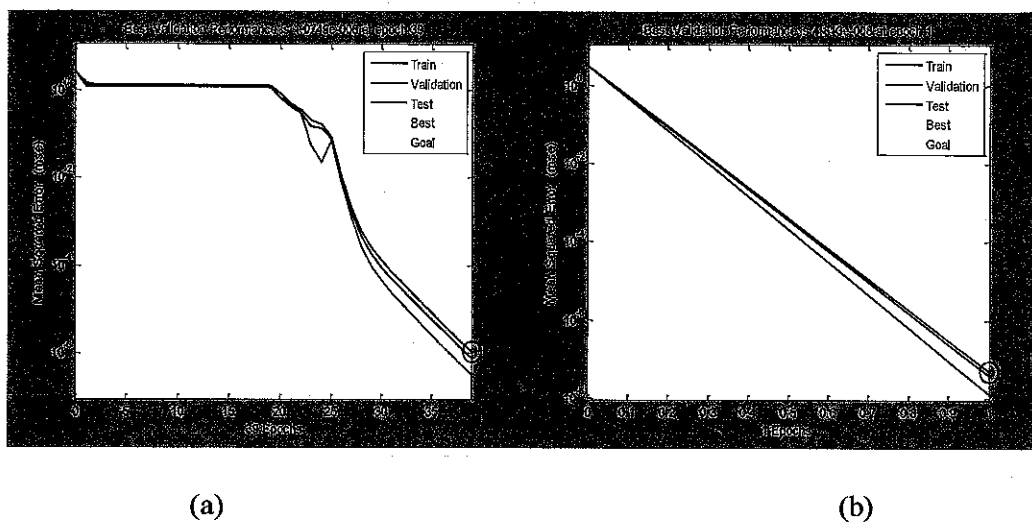


Figure 5.7: Performance (a) before and (b) after optimization for LM algorithm

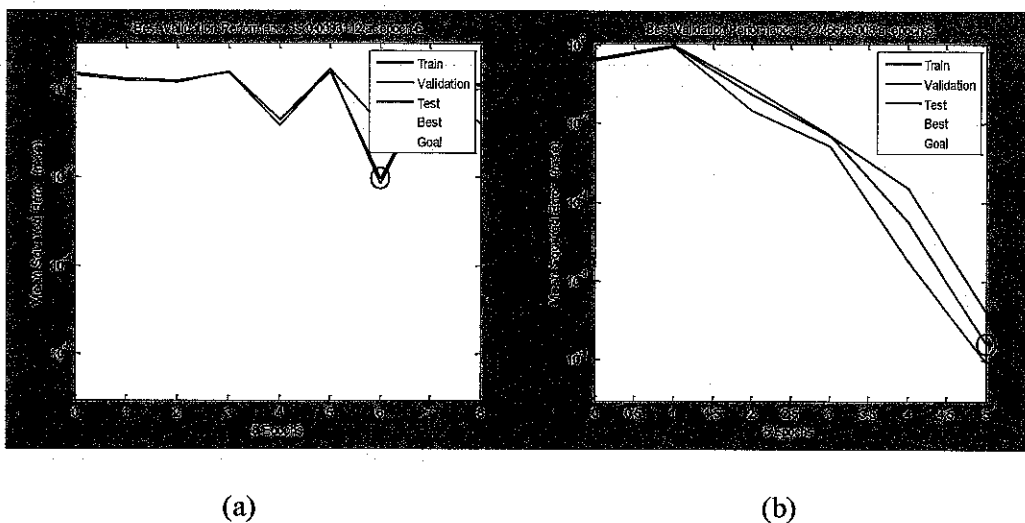


Figure 5.8: Performance (a) before and (b) after optimization for RPROP algorithm

5.3.3. Validation

Once a neural network has been trained and tested, the performance is validated against an independent validation dataset, consisting of unused samples or patterns from the application data. The validation set is distinct from, and independent of, both the training and test sets; hence, it does not influence the method of training and

testing. Validation can also be used to determine when to stop training (when the error for the validation data hits a minimum) [Masters, 1993] and [Reed, 1993]. Figures 5.7 and 5.8 show the trends of training, testing and validation curves with increasing number of iterations. This is an important feature to know if the neural network is properly and effectively trained, and is ready to classify a new input data.

A neural network, once trained and validated can be used on-line to process real-time patterns (real time datasets) directly from the application environment (in this case, the transmission system) and make bold decisions. This processing primarily involves multiplication of the live input vectors by the already optimized network weight vectors, which can often be done in real time, given the speed of today's microprocessors.

5.4. TESTING RESULTS WITH DATA FROM IEEE 14-BUS MODEL

As stated earlier, the data collected from simulation of IEEE 14-bus have been utilized for testing the previously developed neural network that has been optimized for SMIB and IEEE 9-bus models. The test results show the robustness of the method which showed a sound identification performance even for High Impedance Faults (HIFs), which has not been considered in the previous models. The neural network has not been trained with HIFs. But it can still map new data accordingly. Table 5.17 illustrates the results obtained by testing the already optimized and trained neural networks in each of the previous case studies. The response of the neural network for high impedance fault cases (see highlighted) has been outstanding except for EBP algorithm which gave relatively poorer performance compared to LM and RPROP algorithms. In Table 5.17, results which are shown in bold are the 'worst' approximations in each algorithm; yet, quite enough to make decisions. A usual practice in neural network is to set a minimum threshold of 0.8 (corresponding to an output '1') for making decisions. The output from EBP still does not satisfy this threshold. While the results show RPROP has comparable output for this application, LM is exceptionally the most suitable algorithm as far accuracy and robustness are concerned.

Table 5.17: Test results of optimized ANN for the data generated from IEEE 14-bus system

Case	Target	Algorithm		
		EBP	LM	RPROP
1	1	0.9974	0.9999	0.9986
1'	0	0.0025	0.0017	0.0019
2	1	0.7869	0.9200	0.8969
2'	1	0.8090	0.9893	0.8951
3	1	0.9972	0.9997	0.9987
3'	0	0.0027	0.0015	0.0023
4	1	0.9972	0.9997	0.9987
4'	0	0.0029	0.0012	0.0026
5	1	0.9974	0.9974	0.9974
5'	0	0.0029	0.0015	0.0026
6	1	1.0000	1.0000	1.0000
6'	1	1.0000	1.0000	1.0000
7	1	1.0000	1.0000	1.0000
8	1	1.0000	1.0000	1.0000
9	1	1.0000	1.0000	1.0000
10	1	0.7196	0.9952	0.9925
10'	0	0.0027	0.0013	0.0019
11	1	0.8661	0.9673	0.9218
11'	1	0.9264	0.9865	0.9434
12	1	0.9827	0.9996	0.9995
12'	0	0.0027	0.0014	0.0015

5.5. ACCURATE DETERMINATION OF FAULT EXTINCTION TIME

Accurate determination of dead time in the case of temporary faults is another main objective of this work. The AR scheme developed using artificial neural network has the ability to detect secondary arc extinction. This is due to the reason that the neural network has been already trained with cleared fault data patterns obtained from samples of voltage signals following the secondary arc extinction. Basically, a sample fault pattern which is taken before the fault extinguishes is mapped to a neural network output of '1'; whereas, a neural network output of '0' represents a sample taken from a section of the voltage waveform where the fault is vanished out.

Another fact with transmission line faults is that a temporary fault extinguishes out after short time while a permanent fault persists. Thus the neural network output after each sample taken from the fault voltage holds a pattern which assumes 111110000... and 111111111... for temporary and permanent faults, respectively. In other words, the output of neural network while examining a series of consecutive samples will go from '1' to '0' immediately after secondary arc extinction. It is this feature that is employed to accurately determine the fault extinction time. For the sake of clarity, the temporary and permanent fault signals are plotted against the neural network output as illustrated in Figure 5.9.

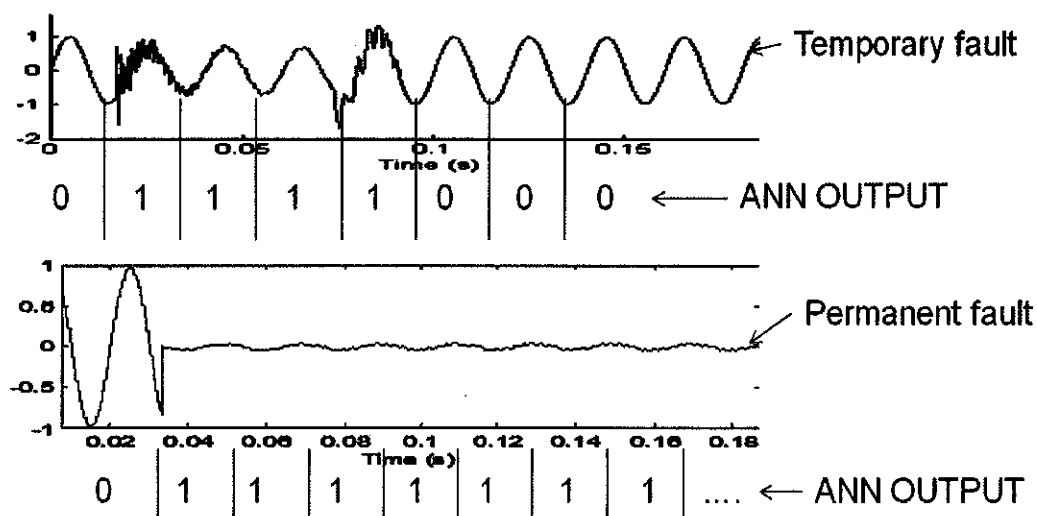


Figure 5.9: ANN output patterns for temporary and permanent faults

5.6. SUMMARY

Data pre-processing techniques and neural network training, testing and validation works (before the data can be fed to the neural network) have been explained plainly in this Chapter. The ANN training processes by using three algorithms (EBP, LM and RPROP), the use of Taguchi's method for optimization of parameters which are understood to pose significant impact on the performance of the neural network during and post training process, and the steps Taguchi's experiments have been also discussed. In addition, the features extracted from the faults generated on IEEE 14-bus system has been employed to test the efficacy of fault identification process

using optimized neural network in the first two case studies (SMIB and IEEE 9-bus system models). The results validate the usefulness of the method developed in terms of fault identification, increasing rate of successful autoreclosing, and other aspects such as improved stability, security of power system, etc.

CHAPTER SIX

CONCLUSIONS AND RECOMMENDATIONS

6.1. CONCLUSIONS

The main objective of this thesis was to propose an adaptive auto-reclosure, based on neural network, for protecting EHV transmission lines by enhancing the performance of conventional auto-reclosure i.e. by increasing the rate of successful reclosure. A technique which has been set forth to discern a temporary fault from a permanent fault and accurately determine the fault extinction time of temporary fault case was presented in Chapter 4. The logic for identifying the type of a fault on the transmission line was handled by a well trained and optimized neural network based on defining the pattern of fault voltage waveforms using FFT method as a means for feature extraction.

To meet the objectives, a number of simulations have been carried out on three different power system models –namely, Single-Machine-Infinite-Bus (SMIB), IEEE 9-bus, and IEEE 14-bus electric system to get input data features for the proposed adaptive AR scheme based on neural network which helps identify temporary from permanent. Illustrations of a number of simulations, which have been carried out on SMIB, IEEE 9-bus and IEEE 14-bus power system models to demonstrate the functionality of the proposed method, were reported in Chapter 4. Extraction of input data features from simulated fault voltages were carried out by decomposing the voltage signals into frequency spectra with the help of Fast Fourier Transform. After allowing the features data set through pre-processing before being fed into neural network, three algorithms –Levenberg Marquardt, Resilient Backpropagation and Error Backpropagation algorithms, whose key parameters have been optimized by Taguchi's methodology, were used for training the neural network.

The results, obtained from the optimized neural network based AR technique are quite reasonable. The developed technique has proved its robust identification capability of the type of fault, and provided correct results by classifying different types of faults in

to their own category (temporary, cleared or permanent). In Chapter 4, it has been shown how accurately the fault extinction can be determined using the proposed technique. The outcomes from SMIB model and the efficacy of the developed methods in the realization of adaptive AR scheme have been exclusively validated by performing similar simulation works on the benchmark IEEE 9-bus and IEEE 14-bus electric systems.

Among the three algorithms used in this study, according to simulation results, LM and RPROP have been identified as the best training algorithms during the fault identification process. Yet, LM yielded better classification results than RPROP; whereas, EBP was found substandard to the other two as far as overall training performance, fast convergence and accuracy are concerned. Regarding the handy optimization tool (Taguchi's method) employed in our study, it has been verified that the optimal parameter combination determined by Taguchi's method yields the maximum accuracy. The parameters decisive in the application of ANN throughout the process have been optimized using Taguchi's Methodology, a powerful and robust process optimization technique. Results and improvements to overall performance of ANN (shown in Chapter 4) prove this fact. Hence, the ANN has been effectively optimized, and testing results (refer to Chapter 4) show the technique developed in this study has the ability to distinguish a transient from a permanent fault, and avoid reclosing onto a line under fault.

Some of the contributions made by this thesis are summarized as follows:

- Avoiding improper reclosing action of a conventional auto-reclosure on to a faulted line in EHV systems. The technique developed has the ability to distinguish between a transient and a permanent fault.
- Increased rate of successful reclosure by accurately determining the fault extinction time (dead time).
- Improved system stability and a reduction in system-equipment damage under a permanent fault. The technique proposed in this report transforms the

conventional auto-reclosure system which is based on 'restore service' into 'reclose only if safe'.

- Improvements to power system security.
- Improvements to ANN performance during and post-training performances by using Taguchi's method.

6.2. RECOMMENDATIONS

The results of the thesis are fully based on simulations. Although the entire results show the efficacy of the proposal, it has to still be verified by practically implementing the method on a real-time network; hence, real-time data recorded over time from real network transmission line faults.

The hardware part of the adaptive auto-reclosure technique with a couple of new features –adaptive fault classification (temporary or permanent) and accurate determination of fault extinction time –is yet to be realized in the future works. There are a number of ways in the modern world which can realize the proposed AR scheme e.g. using transputer card (parallel data processing micro-controller type devices) or with micro-controller itself.

In addition to the above recommendations and future works, the following points are suggested:

Initiation – Another issue here is the initiation of the new AR module which can be done in a number of ways. The assumption made in this study is that data acquisition from line CVT is enabled immediately after fault inception for further investigations. In addition to this, the initiation process can still be made by sensing the circuit breaker opening or trip circuit initiation, which can reduce the processing load to some extent. But these possibilities are left for future verification.

Increasing Number of Examples – Test results from the study show the neural network can robustly accomplish accurate identification process. Apart from over-fitting problem, the general trend with neural networks is increasing examples increases their performance. So, examples prepared for training the neural network can be increased and the effect of the increase can be studied in the future.

Other Artificial Intelligence –Only ANNs have been utilized to propose and add adaptive capability to the existing AR scheme. However, other artificial intelligence techniques such as expert systems, genetic algorithm, artificial neural networks, fuzzy logic, etc. can also be assessed, and the best one be selected.

Expanding Taguchi's Experimentation –Due to lack of available Design of Experiment (DOE) software, Taguchi's experimentations, in this study, have been limited to L₁₆ Orthogonal Array (OA) matrices. If DOE software is readily available, Taguchi's method can be fully utilized to encompass wider range of values of several factors (including new factors e.g. weight initializations which require very big OA matrix). This will make wider range of generalizations.

PUBLICATIONS

1. Desta Zahlay F., K. S. Rama Rao, "An Improved and Self-Adaptive Reclosing Scheme using Neural Network and Taguchi's Methodology on IEEE 9-Bus and 14-Bus System Simulation Case Studies", *Elsevier International Journal of Electric Power Systems Research*, (Submitted).
2. Desta Zahlay F. and K. S. Rama Rao, "Assessment of ANN-Based Auto-reclosing Scheme Developed on Single Machine-Infinite Bus Model with IEEE 14-Bus System Model Data", *IEEE International Conference on Emerging Technologies for Sustainable Development, TENCON 2009, Singapore*, (Submitted).
3. Desta Zahlay F. K. S. Rama Rao, and Perumal A/L N., "Development of an Adaptive Autoreclosure using Taguchi's Method and Artificial Neural Networks on IEEE 9-Bus Electric Power System", *7th IEEE International Conference on Robotics, Vision, Signal Processing & Power Applications, RoViSP 2009, December 19-20, 2009* (Submitted).
4. Desta Zahlay F. and K. S. Rama Rao, "Autoreclosure in Extra High Voltage Lines using Taguchi's Method and Optimized Neural Networks", *IEEE International Conference on Computer Engineering & Technology, ICCET 2009, Jan 22-34, 2009, Singapore*, pp: 151-155.
5. Desta Zahlay F. and K. S. Rama Rao, "Taguchi's Method for Optimized Neural Network Based Autoreclosure in Extra High Voltage Lines", *2nd IEEE International Power & Energy Conference, PECon 2008, 1-3 Dec. 2008, Johor Bahru, Malaysia*, pp. 901-906.
6. Desta Zahlay F., K. S. Rama Rao and Taj Mohd Baloch, "Neural Network Based Optimal Autoreclosure in Extra High Voltage Overhead Lines", *National Postgraduate Conference (NPC 2008), Malaysia, 31st March 2008*.

BIBLIOGRAPHY

- ABB Electric (1994)**, "ABB Electric Utility School -Reclosing", Published by ABB.
- Abdel-Azia Fouad and Vijay Vittal, (1991)**, "Power System Transient Stability Analysis Using the Transient Energy Function Method", Published by Prentice HallPub, USA, ISBN-10: 013682675X.
- Aggarwal P.K., Song Y.H., Johns A.T., (1993)**, "Adaptive Single-Pole Auto-Reclosure Scheme Based on Defining and Identifying Fault Induced Voltage Waveform Patterns," Athens Power Tech, Proceedings. Joint International Power Conference, Vol. 1, pp: 411-416.
- Alessandra S.C., Carlos M.P., Cristina T.M., (2008)**, "Single-phase Auto-reclosure Studies Considering a Robust and Reliable Secondary Arc Model Based on a Gray-box Model", International Conference on High Voltage Engineering and Application, pp: 486-489.
- Anderson P.M. and Fouad A.A. (2003)**, "Power System Control and Stability", 2nd edition, IEEE Press USA, John Wiley and Sons Inc. Publication, pp: 37-48, ISBN: 978-0-471-23862-1.
- Anderson P.M. and Fouad A.A. (1977)**, "Power System Control and Stability", 1st edition, The Iowa State University Press, Ames, Iowa, USA, ISBN: 0813812453 .
- Atif Zaman Khan, (1998)**, "Single Machine Infinite Bus Power System Transient Stability: Software Implementation", Electric Power Components and Systems, Vol. 26, Issue 7, pp: 699 -707.
- Aucoin B.M. and Jones R.H. (1996)**, "High Impedance Fault Detection Implementation Issues", IEEE Transaction on Power Delivery, Vol. 11, Issue 1, pp: 139-148.
- Ban G., Prikler L. and Said A.R. (1999)**, "Use of Neutral Reactors for Improving the Successfulness of Three Phase Reclosing", International Conference Electric Power Engineering, PowerTech Budapest '99, pp: 142 -148.

- Bansal R.C. (2005)**, "Optimization Methods of Electric Power Systems: An Overview", International Journal of Emerging Electric Power Systems, Vol. 2, Issue 1, Article 1021.
- Bartolac T.J. (1993)**. "Parallel Neural Network Training", AAAI Spring Symposium on Innovative Applications of Massive Parallelism, Stanford University, USA.
- Basler Electric (1998)**, "Basler Electric Relay Application School – Reclosing", Published by Basler Electric Press, UK.
- Battiti R. (1992)**, "First- and Second-order Methods for Learning between Steepest Descent and Newton's Method," Neural Computation, Vol. 4, Issue 2, pp: 141-166.
- Caudill and Butler (1994)**, "Understanding neural network", MIT Press, USA.
- Chen T.C. (2003)**, "Acceleration of Levenberg-Marquardt Training of Neural Networks with Variable Decay Rate," IEEE Trans. on Neural Network, Vol. 3, Issue 6, pp: 1873 - 1878.
- Dash P.K. and Samantray S.R. (2004)**, "An Accurate Fault Classification Algorithm using a Minimal Radial Basis Function Neural Network," Journal in Engineering Intelligent Systems, Vol. 12, Issue 4, pp: 205-210.
- Devendra K. Chaturvedi (2008)**, "Soft Computing: Techniques and Its Applications in Electrical Engineering", Published by Springer, ISBN: 3540774807.
- El-Hadidy M.A., Moustafa, D.H. and Attia A.S. (2004)**, "Using Neuro-wavelet Technique for Adaptive Single Phase Autoreclosure of Transmission Lines", Universities Power Engineering Conference, Vol. 39, Issue 2, pp: 684-688.
- Elkalashy N. I., Hatem A. Darwish, Abdel-Maksoud I. Taalab, and Mohammad A. Izzularab (2007)**, "An Adaptive Single Pole Autoreclosure Based on Zero Sequence Power", Electric Power Systems Research, Vol. 77, Issues 5-6, pp: 438-446.
- GEC Alstom T&D (1987)**, "Protective Relays: Application Guide", 3rd edition, Stafford, UK, 1987.

- Golshan M.E.H. and Golbon N. (2005)**, "Detecting Secondary Arc Extinction Time by Analyzing Low Frequency Components of Faulted Phase Voltage or Sound Phase Current Waveforms", *Electrical Engineering*, Vol. 88, Issue 2, pp. 141–148.
- Hagan and Menhaj (1994)**, "Training Feedforward Networks with the Marquardt Algorithm", *IEEE Transactions on Neural Networks*, Vol. 5, Issue 6, pp: 989-993.
- Haykin S. (1998)**, "Neural Networks: A Comprehensive Foundation", 2nd edition, Prentice Hall, USA, ISBN-10: 0132733501.
- Huang Qiang, Li Yongli, Li Bin (2002)**, "A New Adaptive Autoreclosure Scheme to Distinguish Transient Faults from Permanent Faults", *International Conference on Power System Technology*, Vol. 2, pp: 671- 674.
- IEEE Power Systems Committee (1992)**, "IEEE Standard Definitions for Power Switchgear", IEEE Std. C37.100-1992.
- IEEE Power Systems Relaying Committee (1984)**, "Automatic Reclosing of Transmission Lines", *IEEE Transactions*, Vol. PAS-103, Issue 2, pp: 234 – 245.
- IEEE Power Systems Relaying Committee (2003)**, "IEEE guide for auto-matic reclosing of line circuit breakers for AC distribution and transmission lines", IEEE Power Engineering Society, USA.
- Jackson M.C. (1979)**, "Turbine Generator Shaft Torque and Fatigue: Part II - Impact of System Disturbances and High-speed Reclosing", *IEEE Transactions*, Vol. PAS-98, pp: 2308-2313.
- Jan Machowski, Janusz Bialek, James Richard Bumby (1997)** "Power System Dynamics and Stability", published by John Wiley and Sons, USA, ISBN0471956430, 9780471956433.
- Johns A.T., Aggarwal R.K. and Song Y.H. (1994)**, "Improved Technique for Modeling Fault Arcs on Faulted EHV Transmission Systems," *IEE Proc.-Generation, Transmission and Distribution*, Vol. 141, Issue 2, pp: 141-147.

- Joorabian M., S.M.A. Teleghani Asl, and R.K. Aggarwal (2004)**, "Accurate Fault Locator for EHV Transmission Lines Based on Radial Basis Function Neural Networks," *Journal of Electric Power System Research*, Vol. 17, Issue 3, pp: 195-202.
- Kak S. (1998)**, "Artificial Intelligence Techniques in Power Systems", *IEEE Computer Applications in Power*, Vol. 11, Issue 1, pp: 71.
- Kevin Priddy and Paul Keller (2005)**, "Artificial Neural Networks: an Introduction", published by SPIE Press.
- Kevin Warwick, Arthur Ekwue and Raj Aggarwal (1997)**, "Artificial intelligence techniques in power systems", *IEE Power Engineering Series*, Vol. 22, ISBN:0-85296-897-3.
- Khorashadi-Zadeh H. (2005)**, "Artificial Neural Network Approach for Autoreclosure in Transmission Lines", *Power Tech.*, 2005 IEEE Russia: pp: 1-4.
- Kimbark and Wilson, (1998)**, "Power System Stability", 1st edition, John Wiley & Sons Inc., New York.
- Kimbark E.N. (1964)**, "Suppression of Ground-Fault Arcs on Single-Pole Switched EHV Lines by Shunt Reactors", *IEEE Transactions on Power Apparatus and Systems*, Vol. 83, pp: 19-26.
- Kothari D.P. and Nagrath I.J. (2004)**, "Modern Power System Analysis", 3rd edition, published by Tata McGraw-Hill, USA, ISBN: 0070494894.
- Kuffel E. and Zaengl W.S. (2000)**, "High Voltage Engineering – Fundamentals", 2nd edition, Newnes Publisher, ISBN: 0750636343, 9780750636346.
- Laszlo Prikler and Mustafa Kizilcay (2002)**, "Improved Secondary Arc Models Based on Identification of Arc Parameters from Staged Fault Test Records", 14th PSCC, Sevilla, Session 24, Paper 3, pp: 1-7.
- Lei Lai (1998)**, "Intelligent System Applications in Power Engineering Evolutionary Programming and Neural Networks", John Wiley & Sons, Inc. Publication, USA, ISBN: 978-0-471-98095-7.

- Leonard L. Grigsby, (2007)**, "Power system stability and control", CRC Press, Taylor and Francis Group, USA, ISBN: 0849392918, 9780849392917.
- Li Bin, Zhang Shuo, Crossley P. and Bo Zhiqian (2008)**, "The Scheme of Single-Phase Adaptive Reclosing on EHV/UHV Transmission Lines", IET 9th International Conference on Developments in Power System Protection (DPSP 2008), Glasgow, UK, pp: 116-120.
- Lochner H.R. and Joseph E. M. (1990)**, "Designing for Quality. An Introduction to the Best of Taguchi and Western Methods of Statistical Method Design", Chapman and Hall.
- Lukomski R. and Wilkosz R. (2003)**, "Power System Topology Verification Using Artificial Neural Network Utilization of Measurement Data", IEEE PowerTech Conference, Vol. 3, pp: 180-186.
- Lukowicz M. (2004)**, "A New Scheme for Single-pole Autoreclosure Based on Recurrent ANNs", Developments in Power Systems, Vol. 2, pp: 591- 594.
- Madsen K., Hans Bruun Nielsen and Ole Tingleff (2004)**, "Methods for Non-Linear Least Squares Problems", 2nd edition, Informatics and Mathematical Modelling, Technical University of Denmark, DTU, Lecture notes, available at <http://www.imm.dtu.dk/courses/02611/nllsq.pdf>.
- Math H.J. Bollen and Irene Yu-Hua Gu, (2006)**, "Signal processing of power quality disturbances", IEEE Series on Power Engineering, John Wiley & Sons, Inc., Publication, USA.
- Megahed A.I., Hany M.J., Fathy M.A. and Mahmoud A.E. (2006)**, "Arc Characteristics and a Single-Pole Auto- reclosure Scheme for Alexandria HV Transmission System," Journal of Electric Power Systems Research, Vol. 76, Issue 8, pp: 663–670.
- Minai and Williams (1990)**, "Acceleration of Back-propagation", International Joint Conference on Neural Networks.
- Mittelmann H.D. (2004)**, "The Least Squares Problem", webpage: <http://plato.asu.edu/topics/problems/nlolsq.html>

- Pai A.M. (2004)**, "Computational Methods for Electric Power Systems", Power and Energy Magazine, IEEE, Vol. 2, Issue 1, pp: 66 – 72.
- Pai A.M., (2005)**, "Computer Techniques in Power System Analysis", 2nd edition, Published by Tata McGraw-Hill, USA, ISBN: 0070593639.
- R.D. Reed and R.J. Marks II (1999)**, "Neural Smithing: Supervised Learning in Feedforward Artificial Neural Networks", The MIT Press, USA.
- Radojevic Z.M. and Terzija V.V. (2008)**, "A New Digital Algorithm for Overhead Lines Disturbance Records Analysis", IET 9th International Conference on Developments in Power System Protection (DPSP 2008), pp: 658 – 663.
- Riedmiller M. (1994)**, "Advanced Supervised Learning in Multi-layer Perceptrons-from Backpropagation to Adaptive Learning Algorithms," International Journal on Computer Standards and Interfaces, Vol. 16, pp: 265-278.
- Riedmiller M. and Braun H. (1993)**, "A direct Adaptive Method for Faster Backpropagation Learning: The RPROP Algorithm", Proceedings of the IEEE International Conference on Neural Networks (ICNN 1993), San Francisco, USA, pp: 586-591.
- Riedmiller M., (1994)**, "Advanced Supervised Learning in Multi-layer Perceptrons-from Backpropagation to Adaptive Learning Algorithms", International Journal on Computer Standards and Interfaces, Vol. 16, pp: 265-278.
- Riedmiller M., (1994)**, "Rprop - Description and Implementation Details, Technical Report", Published by University of Karlsruhe Press.
- Roger C. Dugan, Mark F. M. and Beaty H. W. (2003)**, "Electrical Power Systems Quality", 2nd edition, Published by McGraw-Hill Inc., Publication, USA, ISBN-10: 0070180318.
- Rolim G. and Zurn J.G. (2003)**, "Interpretation of Remote Backup Protection for Fault Section Estimation by a Fuzzy Expert System", IEEE International PowerTech Conference, Bologna, Spain, pp: 312 - 315.
- Sang-Pil Ahn, Chul-Hwan Kim, Aggarwal R.K. and Johns A.T. (2001)**, "An Alternative Approach to Adaptive Single Pole Auto-Reclosing in High Voltage

- Transmission Systems Based on Variable Dead Time Control”, IEEE Transactions on Power Delivery, Vol. 16, Issue 4, pp: 676–686.
- Sidhartha Panda (2007)**, “MATLAB/SIMULINK Based Model of Single-Machine Infinite-Bus with TCSC for Stability Studies and Tuning Employing GA”, International Journal of Computer Science and Engineering, Vol. 1, Issue 1, pp: 50-59.
- Sultan A.F.**, Swift G.W. and Fedirchuk D.J. (1992), “Detection of High Impedance Arcing Faults Using a Multi-layer Perceptron”, IEEE Transaction Power Delivery, Vol. 7, Issue 4, pp.1871–1877.
- Terzija V.V. and Radojevic Z.M. (2004)**, “Numerical Algorithm for Adaptive Auto-reclosure and Protection of Medium-Voltage Overhead Lines,” IEEE Transactions on power delivery, Vol. 19, Issue 2, pp: 554 - 559.
- Vakil M.B. and Pavesic N. (2003)**, “A Fast Simplified Fuzzy ARTMAP Network”, Kluwer Academic Publishers, USA, Vol. 17, Issue 3, pp: 273-316.
- Wang H.F. and Swift F.J. (1997)**, “A Unified Model for the Analysis of FACTS Devices in Damping Power System Oscillations Part I: Single-Machine Infinite-Bus Power Systems,” IEEE Transaction on Power Delivery, Vol. 12, Issue 2, pp: 941-946.
- Warwick K.**, Arthur E. and Raj A. (1997), “Artificial Intelligence Techniques in Power Systems”, IEE Power Engineering, Vol. 22, Bookcratt Printed, ISBN:0-85296-897-3.
- Xiangning Lin, et al. (2008)**, “A Novel Adaptive Reclosure Criterion for EHV Transmission Line”, IET 9th International Conference on Developments in Power System Protection, pp: 121–125.
- Yaoshong G.**, Bing W., Xiangli D., Bo Z.Q. and Klimek A. (1989), “Prediction Method for Preventing Single-phase reclosing on Permanent Fault”, IEEE Trans Power Delivery, Vol. 4, pp: 114–121

- You-Jin Lee, No-Kyu S., Chul-Hwan K. and Aggarwal R.K. (2008)**, “Development of Auto-Reclosing Algorithm Using Multi Agent System”, IET 9th International Conference on Developments in Power System Protection, pp: 126 – 131.
- Yu I.K. and Song Y.H. (1998)**, “Wavelet Analysis and Neural Network Based Adaptive Single Pole Autoreclosure Scheme for EHV Transmission Systems,” Journal, Electrical Power and Energy Systems, Vol. 20, Issue 7, pp: 465-474.
- Zengping W., Liu H., Xu Y., Ma J. and Liu J. (2006)**, “Prediction method for preventing reclosing on permanent fault of shunt compensated EHV/UHV transmission lines,” IEEE Power Engineering Society.
- Zoric K.J., Djuric M.B. and TERZIJA V.V. (1997)**, “Arcing Faults Detection on Overhead Lines from the Voltage Signals,” Journal of Electrical Power and Energy Systems Research, Vol. 19, Issue 5, pp. 299-303.

APPENDIX A

DISTRIBUTED TRANSMISSION LINE PARAMETERS

Voltage level: 400-kV three-phase line-to-line RMS.

Transmission line length: 300 km

Conductors: Three bundles of 4 Bersfort ACSR 1355 MCM conductors; two 1/2 inch-diameter steel ground wires.

Note: Ytower and Ymin are the average heights of conductors.

LINE GEOMETRY:

Frequency (Hz): 50.00

Ground resistivity (Ω .m): 100.000

Number of phase conductors (bundles): 3

Number of ground wires (bundles): 2

Conductor (bundle)	Phase number	X (m)	Ytower (m)	Ymin (m)	Conductor bundle type
1	1	-12.802	20.726	20.726	1
2	2	0.000	20.726	20.726	1
3	3	12.802	20.726	20.726	1
4	0	-8.992	32.918	32.918	2
5	0	8.992	32.918	32.918	2

CONDUCTOR AND BUNDLE CHARACTERISTICS:

Conductor (Bundle) Type	Conductor Outside Diam.(cm)	Conductor T/D ratio	Conductor GMR (cm)	Conductor DC resistance (Ohms/km)	Conductor relative permeab.
1	3.556	0.375	1.427	0.043	1
2	1.270	0.500	0.495	3.107	1

Number of conductor	Bundle diameter (cm)	Angle of conductor one (deg.)
4	64.658	45.00
1	0.000	0.00

R, L, AND C LINE PARAMETERS:

Resistance matrix R_matrix (ohm/km):

0.0890 0.0790 0.0773
 0.0790 0.0915 0.0790
 0.0773 0.0790 0.0890

Inductance matrix L_matrix (H/km):

1.6100×10^{-003} 7.8539×10^{-004} 6.4938×10^{-004}
 7.8539×10^{-004} 1.6053×10^{-003} 7.8539×10^{-004}
 6.4938×10^{-004} 7.8539×10^{-004} 1.6100×10^{-003}

Capacitance matrix C_matrix (F/km):

1.1661×10^{-008} -2.1268×10^{-009} -5.8362×10^{-010}
 -2.1268×10^{-009} 1.2117×10^{-008} -2.1268×10^{-009}
 -5.8362×10^{-010} -2.1268×10^{-009} 1.1661×10^{-008}

Positive- & zero- sequence resistance [R1 Ro] (ohm/km):

[0.0114, 0.2466]

Positive- & zero- sequence inductance [L1 Lo] (H/km):

[8.6839×10^{-004} , 3.0886×10^{-003}]

Positive- & zero- sequence capacitance [C1 Co] (F/km):

[1.3426×10^{-008} , 8.5885×10^{-009}]

APPENDIX B

TRAINING DATA PATTERNS AND TESTING RESULTS OF NEURAL NETWORK

1. Training Data Patterns Obtained from SMIB Model Simulation

Following are data patterns with target values for training ANN in SMIB study (DC = DC component, T = Targets, FT = Fault Type, L = Location (km), D = Duration of fault (cycles), TF = Temporary Fault, CF = Cleared Fault, PF =Permanent Fault, A = phase A, B = phase B, C = phase C, G = Ground, HIF = High Impedance Fault).

DC	50 Hz	100 Hz	150 Hz	200 Hz	250 Hz	T	FT	L	D
0.295922	4.379843	0.580938	1.307111	0.078427	0.871407	1	TF (AG)	10	3
0.416842	5.235014	1.280322	1.965572	0.172844	1.522152	1	TF (ACG)	25	2
0.537762	6.090184	1.166236	2.624032	0.157442	1.749355	1	TF (AG)	50	3
0.659353	3.996999	0.355376	0.799596	0.047976	0.533064	1	TF (ABG)	75	3
0.675066	4.224059	0.373300	1.014067	0.050396	0.696414	1	TF (AB)	75	4
0.864639	4.146167	0.209866	0.867545	0.028332	0.500731	1	TF (AG)	100	4
1.069924	4.295334	0.415775	0.935493	0.056130	0.623662	1	TF (AG)	125	5
1.262222	8.452317	3.603709	3.545567	0.486501	1.817916	1	TF (AG)	150	3
1.986682	10.814449	1.985379	4.467102	0.268026	2.978068	1	TF (AG)	175	6
2.339997	16.762474	0.209368	0.471079	0.028265	0.314053	1	TF (AC)	200	3
2.780251	15.372602	3.040255	2.091958	0.410434	1.106811	1	TF (ACG)	225	4
3.177036	17.651679	1.886911	0.904386	0.254733	0.820562	1	TF (AG)	250	4
4.014074	18.540884	0.594530	1.337692	0.080262	0.891795	1	TF (AG)	275	5
4.523346	16.226844	0.005688	0.012798	0.000768	0.008532	0	CF (AG)	10	3
4.647156	16.226204	0.027414	0.013150	0.003701	0.011968	0	CF (ACG)	25	2
4.770965	16.225564	0.006001	0.013502	0.000810	0.009001	0	CF (AG)	50	3
4.775648	16.225514	0.028209	0.013532	0.003808	0.012315	0	CF (ABG)	75	3
5.032634	16.224133	0.006353	0.014295	0.000858	0.009530	0	CF (AB)	75	4
5.171497	16.223308	0.030759	0.014755	0.004152	0.013428	0	CF (AG)	100	4
5.310360	16.222483	0.006762	0.015214	0.000913	0.010143	0	CF (AG)	125	5
5.458673	16.221505	0.032858	0.015761	0.004436	0.014346	0	CF (AG)	150	3
5.606986	16.220527	0.007248	0.016308	0.000978	0.010872	0	CF (AG)	175	6
5.925262	16.217907	0.007813	0.017579	0.001055	0.011719	0	CF (AC)	200	3
6.126492	16.197885	0.085236	0.042327	0.011507	0.033420	0	CF (ACG)	225	4
6.386246	16.186564	0.110855	0.055337	0.014965	0.042707	0	CF (AG)	250	4
6.847229	16.155221	0.041376	0.093095	0.005586	0.062063	0	CF (AG)	275	5

0.000250	0.150707	0.000034	0.000076	0.000005	0.000051	1	PF (AG)	10	-
0.001032	0.150698	0.000236	0.000113	0.000032	0.000103	1	PF (ABG)	25	-
0.001083	0.150716	0.000088	0.000042	0.000012	0.000038	1	PF (ABC)	50	-
0.001270	0.150717	0.000016	0.000036	0.000002	0.000024	1	PF (ABCG)	75	-
0.001500	0.150720	0.000053	0.000026	0.000007	0.000023	1	PF (ABG)	75	-
0.001729	0.150723	0.000007	0.000015	0.000001	0.000010	1	PF (AG)	100	-
0.001814	0.150689	0.000067	0.000015	0.000009	0.000100	1	PF (ABC)	125	-
0.003811	0.150673	0.000456	0.000219	0.000062	0.000199	1	PF (ABCG)	150	-
0.005808	0.150657	0.000128	0.000287	0.000017	0.000191	1	PF (ACG)	175	-
0.008609	0.279653	0.064918	0.146066	0.008764	0.097377	1	PF (ABC)	200	-
0.009584	0.150630	0.000861	0.000413	0.000116	0.000375	1	PF (ABCG)	225	-
0.013359	0.150602	0.000240	0.000539	0.000032	0.000359	1	PF (ABCG)	250	-
0.020412	0.150557	0.001617	0.000774	0.000218	0.000712	1	PF (ABC)	275	-
0.027465	0.150511	0.000448	0.001008	0.000060	0.000672	1	PF (ABG)	10	-
0.030132	0.193420	0.138529	0.049691	0.018701	0.109666	1	PF (ABC)	150	-
0.031465	0.214874	0.206738	0.074032	0.027910	0.164032	1	PF (ABC)	10	-
0.054321	0.150095	0.000888	0.001998	0.000120	0.001332	1	PF (ACG)	10	-

2. Responses of Optimized Neural Network to Testing Data Patterns in Case Study I ($T = Target$, $LM = Levenberg-Marquardt Algorithm$)

DC	50 Hz	100 Hz	150 Hz	200 Hz	250 Hz	T	LM
0.344722	4.478543	0.578798	1.305881	0.076127	0.871244	1	1.000000
0.465642	5.333714	1.278182	1.964342	0.170544	1.521989	1	0.999973
0.586562	6.188884	1.164096	2.622802	0.155142	1.749192	1	0.999974
0.708153	4.095699	0.353236	0.798366	0.049876	0.532634	1	0.999974
0.723866	4.322759	0.371160	1.012837	0.052296	0.695984	1	0.999974
0.913439	4.244867	0.207726	0.866315	0.030232	0.500301	1	0.999974
1.118724	4.394034	0.413635	0.934263	0.058030	0.623232	1	0.999973
4.572146	16.010614	0.003548	0.011568	0.000788	0.008498	0	0.000027
4.695956	16.009974	0.025274	0.013161	0.003721	0.012110	0	0.000026
4.819765	16.009334	0.005791	0.013513	0.000830	0.009112	0	0.000024
4.488648	16.009284	0.027999	0.013543	0.003828	0.012131	0	0.000023
4.745634	16.007903	0.006143	0.014306	0.000878	0.009450	0	0.000022
4.884497	16.007078	0.030549	0.014766	0.004172	0.013432	0	0.000027
5.023360	16.006253	0.006552	0.015225	0.000933	0.010242	0	0.000028

0.008409	0.280653	0.064708	0.146077	0.008784	0.097417	1	1.000000
0.009384	0.151630	0.000871	0.000511	0.000120	0.000384	1	1.000000
0.013159	0.151602	0.000250	0.000520	0.000029	0.000389	1	1.000000
0.020212	0.151557	0.001627	0.000698	0.000195	0.000714	1	1.000000
0.027265	0.151511	0.000458	0.001042	0.000050	0.000686	1	1.000000
0.029932	0.194420	0.138539	0.048961	0.018642	0.110060	1	1.000000
0.031265	0.215874	0.206748	0.074043	0.026920	0.165402	1	1.000000
0.054121	0.151095	0.000898	0.002000	0.000131	0.001400	1	1.000000
0.001300	0.151720	0.000063	0.000030	0.000006	0.000019	1	1.000000

APPENDIX C

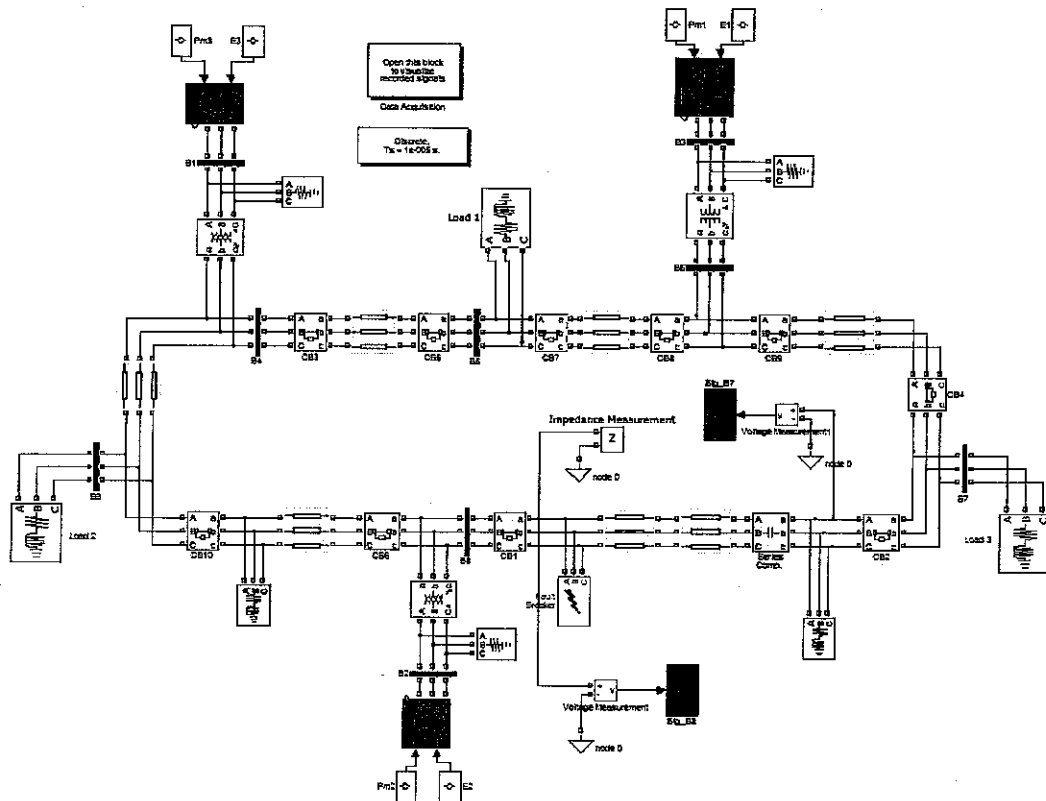
SOME OF THE DATA PATTERNS FOR TRAINING ANN WITH TARGET VALUES

(DC = DC component, T = Targets, FT = Fault Type, L = Location (km), D = Duration of fault (cycles), TF = Temporary Fault, CF = Cleared Fault, PF = Permanent Fault).

Input Features						T	TF & Sample cycle from inception	L (% of length of line)
DC	50 Hz	100 Hz	150 Hz	200 Hz	250 Hz			
0.438101	4.690590	0.745094	1.416558	0.100588	1.011441	1	TF 1 st cycle	20%
4.585251	16.222300	0.035060	0.016998	0.004733	0.014832	0	CF 10 th cycle	20%
0.640740	4.146167	0.385575	0.867545	0.052053	0.578363	1	TF 1 st cycle	40%
4.897615	16.221990	0.006883	0.015488	0.000929	0.010325	0	CF 10 th cycle	40%
0.864639	10.109350	1.954640	1.821340	0.263876	1.111631	1	TF 1 st cycle	60%
5.384517	16.212600	0.069976	0.029241	0.008030	0.024424	0	CF 10 th cycle	60%
1.704775	17.207080	0.305659	0.687732	0.041264	0.458488	1	TF 1 st cycle	80%
5.658947	16.186560	0.024594	0.055337	0.003320	0.036891	0	CF 10 th cycle	80%
2.758516	0.150709	0.000145	0.000069	0.000020	0.000063	1	PF 1 st cycle	5%
6.386246	0.165157	0.040264	0.017053	0.006400	0.032250	1	PF 10 th cycle	5%
0.001266	0.150800	0.000012	0.000027	0.000002	0.000018	1	PF 1 st cycle	20%
0.013169	0.151009	0.021030	0.000659	0.000038	0.020045	1	PF 10 th cycle	20%
0.001495	0.150690	0.000065	0.000147	0.000009	0.000098	1	PF 1 st cycle	40%
0.016926	0.171995	0.069715	0.024982	0.009399	0.055101	1	PF 10 th cycle	40%
0.002031	0.150857	0.000098	0.000223	0.000014	0.000151	1	PF 1 st cycle	60%
0.019918	0.182715	0.104178	0.037403	0.014064	0.082372	1	PF 10 th cycle	60%
0.003791	4.690590	0.745094	1.416558	0.100588	1.011441	1	TF 1 st cycle	20%
0.025939	16.222300	0.035060	0.016998	0.004733	0.014832	0	CF 10 th cycle	20%

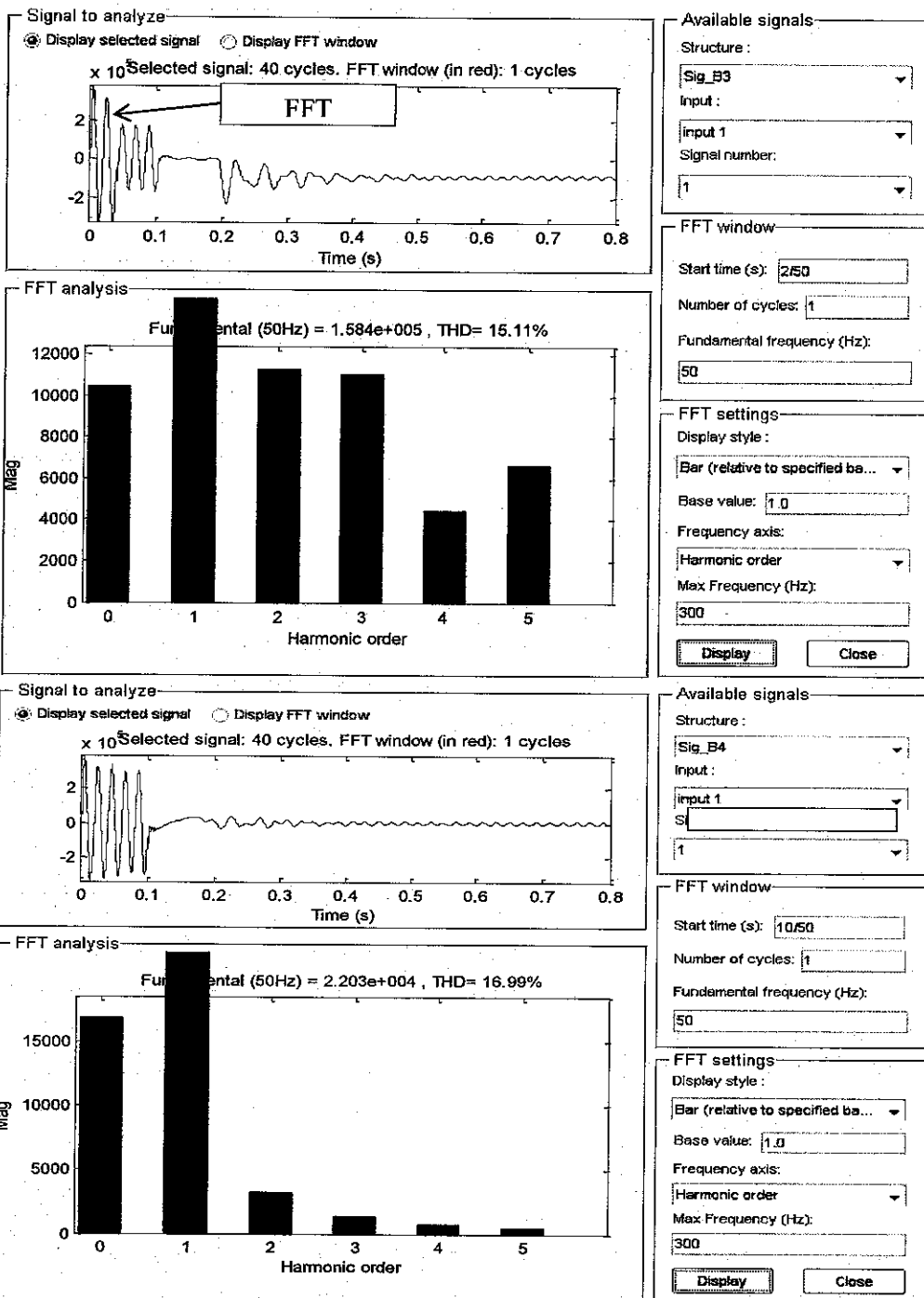
APPENDIX D

A SET UP OF IEEE 9-BUS POWER SYSTEM MODEL IN SIMULINK



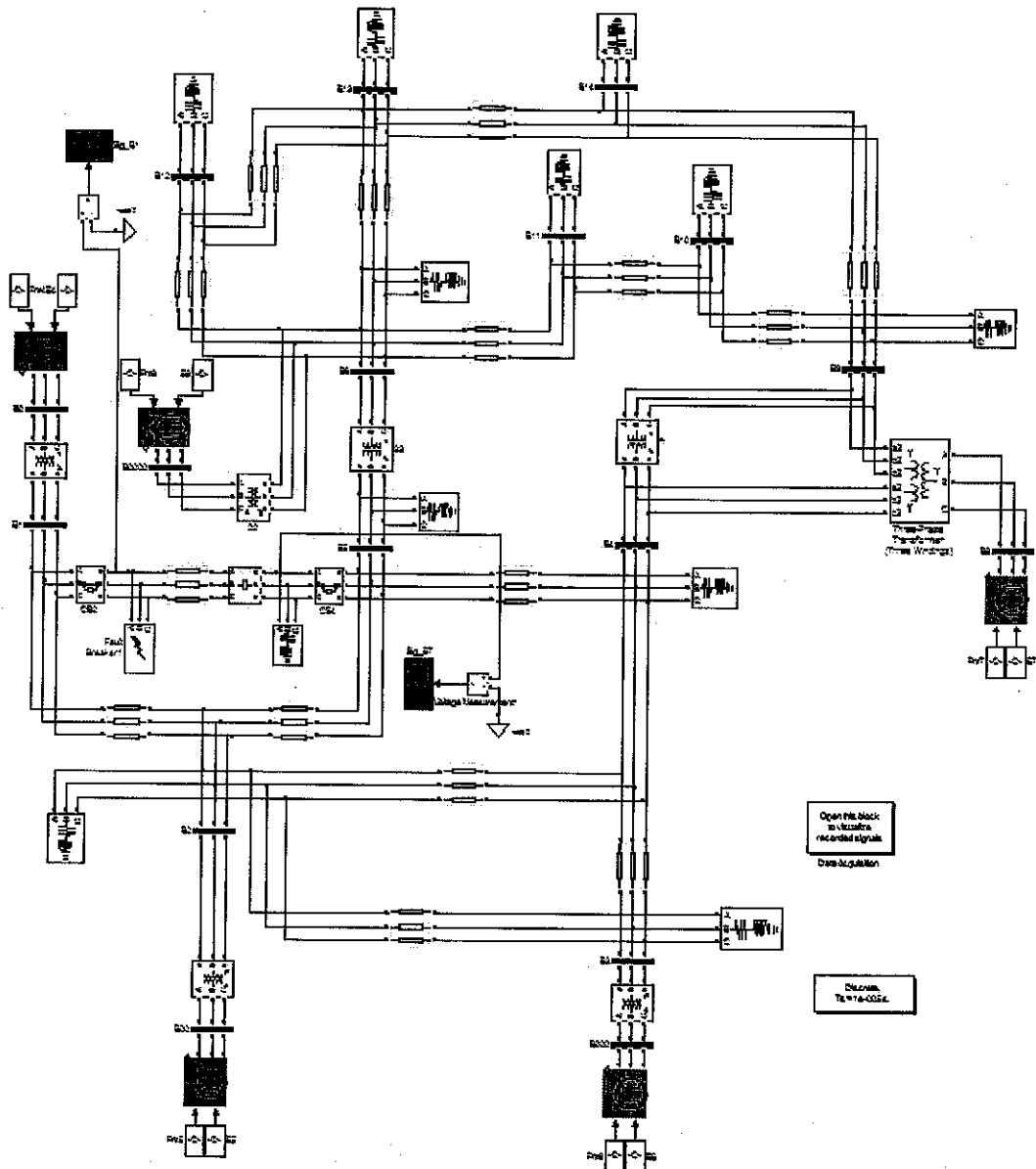
APPENDIX E

FFT OUTPUTS OF TEMPORARY FAULT AFTER AND BEFORE EXTINCTION



APPENDIX F

A SET UP OF IEEE 14-BUS POWER SYSTEM MODEL IN SIMULINK



APPENDIX G

MATLAB CODES

1. Part of the Graphical User Interface for EBP Algorithm

```
% Note this program is a GUI for the simulating Neural network proposed for %
ADAPTIVE          AUTORECLOSURE
```

```
%=====
%
```

```
function GUIDemonew(fcn)
```

```
%demo of user interface construction
%this function CALLS ITSELF via GUI callbacks
```

```
% By default make the GUI
%This code detects the first entry into the function
%from the command line with no parameters
if nargin == 0
    fcn = 'makeGUI';
end
```

```
%This is the main decision point of the function.
%The switch statement is executed once-per-fuction call
switch fcn
```

```
    %This code is executed ONCE when the function enters with
    %no arguments
case 'makeGUI'
```

```
    % Determine the name of this function and store it in the
    %figure plotinfo variable.
    %Since variables used in a function are not persistent after
    %the function exits we will need to store the state-variables
    %in a data structure associated with the persistent Figure-window.
    %The plotinfo sturcture will be saved into the Figure's UserData
    %area and retrieved from there as necessary.
    plotinfo.myname = mfilename;
```

```
%====Create main figure=====
fig = figure('Position',centerfig(660,630),...
    'Resize','on',...
    'NumberTitle','off',...
    'Name','GUI DEMO FOR OPTIMIZATION',...
    'Interruptible','off',...
    'Menubar','none',...

```

```

.
.
.
.

    set(gcf,'UserData',plotinfo);

case 'editNumHidden'
    plotinfo=get(gcf,'UserData');
    plotinfo.NumHidden=str2num(get(plotinfo.s11,'string'));
    set(plotinfo.s12,'value',plotinfo.NumHidden);
    set(gcf,'UserData',plotinfo);

case 'editMCode'
    edit backpropnew;
case 'rate'
    plotinfo=get(gcf,'UserData');
    plotinfo.dlg1=get(plotinfo.dlgbox1,'value');
    n=plotinfo.dlg1;
    set(gcf,'UserData',plotinfo);

case 'editHelp'
    edit ETEXT;

case 'editFunCode'
    edit a2d;pause(4);

%
case 'dialog'
    plotinfo=get(gcf,'UserData');
    plotinfo.dlg=get(plotinfo.dlgbox,'value');
    choice=plotinfo.dlg;
    set(gcf,'UserData',plotinfo);

case 'edttl'
    plotinfo=get(gcf,'UserData');
    plotinfo.title=get(plotinfo.ttl,'string');
    title(plotinfo.title);
    set(gcf,'UserData',plotinfo);

case 'linemenu1'
    plotinfo=get(gcf,'UserData');
    set(plotinfo.line, 'LineStyle', '--')

case 'linemenu2'
    plotinfo=get(gcf,'UserData');
    set(plotinfo.line, 'LineStyle', ':')

```

```

case 'linemenu3'
    plotinfo=get(gcf,'UserData');
    set(plotinfo.line, 'LineStyle', '-')

end

%====A utility to center the window on the screen=====
function pos = centerfig(width,height)

% Find the screen size in pixels
screen_s = get(0,'ScreenSize');
pos = [screen_s(3)/2 - width/2, screen_s(4)/2 - height/2, width, height];
%=====

```

2. Main Program for EBP Algorithm

```

tic % Start counting the time elapsed during simulation

% Load the input patterns /the energies of dc,50Hz, and the first 4 harmonics/
patterns = xlsread('input_data', 'sheet1');

% The corresponding desired outputs
desired_out = xlsread('target','sheet1');

% Will hold a record of all sum-squared-errors. Nice to plot
sse_rec = [];sse_rec1 = [];sse_rec2 = [];sse_rec3 = [];
%variable parameters
etha, alpha,NumHidden,tolerance
% sse = 10; % A dummy initial sse. Must be large, for the "while" below
% %etha = 0.6; % Learning rate.
% %alpha = 0.2; % Momentum term
patterns = [patterns ones(size(patterns,1),1) ]
% Add a column of 1's to patterns to make a bias node
num_inp = size(patterns,2) % No. of input nodes (including bias)
% Note: size(x,2) is Matlab for the no. of columns in matrix x
num_hid = 10; % No. of hidden nodes (including bias node)
num_out = size(desired_out,2) % No. of output nodes

%%%%%%%%%%%% Giving the weights small initial values in range [-1,1]%
w1 = (1-2*rand(num_inp,num_hid-1))
    % Input to hidden weights. NB: no weights to bias hidden node

w2 = (1-2*rand(num_hid,num_out)) % Hidden-to-output weights
% Note: rand(rows,cols) is a matrix of random numbers of that size

dw1_last = zeros(size(w1)); % Last w1 change, set to a zero matrix
dw2_last = zeros(size(w2)); % Last w2 change, set to a zero matrix

```

```

epoch = 0;          % Initialise count of training epochs

%%%% Main loop %%%
while sse > tolerance % When sse is low enough, we'll stop
    winp_into_hid = patterns * w1; % Pass patterns through weights
    % Sigmoid of weighted input
    hid_act = 1./(1+exp(- winp_into_hid));
    % Add bias node
    hid_with_bias = [ hid_act ones(size(hid_act,1),1) ];
    % Pass hidden acts through weights
    winp_into_out = hid_with_bias * w2;
    % Sigmoid of input to output
    out_act = 1./(1+exp(- winp_into_out));
    % Error matrix
    output_error = desired_out - out_act;
    % Sum sqr error, matrix style
    sse = trace(output_error*output_error);
    sse_rec = [sse_rec sse]; % Record keeping
    % delta=dE/do * do/dnet
    deltas_out = output_error .* out_act .* (1-out_act);
    deltas_hid = deltas_out*w2' .* hid_with_bias.*(1-hid_with_bias);
    deltas_hid(:,size(deltas_hid,2)) = [];
    % Take out error signals for bias node
    dw1 = etha * patterns' * deltas_hid + alpha * dw1_last;
    % The key backprop step, in matrix form
    dw2 = etha * hid_with_bias' * deltas_out + alpha * dw2_last;
    w1 = w1 + dw1; w2 = w2 + dw2; % Weight update
    dw1_last = dw1; dw2_last = dw2; % Update momentum records
    epoch = epoch + 1;
    if rem(epoch,50)==0
        % Every 50 epochs, show how training is doing
        disp([' Epoch ' num2str(epoch) ' SSE ' num2str(sse)]);
    end
end

% Testing for convergence

if epoch==1000
    if(sse_rec(1,1000)>=1)
        disp(' ');
        disp(' ');
        disp('Warning!! Training may not be successful!!! ');
        disp('N.B: It is diverging.....');
        disp('Please adjust your parameter combinations');
        disp(' 1. learning rate,');
        disp(' 2. momentum,');
        disp(' 3. number of hidden layers and/or ');
        disp(' 4. tolerance');
        disp('Update, save and run it again');
    end
end

```



```
plot((100:1000),sse_rec2); xlabel('Epochs'); ylabel('Sum squared error
(SSE)');grid on
title(['SSE Vs. epochs plot for tolerance =
',num2str(tolerance)]);waitforbuttonpress;
for i=1000:1:epoch
    sse_rec3=[sse_rec3 sse_rec(1,i)];
end
%figure;
plot((1000:1:epoch),sse_rec3); xlabel('Epochs'); ylabel('Sum squared error
(SSE)');grid on
title(['SSE Vs. epochs plot for tolerance = ',num2str(tolerance)]);
end;
toc %Stop counting the time elapsed during simulation

% The end
```